M 2015

U.PORTO
FEUP FACULDADE DE ENGENHARIA
UNIVERSIDADE DO PORTO

Nanostructured Lipid Carriers: a new approach for Psoriasis dermal therapy

MARA ALEXANDRA PALHETE FERREIRA
DISSERTAÇÃO DE MESTRADO APRESENTADA
À FACULDADE DE ENGENHARIA DA UNIVERSIDADE DO PORTO EM 14 DE JULHO DE 2015
ENGENHARIA BIOMÉDICA

U.PORTO
FEUP

MEB - MESTRADO EM ENGENHARIA BIOMÉDICA | **2014/2015**

A Dissertação intitulada

"Nanostructured Lipid Carriers: a new approach for Psoriasis dermal therapy"

foi aprovada em provas realizadas em 14-07-2015

o júri

Presidente Professor Doutor José Alberto Peixoto Machado da Silva
Professor Associado do Departamento de Engenharia Eletrotécnica e de Computadores da Faculdade de Engenharia da U. Porto

Professora Doutora Maria Benedita Almeida Garrett de Sampaio Maia
Professora Auxiliar do da Faculdade de Medicina Dentária da U. Porto

Doutora Sofia Teresa Coimbra Antunes Costa Lima
Investigadora do Departamento de Ciências Químicas da Faculdade de Farmácia da U. Porto

O autor declara que a presente dissertação (ou relatório de projeto) é da sua exclusiva autoria e foi escrita sem qualquer apoio externo não explicitamente autorizado. Os resultados, ideias, parágrafos, ou outros extratos tomados de ou inspirados em trabalhos de outros autores, e demais referências bibliográficas usadas, são corretamente citados.

Autor - Mara Alexandra Palhoto Ferreira

Faculdade de Engenharia da Universidade do Porto

Faculdade de Engenharia da Universidade do Porto

Nanostructured Lipid Carriers: a new approach for Psoriasis dermal therapy

Mara Alexandra Palhete Ferreira

FINAL VERSION

Dissertation carried out in the
Master in Biomedical Enginnering

Orientation by: Salette Reis and Sofia Lima

June of 2015

Faculdade de Engenharia da Universidade do Porto

Nanostructured Lipid Carriers: a new approach for Psoriasis dermal therapy

Mara Alexandra Palhete Ferreira

FINAL VERSION

Dissertation carried out in the
Master in Biomedical Enginnering

Orientation by: Salette Reis and Sofia Lima

June of 2015

Resumo

Durante as ultimas décadas, transportadores coloidais e inorgânicos têm sido estudados na veiculação dérmica/transdérmica de fármacos. O sucesso da implementação destes sistemas neste tipo de veiculação prende-se com a sua capacidade de atravessar várias barreiras anatómicas, a capacidade de libertar o fármaco de forma controlada e ainda da sua estabilidade à escala nanométrica.

No início dos anos 90, entre os transportadores coloidais lipídicos surgiram as nanopartículas lipídicas sólidas (SLN) como sistemas bastante promissores na veiculação de fármacos.

Por isto, estas nanoparticulas são amplamente aceites por combinar as vantagens e ultrapassar as desvantagens associadas a outros transportadores coloidais. Contudo, a baixa capacidade de retenção do fármaco e a sua expulsão durante o armazenamento são as suas grandes desvantagens. Transportadores lipídicos nanoestruturados (NLC) foram desenvolvidos para ultrapassar a baixa capacidade de retenção do fármaco nas SLN, ao diminuir o grau de organização da sua matriz lipídica. Baseiam-se numa mistura de lipidos que resulta em várias imperfeições na sua matriz promovendo a maior acomodação do fármaco. Como os lípidos liquídos exibem maior solubilidade para os fármacos, transportadores lipidicos nanoestruturados têm maior capacidade de retenção dos fármacos bem como uma libertação mais controlada do mesmo. Várias vias de administração têm sido investigadas para estas nanoparticulas de matriz lipídica: tópica, oral ou parental.

O metotrexato (MTX) é um antagonista do ácido fólico que se liga competitivamente à enzima dihidrofolato redutase que impede o crecimento da célula, retém o ciclo celular nas fases G1/S e é utilizado em ensaios clínicos, desde os anos 50, no tratamento de diferentes tumores sólidos e ainda na terapida de doenças autoimunes e inflamatórias como a artrite reumatóide e psoríase. Para ultrapassar os inconvenientes associdas à terapêutica com MTX (por ex. hepatotoxicicidade, colite ulcerativea, nefrotoxicidade), os veiculadores coloidais poderão ser aplicados.

A produção de nanopartículas requer um elevado conhecimento de todos os parâmetros e propriedades do processo. Utilizar a abordagem tradicional (um factor de cada vez) para

obter uma formulação optimizada é difícil de conceber, ineficiente e bastante morosa. O desenho estatístico das formulações é uma estratégia validada e bastante útil na preparação de uma formulação com menos ensaios experimentais e, que fornece informação suficiente entre as variáveis dependentes e independentes no processo. Alguns estudos descreveram nanopartículas lipídicas optimizadas através de um modelo factorial. Neste trabalho, o efeito da composição da formulação na optimização de NLCs com MTX foi realizada recorrendo a um modelo denominado Box-Behnken. A formulação foi produzida pelo método de ultrasonicação utilizando Witepsol®E85 como lípido sólido e Migliol®812 como lípido liquido e as suas propriedades físico químicas (morfologia, tamanho, índice de polidispersão e eficiência de incorporação), libertação in vitro do fármaco e viabilidade celular foram estudadas. As NLCs optimizadas exibiram uma forma praticamente esférica, com tamanhos de 252-nm, índice de polidispersão de 0.06 ± 0.02, potencial zeta de -14 mV e eficiência de incorporação de 87%. Os estudos de libertação mostraram que o fármaco tem uma libertação inicial rápida seguida de uma fase controlada durante 24 horas. O modelo matemático de Peppas-Korsmeyer descreve a cinética desta libertação para ambientes fisiológicos e inflamatórios e o modelo Hixson-Crowell nas condições simuladas da pele. Não foi observada citotoxicidade em fibroblastos. Assim, NLCs com MTX têm potential para ser exploradas como sistemas veiculadores de fármacos.

A segunda abordagem do trabalho consistiu no desenvolvimento de um modelo para veiculação de fármacos com alvo local de acção para o tratamento da psoríase. Para veicular MTX, foram produzidas, NLC e SLN funcionalizadas com Etanercept, anticorpo monoclonal comumente usado na terapia biológica da psoríase para assim obter uma terapia direcionada.

Estas nanoformulações foram incorporadas num hidrogel para eventualmente facilitar a sua penetração na barreira dérmica. A formulação foi produzida pelo método descrito acima, utilizando palmitato de cetilo como lípido sólido e Migliol® 812 como lípido líquido e caracterizadas em termos de propriedades físico-quimicas, perfil de libertação do fármaco e citotoxicidade em fibroblastos e queratinócitos, ensaios de permeação e propriedades reológicas.

Todas as nanoformulações apresentam tamanhos à volta dos 400-nm, potencial zeta de -30 mV, índice de polidispersão inferior a 0.3 e elevados valores de eficiência de incorporação do fármaco. Para além disso, microscopia por TEM e Cryo-SEM mostrou que todas as nanopartículas exibem forma esférica independentemente da sua composição e foram estáveis durante 6 semanas, à temperatura ambiente. A libertação do MTX mostrou o mesmo comportamento das formulações anteriores: rápido seguido de um perfil controlado. Para além disso, um hidrogel (Carbopol 934®) foi enriquecido com ambas as nanoparticulas lipídicas com e sem MTX, e a mesma combinação das nanopartículas funcionalizadas. Análises reológicas revelaram que estas nanoformulações possuem comportamento não-Newtoniano, pseudoplástico e tixotropia, sugerindo que são apropriadas para veiculação tópica. No entanto, possuem uma ligeira perda de consistência após 2 semanas de preparação. Ensaios de permeação da

pele demonstraram, mimetizando condições fisiológicas, as nanopartículas lipídicas com MTX possuem bons níveis de penetração do fármaco e proteína funcionalizada, através da pele de porco. Observa-se um pequeno decréscimo quando as nanopartículas são incorporados no hidrogel.

Os principais resultados obtidos para ambas as nanopartículas permitem afirmar que possuem propriedades interessantes para veicular MTX. Estes resultados revelam ainda que estes sistemas são uma plataforma promissora para a terapia tópica de doenças inflamatórias, como a psoríase.

***Palvras-chave**: desenho factorial Box-Behnken, Etanercept, hidrogel, metotrexato (MTX), nanopartículas sólidas lipídicas (SLN), terapia direcionada, transportadores lipídicos nanoestruturados (NLC)*

Abstract

During the last decades, inorganic and colloidal carriers have been discovered for dermal/transdermal drug delivery. The successful implementation of these systems for drug delivery entirely depends on their ability to go through numerous anatomical barriers, sustained release of their content and their stability in the nanometer siz.

Among these lipid colloidal delivery systems Solid Lipid Nanoparticles (SLN) emerged in the early nineties as an alternative and, current trials applying SLN consider them very promising in drug delivery. In fact, it is widely accepted that SLN combine the advantages and avoid the disadvantages of other colloidal carriers. Low drug loading and drug expulsion during storage period are taken as the disadvantage of solid lipid nanoparticles. Nanostructure Lipid Carriers (NLC) have been developed to overcome the drug loading limitation of SLN, by decreasing the degree of the lipid matrix organization. NLC are based on a mixture of solid and liquid lipids that results in an imperfect matrix thus, in an increase of the drug loading. As liquid lipids exhibit higher solubility for drugs, NLC have a higher loading capacity than SLN, as well as an improved drug controlled release. Many administration routes are being investigated for lipid nanoparticles, including topical, oral and parenteral ones.

Methotrexate (MTX) is a folate antagonist used in the clinics for the treatment of different solid tumours and in the therapy of autoimmune and inflammatory diseases as rheumatoid arthritis and psoriasis. To overcome the drawbacks (e.g. hepatotoxicity, ulcerative colitis, nephrotoxicity) associated with MTX administration colloidal delivery systems can be applied. The first aim of the present research was to develop a lipid based delivery system for MTX safe administration.

A formulation design requires full knowledge of the relationship between the process parameters and the quality attributes. To reach an optimized formulation using traditional screening approach (one factor at a time) is difficult, inefficient and time consuming. A

The statistical formulation design is a validated and useful approach to develop a formulation with less experimentation and providing enough information on the relationship between independent and dependent variables. Few studies have optimized lipid nanoparticles using factorial design and is widely accepted that the ingredients have great influence on the

physicochemical properties. Here, the effect of the formulation composition in the optimization of MTX-loaded NLC by means of a Box-Behnken factorial design is described. The formulation was produced using the hot ultrasonication method, using Witepsol®E85 as the solid lipid and Mygliol®812 as liquid lipid, and their physicochemical properties (morphology, particle size, polydispersity, zeta potential, and entrapment efficiency), in vitro drug release studies and cytotoxicity were investigated. Optimized NLCs loaded with MTX exhibited spherical shape with 252-nm, a polydispersity of 0.06 ± 0.02, zeta potential of -14 mV and an entrapment efficiency of 87%. In vitro release studies revealed a fast initial release followed by a sustained release of MTX from the NLC up to 24-hours. The release kinetics of the optimized NLC best fitted the Peppas-Korsmeyer model for physiological and inflammatory environments and the Hixson-Crowell model skin simulation conditions. No toxicity was observed in fibroblasts. Thus, the optimized MTX-loaded NLC have the potential to be exploited as delivery system.

The second aim of this research was to design and characterize a targeted delivery system for topical application in psoriasis. Besides delivery of MTX, NLC and SLN were functionalized with Etanercept, a monoclonal antibody currently used in psoriasis biological therapy, to obtain a target therapy. These nanoformulations were incorporated into a hydrogel to eventually facilitate their penetration in a dermal barrier. The formulation was produced by the method described above, using cetyl palmitate as solid lipid and Miglyol 812 as liquid lipid, and were characterized in terms of: physico-chemical properties, in vitro drug release profile, in vitro cytotoxicity in keratinocytes (KC) and fibroblasts, skin permeation profile and rheological properties. All nanoformulations presented size closer to 400 nm, -30 mV, polydispersity index below 0.3 and high values of drug content. Furthermore, morphological investigations by TEM and Cryo-SEM showed that all nanoparticles exhibit a spherical shape and a smooth surface independently of their composition and were stable at least 6 weeks at room temperature. MTX release showed a fast initial phase followed by a sustained drug release. Furthermore, we produced a hydrogel (Carbopol® 934) enriched with empty LNs, MTX loaded LNs, F-LNs and MTX loaded F-LNs. Rheological tests showed that all the designed formulations had a non-Newtonian, pseudoplastic, thixotropic behavior, suggesting that they are suitable for topical drug delivery with a small decrease of it consistency in 2 weeks. Skin permeation assays demonstrated that, mimicking physiological values and temperature, LNs loaded with MTX have good levels of MTX and protein penetration through pig ear skin. A small decrease of MTX permeation was observed when LNs were embedded in the hydrogel.

The main results obtained for both approaches of this work reveal that produced lipid colloidal carriers show interesting properties for delivering MTX. Present results demonstrated that these systems could be a promising platform for inflammatory diseases, in particular for psoriasis topical therapy.

Keywords: *Box-Behnken factorial design, Etanercept, hydrogel, Methotrexate (MTX), Nanostructure Lipid Carriers (NLC), Solid Lipid Nanoparticles (SLN)*

Acknowledgments

This study was carried out in the period between September of 2014 and June of 2015 at the Departamento de Química da Faculdade de Farmácia, under the supervision of Professor Doctor Salette Reis and Doctor Sofia Costa Lima, at the Universidade do Porto for my master thesis at Biomedical engineering.

I would like to express my gratitude to my supervisors Prof. Dr. Salette Reis and Dr. Sofia Costa Lima, for constant advice, guidance and support, for giving me the opportunity to work on this interesting topic, and also for the kindness and motivation during all the time.

I would like to thank Luise Lopes for her help to performe a statistical analysis of experimental designs, thank Prof. Dr. Marcela Segundo and Dr. Luisa Barreiros of Departamento de Química da Faculdade de Farmácia for help and guidance during HPLC experiments and also recognize help provided by Dra Helena Amaral in rheological measurements with hydrogel.

I would like to thank all the people of Molecular Biophysics and Biotechnology Unit from GABAI at Faculdade de Farmácia, my colleagues for the excellent working environment provided; it was a great and unbelievable experience.

Finally, I want to thank my family and friends, especially my mother and father for their support and unconditional love, thank you for always being there for me.

List of contents

List of figures

List of tables

List of abbreviations

APCs	Antigen presenting cells
BSA	Bovine serum albumin
CCR	Chemokine receptor
CD	Cluster of differentiation
CXCL	Chemokine ligand
Cryo-SEM	Cryo-Scanning electron microscopy
CyA	Cyclosporine A
DC	Dentritic cells
DCM	Dichloromethane
DLS	Dynamic light scattering
DMSO	Dimethil sulfoxide
DSPE-PEG-NH_2	1,2-distearoyl-*sn*-glycero-3-phosphoethanolamine-N-[amino(polyethylene glycol)
EDC	1-etliyl-3-(3-dimethylaminopropyl)carbodiimide
EE	Entrapment efficiency
FBS	Fetal bovine serum
FDA	Food and Drug Administration
F-LNs	Functionalized lipid nanoparticles
ICAM	Intercellular adhesion molecule
IL	Interleukin
IFN	Interferon
KC	Keratinocytes
LFA	Lymphocyte function associated
LNs	Lipid nanoparticles
NLC	Nanostructured lipid carrier
MTX	Methotrexate
PBS	Phosphate buffered saline
PCS	Photon Correlation Spectroscopy
PDI	Polydispersity index
PSO	Psoriasis
PSA	Psoriatic arthritis
PVA	Polyvinil alcohol
QELS	Elastic Light Scattering

RA	Rheumatic arthritis
SC	*Stratum corneum*
SLN	Solid lipid nanoparticles
TCR	T-cell receptor
TEM	Transmission electron microscopy
Th	T-helper cells
TNF	Tumor necrosis factor
UV	Ultraviolet
VEGF	Vascular endothelial growth factor

List de symbols

ζ	Zeta
μ	Micro
τo	Yield stress
λ	Wavelength

Chapter 1- Aims and Organization of dissertation

This dissertation aims to improve methotrexate (MTX) administration in psoriasis (PSO) topical therapy. To achieve this goal specific objectives were defined: (1) to ascertain if Box-Behnken design approach is suitable to optimize the production of lipid nanoparticles containing MTX; (2) to develop a topical therapy through the design of an innovative hydrogel enriched with MTX loaded lipid nanoparticles; (3) to produce a combination therapy with currently used psoriatic drugs: Etanercept and MTX, eventually for a systemic or topical administration.

Since the beginning of the 1990s, lipid based nanoparticles have features that make them interesting for the pharmaceutical and cosmetic technology research. Lipid nanoparticles as solid lipid nanoparticles (SLN) and their second generation, the nanostructured lipid carriers (NLC) have been investigated as carrier systems for many applications, and will be used in this work.

This dissertation is organized as follows: Aims and organization of dissertation, introduction and state of art, materials and methodology, results and discussion and conclusions including future work. In the introduction the skin histology and physiology are described, as well as the different types of drug for skin as administration route; also PSO is exhaustively detailed through its epidemiology, clinical and histopathology features and, its pathogenesis and genetics basis as well the traditional treatment according to class of drugs and administration routes. A particular focus will be given to skin as administration route for PSO, with respect to the uses of lipid nanoparticles, novel therapeutic approaches for PSO in general and the features of lipid nanoparticles in particular were mentioned. After the methodology section where the theoretical principals and experimental details for each method are described, the results of this dissertation are detailed and discussed.

Within the results section two parts are described, at first the application of formulation design approach to optimize the production of NLCs loaded with MTX, including their

physico-chemical properties and biological safety. The second part of the results section focus two therapeutic strategies for PSO: a topical therapy based on a hydrogel enriched with lipid nanoparticles and a targeted combined therapy using etanercept and MTX. The developed delivery systems were characterized and investigated with regard to physical (size, charge, morphology, storage stability), chemical (drug loading, *in vitro* drug release), biological (*in vitro* cytotoxicity and skin permeation profile) and rheological properties. All of the results and main conclusions obtained were exposed in next sections.

Chapter 2- Introduction and State of art

2.1 Psoriasis

2.1.1 Epidemiology of psoriasis

Originally, this disorder thought to be associated with abnormal differentiation and hyperproliferation of epidermal keratinocytes (KC), but now is known as one of the commonest immune-mediated disorders [1]–[3].

Around 2-3% of the world's population live with PSO and the prevalence appearing to be relatively highest in Scandinavian countries (8.5% in Norway), Northern Europe, American and Canadian populations (4.6 and 4.7%, respectively) [4]–[8]. The prevalence varies substantially between countries and appears to be relatively frequent in countries of higher latitude [9].

Studies of monozygotic twins propose a 70% possibility of a twin developing PSO if the other twin has the disease. These findings suggest both a genetic predisposition and an environmental response in developing PSO [23–25]. Though, PSO can be transmitted genetically it does not spread from one person to another by contact [14, 25, 26].

PSO affects people of all ages but occurs most usually in the third decade of life (a peak between 15 and 30 years) and another peak between 50 and 60 years [20, 24, 27], [28]. Children are rarely affected [14, 25]. Psoriatic arthritis (PSA) is a chronic inflammatory type of arthritis associated with PSO, usually seronegative for rheumatoid factor [24, 29, 30]. Its pain, stiffness and swelling in and around the joints and the sites where tendons and ligaments attach to bone [17].

2.1.2 Clinical features of psoriasis

In early-onset of PSO, developing before the age of 40 years, genetic and environmental factors have a crucial role. The triggers include emotional stress, skin injury, systemic infections, among others [14, 17]. PSO can be an enormously disabling disease which could impact significantly on a patient's quality of life (QoL) [4].

The common type of PSO is called PSO vulgaris or large plaque PSO and is caused by unsuitable activation of the cellular immune system [15, 22, 27, 31]. PSO is a papulosquamous disease with formation of erythematous, inflamed and raised plaques that are well-demarcated in the region of normal skin [14, 15]. The plaques are red or salmon pink in colour, covered by grey or silvery-white, dry scales and could be thick and have few or more millimeters [15, 24]. Plaques are frequently dispersed symmetrically and take place in any part of the body (Figure 2.1) on the extensor aspects of elbows and knees; scalp, where they not often invade beyond the hairline, lumbosacral region, and umbilicus [15, 24].

Figure 2.1 - Psoriasis vulgaris localizations. Adapted from [19], [20].

PSO vulgaris to be associated with phenotypically and genotypically distinct conditions, which might account for the variability of response to therapy, mainly with the T-cell targeted biological agents [2].

Occasionally PSO may involve the oral mucosa or the tongue and when that happens, the dorsal surface may have stridently gyrate red patches with a white -yellow border [11].

In addition, diverse forms of PSO may be limited to a small or extensive area. Further, PSO may have a variable course exhibiting as chronic, stable plaques or can present acutely, with a rapid progression and widespread [11].

Regardless of advances in our understanding of the pathogenesis of PSO, there have been no large, representative, prospective and longitudinal studies about the natural history of the disease, mainly predictors of disease severity [15, 22].

2.1.3 Histopathology of psoriasis

The characteristic histological features can be traced to specific immunological responses and will be listed:

- Hyperproliferation of basal KC gives rise to acanthosis, thickening of the epidermis resulting from augmented numbers of acanthocytes (‘prickle cells’). This thickening occurs in ridges, with surrounding areas of thinning taked by elongated dermal papillae, and elongation of the epidermal rate ridges (papillomatosis). Hyperproliferation is accompanied by incomplete differentiation and maturation so that the cells are shed abnormally in large clumps. In addition, the loss of the granular layer (hypogranulosis) [20, 34].

- The thickening of the epidermis and the connected silvery scale are due to premature KC maturation and succeeding incomplete cornification, which result in retention of nuclei inside the cells of the *stratum corneum* (SC) (parakeratosis) [7].
- Dilatation and elongation of capillaries occurs induced by angiogenic factors [such as vascular endothelial growth factor (VEGF)]. Auspitz sign is a typical finding in PSO and it is relates to the manifestation of small bleeding points following consecutive layers of scale from the surface of psoriatic papules or plaques. These reach the top of the dermal papillae and almost enter to the surface of the skin [20, 34, 35].
- Infiltration of the dermis and epidermis by neutrophils, lymphocytes, macrophages and dendritic antigen presenting cells (APCs). The neutrophils frequently form cumulations termed 'microabscesses of Munro' (in the *SC*) or 'micropustules of Kogoj' (in the upper epidermis) [21].

2.1.4 Pathogenesis of psoriasis

An insight of the molecular mechanisms associated with pathogenesis of PSO gives crucial importance to the interaction between acquired and innate immunity [23]. Both clinical and fundamental investigation specify that the cellular innate and adaptive immunological responses, in particularly the activation of T cells, play a crucial role in the pathogenesis of PSO [24].

The activation of T-cells is necessary upon its binding with the APCs. This process is mediated through surface molecules used for adhesion, counting leukocyte function connected with antigen lymphocyte function-associated (LFA)-1 and cluster of differentiation (CD2) on the T cells and, intercellular adhesion molecule (ICAM)-1, and LFA-3 on the APCs [25]. T-cell receptor is specific for T-cell acknowledge an antigen existing on the histocompatibility complex (MHC I or II) by the APC Figure 2.2. Activated T cells propagate and go in the circulation via trafficking through the interaction between LFA-1 and ICAM-1.

Then, extravasate via diapedesis through the endothelium at place of inflammation in the skin [26]. The activation of intracellular signal transduction pathways and production of cytokines/chemokines plays a vital position in reinforcing the inflammatory immune process as it transports lymphocytes to the site of inflammation and disrupt their proliferation [18].

Antimicrobial peptides (AMPs) are a significant constituent of the innate immune system and play a main role in the homeostasis of surface organs such as the skin. The overexpression of AMPs is a feature of PSO and can be exposed as a sign of activation of the innate immune system [23].

The elevated production of VEGF by KC, activated T cells and endothelial cells is persuaded by cytokines such tumor growth factor-α (TGF-α), interferon (IFN-γ) and tumor necrosis factor-α (TNF-α) and the neutrophils that are found in great number, increasing vascular permeability [26].

In the beginning of the disease, there are a significant quantity of macrophages, followed by cells such monocytes, lymphocytes, granulocytes in epidermis, as illustrated on Figure 2.2 [37, 39]. Histological features leading to the development of clusters of cells

are composed by dendritic cells (DC) and $CD4^+$ T cells in the dermis or $CD8^+$ T in the epidermis [37,40]. DCs generate cytokines TNF-α, IFN-γ and interleukin IL-23 (heterodimeric cytokine draw up of a single IL-23p19 subunit coupled with a common IL-12p40 subunit, which is shared with IL-12) and are able to establish inflammation and possibly stabilize the phenotype of T helper cells (Th-17). This may occur throughout mechanisms dependent on the transcription factor STAT3, mediating Th17 terminal effector functions, IL-22 motivate the development of specific subclasses of T cells (Th1, Th17, Th22) and pro-inflammatory [20, 31, 36, 41, 42].

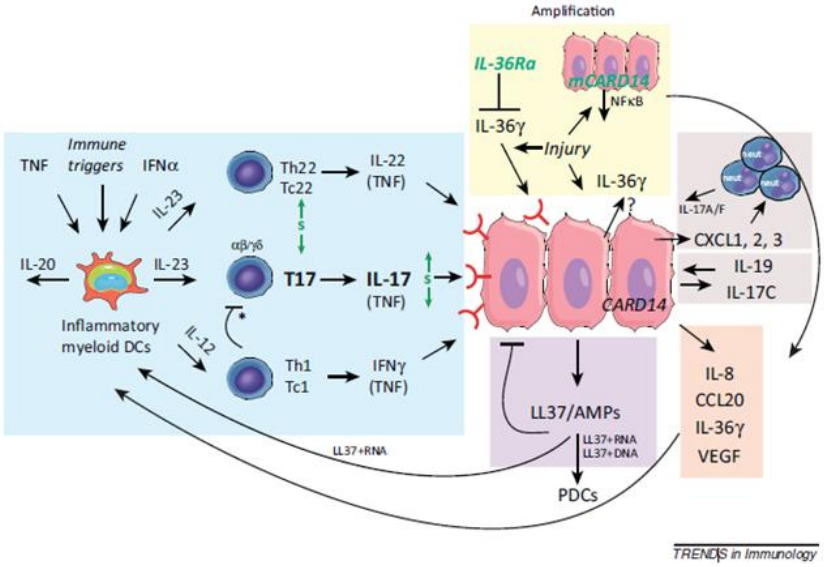

Figure 2.2 - Representation of psoriasis pathogenesis. Adapted from [29]

IL-22 induces hyperproliferation of KC and both IL-17 and IL-22 persuade activation and to the production of AMPs that leads to activation of the immune system and plentiful cytokines and inflammatory mediators persist in psoriatic skin lesions (e.g. IL 8/chemokine CXC ligand (CXCL)8, monocyte chemotactic protein (MCP)-1/chemokine CC ligand (CCL)2, CXCL1, CXCL2, and CXCL3, and CCL20)[31, 41, 43]. These chemokines attract leukocytes such as neutrophils, DCs, chemokine CC receptor (CCR)6+ and also CXCL9, CXCL10 and CXCL11. IFNγ is released throughout Th1 cells and a subset of Th17 cells and plays a vital role in the maintenance phase of PSO, additional activating myeloid DCs and amplifying response circuits [29].

There are others cytokines (e.g. IL-22, IL-19, IL-20 and KC-derived IL-36) that induce epidermal proliferation [29]. Indeed, KC products influence immune activation and induce of new adhesion molecules for T cells [44, 45].

An unregulated function of resident skin cells such as fibroblasts and endothelial cells may possibly also supply to the pathogenesis of PSO [32].

Mutations in epidermal CARD14 (mCARD14) in familial PSO may amplify endogenous activation in response to a trigger, inducing abundant cytokine and chemokine production (such as IL-8, CCL20, and IL-36) [29].

2.1.5 Clinical types of psoriasis

The clinical phenotypes of PSO, illustrated on Figure 2.3, have been sorted based on a variety of features such as: age of onset, degree of skin involvement, morphologic pattern and predominant involvement of specific anatomic location of the body [34]. Following, are described the main diagnostic features of four clinical phenotypes:

Type I - Plaque or vulgaris psoriasis

The plaque PSO is the most frequent form [1]. Patients have sharply well-delineated, round/oval or nummular (coin-sized), scaly and dry plaques (Figure 2.3 a,b). The lesions may at first begin as erythematous macules or papules, extend peripherally, in a fairly symmetrical distribution [34, 46]. The rupioid and ostraceous notions speak about to morphological subtypes of plaque PSO meaning small plaques and ostraceous PSO refers to hyperkeratotic plaques with relatively concave centres [11].

The quantity of scaling varies among patients and even at different sites and their removal may expose tiny bleeding points (Auspitz sign) [34]. The lesions can emerge at any part of body but the majority sites are elbows and knees [24, 46].

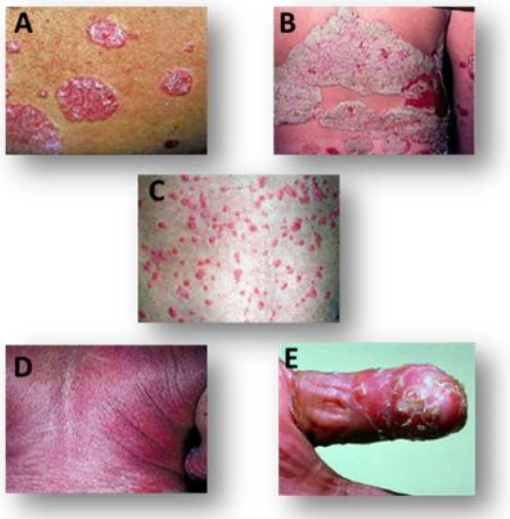

Figure 2.3- Images of types of psoriasis. A) small plaque psoriasis; B) large plaque psoriasis; C) guttate psoriasis; D) erythodermic psoriasis; E) pustular psoriasis. Adapted from [49, 50]

Type II - Guttate psoriasis

Guttate PSO Figure 2.3 c , from the Greek word *gutta* meaning a droplet [1]. It appears on as small diameter lesions of PSO and affects specially children and adolescents, under a streptococcal infection of the pharynx or tonsils or the upper respiratory infection [24, 46]. These are usually distributed in a centripetal away but can also involve the head and limbs. Sometimes lesions form on scalp, face and ears [24, 47].

This type of PSO accounts for 2% of the overall cases of PSO. In children, an acute episode of guttate PSO is usually self-limiting but in adults, these events may development to chronic plaque disease. One small study exposed that 33% of patients with acute guttate PSO perhaps developed chronic plaque disease. In other words, patients have a significantly higher risk for developing plaque PSO in the future. As a result, this form co-exist with other forms of PSO [24, 46, 47].

III - Erythroderma

This type involve almost the skin with active PSO [24, 46] as shown on Fugure 2.3 d. Firstly, chronic plaque PSO may gradually progress as plaques resulting in an exacerbation of instability of this plaques [14, 46]. Secondly, erythroderma may be a manifestation of a withdrawal of a systemic medication [34]. Erythroderma may harm the thermoregulatory capacity of the skin, metabolic changes including hypoalbuminaemia, high output cardiac failure and anaemia due to loss of iron, vitamin B12, and folate [11].

IV- Pustular psoriasis

This form is rare and this events may occur randomly on any part of the body when the collections of neutrophils are great enough to be evident clinically, it is termed 'pustular PSO', as illustrated on Figure 2.3 e [46, 48]. There are two main forms: generalized pustular PSO (*Vom Zumbusch*) and localized pustular PSO. Both types lead to red, painful and inflamed skin with a multiple pustules in a erythematous base [24, 46]. Generalized pustular PSO (*von Zumbusch*) is rare and represents active and unstable disease [11]. Patients with this type frequently need to be admitted to the hospital for management and close monitoring. Localized pustular PSO that admits *acrodermatitis continua of Hallopeau* is characterized by eruption of the fingers and toes and, palmoplantar pustulosis manifests as pustules on palms and soles. Plaque formation is not characteristically seen in this type [34].

Phenotypes of psoriasis in accordance with involvement of anatomical region

PSO can also be classified according to the affected anatomical sites, as illlustrated in Figure 2.4, and can be classified in five types:

- **Palmoplantar pustulosis:** is presented as thick and yellow pustules on a background of erythema and scaling have an effect on the palms and/or soles, Figure 2.4 a[24, 46] .
- **Psoriatic nail disease:** occurs approximately in 15% to 53% of Pso patients and, up to 10% announce with only nail manifestations with no other manifestations [49, 50]. Fingernails are more usually affected than toenails (Figure 2.4 b). The frequent finding are small pits in the nail plate, onycholysis, oil spots (orange-yellow areas), hyperkeratosis [46, 49], 50]. In addition, the site around nail plate may become, thickened, dystrophic, and yellowish-brown nail discoloration[46, 50] .
- **Flexural (inverse) psoriasis**: affects 2% to 7% of patients with PSO and has repercussions on flexures, particularly inframammary, genitalia, and axillary (Figure 2.4 c). In other words, there are intertriginous involvement whilst plaque PSO affects trunk and limbs [46, 49, 50]. In general, this type of lesions are deprived of scale and appear as smooth, red, shiny, well demarcated plaques occasionally confused with candidal, intertrigo, and dermatophyte infections.
- **Scalp psoriasis:** is one of the most frequent site with manifestation of plaque PSO (Figure 2.4 d) and may be present in up to 79% of patients with PSO [49, 50]. The lesions are typically sharply demarcated, asymmetrical and sometimes advanced beyond hair border on the face, neck or auricular regions [38]. It is

linked with seborrheic dermatitis and is difficult to distinguish from scalp PSO [38].

- **Genital psoriasis:** occur in all age groups from infants to the elderly. Nearly one-third of patients with PSO suffer from genital PSO [34].

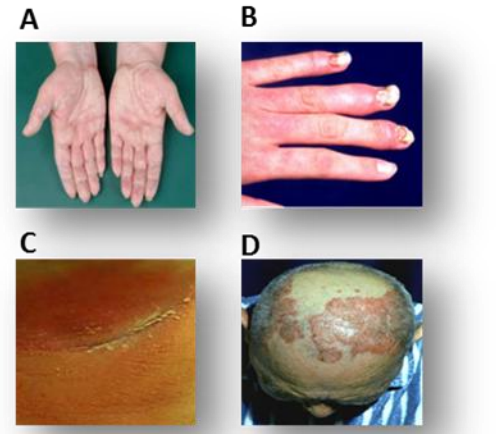

Figure 2.4 - Images of psoriasis classified in accordance with involvement of anatomical region. A) palmoplantar; B) psoriatic nail disease; C) flexural (inverse) psoriasis; D) scalp psoriasis**.** Adapted from [51, [2]

2.2 Treatment and drugs applied in psoriasis

Most patients are mildly affected by PSO and can be treated effectively with topical medication, but 10–20% of patients have moderate-to-severe disease and need a systemic treatment or phototherapy [16, 53]. Also, in patients with moderate-to-severe PSO, combination therapy is frequently [42].

The selection of an adequate therapy depends on several factors: extent of body surface area and severity, patient predilection, practitioner experience, characterization of PSO phenotype, genotype, co-morbidities and the risk of adverse events from therapies [17, 45, 53].

2.2.1 Topical therapies

First-line management of adult mild-to-moderate PSO is with topical treatment, listed on Table 2.1[17, 40, 55, 56].This kind of treatment have a favorable risk/benefit profile when used and is very efficient against itching [23]. Tar has been used on PSO for a long time. **Coal** tar is the mainly form used and is a product obtained of coal distillation containing more than 10,000 compounds. Its effect is probably throughout DNA suppression [45]. The accurate effectiveness of anthralin is complicated to establish**,** but it is known to inhibit human monocytes resulting in a decrease production of cytokines [46]. Furthermore, anthralin is often used in combination with phototherapy (ultraviolet B) [45]. **Retinoids** have proved to be useful in modulating KC proliferation and in reducing inflammation.

These compounds have been used as oral treatment for PSO for a long time, but recent innovations lead to development of a topical formulation based in tazarotene [47]. This agent is thought to perform at the gene level, via retinoic acid receptors, which mediate KC proliferation and differentiation and, their use is likely to increase over time due to their capability to induce long remission periods [45]. **Calcineurin inhibitors** have a role in the management of PSO associated with the activation of T-lymphocytes binding to intracellular proteins and blocking the effect of calcineurin. This leads to a reduced production of interleukin-2 and reduced proliferation of T-cells [60, 61]. **Topical corticosteroids** (steroids) form the base of therapy for PSO due to their anti-inflammatory (dermal) effects, with high potency steroids being the most efficacious [52, 62]. They stimulate or inhibit of genes involved in inflammatory pathways, including inhibition of cytokine production and reduction in inflammatory mediators [51]. There is a scale, ranging from class 1 (highest potency) to class 7 with efficacy rates ranging from 41- 92% [51, 55]. Topical corticoids should not be used over extended periods (more than 6 weeks constantly) without disruption due to it typical corticoid side effects such local cutaneous like skin atrophy [36, 51]. **Vitamin D analogues** (calcipotriol, calcitriol, tacalcitol) have come into broad use recently. They restrain KC growth, support their differentiation, and reduce inflammation in psoriatic lesions via vitamin D receptors on KC and T lymphocytes [45]. These, too, have a positive risk/benefit profile. Although they are a little less efficient than elevated potency corticosteroids [23].

In resume, corticosteroids stay essential to PSO treatment, but vitamin D derivatives are important to be used either in conjunction with steroids or alone, due to their antiproliferative (epidermal) effects [56, 57]. The combination of medications is maybe the most promising topical treatment with amplified efficacy and less side effects [57, 63].

The principle of blending two drugs may be prosperous, but not all combinations offer positive or synergistic effects [48].

Table 2.1 - Current treatment options for psoriasis

Class	Examples of agents	Mode of action	Side effects	Refs
Vitamin D analogue	Calcipotriol	Reduce production of pro-inflammatory cytokines	Pruritus, burning, sharp pain, erythema	[60, [63]
	Calcitriol	-	Anorexia, headache, sweting, polyuria and hypercalmia	[50]
Keratolytic agents	Salicylic acid	Reduce the intercellular bonding of corneocytes and the SC pH	Skin irritation, stinging in the applied area, headache, fast breading, ringing in ears	[52]
	Urea	Dissolves intercellular matrix	Severe skin irritation, mild stinging, itching and skin rash	[55, [65]
	Omega 3 fatty acid	Inhibition of lymphoproliferation and T-cells immune responses; prevents production of pro-inflammatory cytokines	Rash, itching, wheezing, difficult breading or swallowing	[54]
Calcineurin inhibitors	Tacrolimus	Inhibition of T-cell activation by the calcineurin pathway and inhibition of the release of numerous inflammatory cytokines	Burning or itching sensation, flu-like symptoms and headache	[48]
	Pimecrolimus	Similar to tracolimus but more selective, with no effect on dendritic (Langerhans) cells	Burning, soreness of treated skin, swelling of lips, face, tongue and throat.	[55]
Hydroxyanthrone	Dithranol	interferes with mithocondrial supply of energy to the cell and DNA replication	Skin irritation, burning, itching, bron discoloration of diseased skin	[46]
Coal	Coal tars	Suppression of hyperplastic skin	Staining, irritation and carcinogenic risk	[53]
Retinoids	Tazarotene	Decrease of inflammation in the epidermis and dermis	Pruritus, burning sensation, erythema, irritation and dried skin.	[59, 60]
	Acitretin	Modulates mitotic activity and differentiation of KC	Vitamin A toxicity (xerosis, alopecia, bleeds, skin fragility)	[12, 68]
Corticosteroids	bethamethasone diproprionate	Control cellular proteins leading to a broad range of anti-inflammatory, immunosuppressant and vasoconstriction actions.	Skin infections, perioral dermatitis, skin atrophy and hypertrichosis.	[52, 55]
	fluocinolone acetonide		Skin thinning, striae, skin atro-	[58]

			phy, itching, irritation, purpura and hypertrichosis.	
	prednicarbate	Down regulation of IL-1¤, inhibiting cytokines in KC.	Burning sensation, itching, rash, reddening of skin and folliculitis.	[60, 69]
	flurandrenoline	Act on phospholipase A2 inhibitory proteins. It will inhibit arachidonic acid and regulate biosynthesis of inflammation.	Polyuria, polyphasia, weight gain, gastro-intestinal ulceration, pancreatitis, osteoporosis and hyperglycemia.	[60]
	bethamethasone valerate		Irritation, dryness, folliculitis, striae, hypertrichosis, acneiform eruptions and perioral dermatitis.	[52, 55]

Adapted from [8, 12, 51, 52, 55, 57–60, 62, 63, 66–72].

2.2.2 Systemic therapy

Systemic therapy, listed on Table 2.2, should be considered when topical treatments fail in a clinical benefit and in patients with widespread cutaneous disease. In other words patients with moderate-to-severe PSO and/or related PSA [36, 40, 73]. This therapy can be complex compared with topical therapy by severe side-effects and their use demands a precise monitoring of patients [28]. So far, the systemic agents available for the treatment of PSO includes retinoids (acitretin), cyclosporine A (CyA) and MTX [57].

Oral retinoids such acitretin are a group of natural and synthetic derivatives of vitamin A, and have been advanced for the treatment of PSO since the early 1980s. Acitretin due to low efficacy and frequent side effects, is presently given almost exclusively in association with UV therapy, but this monotherapy with this drug can be efficient against pustular PSO [23]. Unpleasant reactions to retinoid such as teratogenicity, mucocutaneous effects and lipid changes have received much attention. Another side-effect interrelated to retinoid is skeletal toxicity [57]. Topical management of acitretin help to control the multiplication of cells, including the speed at which skin cells will grow and may decrease the risk of systemic toxicity as growing local bioavailability in the skin [64].

CyA is an oral calcineurin inhibitor accepted for the treatment of plaque PSO since early 1990s. It suppresses the immune system and stops the activity of certain immune cells [65]. It is tremendously useful and thus appropriate for induction therapy, though not for long-term maintenance therapy due to the risk of irreparable renal crash and also because of the eminent risk of skin cancer in patients who have before undergone phototherapy [42], [65]. CyA is normally used as a rescue drug or binding agent [66].

Table 2. 2- Available systemic treatment options for psoriasis (Adapted from [47-61])

Class	Examples of agents	Mode of action	Side effects	Refs
Non-biologics	Cyclosporine (CyA)	Inhibits activity of phosphatase of calcium-calmodulin-calcineurin complex and promotes translocation of NFAT.	Renal and liver failure, hypertension, nausea, vomiting, diarrhea, hypertrichosis and tremor.	[47, 48]
	MTX	Folic acid antagonist that causes competitive inhibition of the enzyme dihydrofolate reductase.	Liver fibrosis/ cirrhosis, bone marrow depression, renal damage, necrosis of soft tissue and bone.	[49, 50]
Biologics	Efalizumab	Prevents interaction of T-cell with endothelial cells and KC, movement of T-cell from the blood vessels into the tissue and activation of T-cell.	Flu-like reactions, leukocytosis, lymphocytosis and arthralgia.	[51, 52]
	Alefacept	Interact with CD2 on T-cells and interferes with T-cell activation.	Decrease in CD4+ T cells, itching, nausea, muscle aches and allergies risk of infections.	[53, 54]
	Infliximab	Bind both to soluble and membrane-bound TNF-α	Infusion reactions, severe infections and progression of heart failure.	[55, 56]
	Etanercept	Interacts with soluble TNF-α and blocks the cascade of inflammation stimulated by TNF-α.	Infections, local reactions, sore throat, headache, hair loss, and rash.	[57]
	Adalimumab	Binds with high affinity to soluble and membrane-bound TNF-α.	Locally: swelling, redness, pain and itching and shortness of breath.	[58, 59]
	Ustekinumab	Bind p40 subunit of IL-12 and IL-23 and prevents their interaction with the corresponding receptors.	pharmacokinetics are strongly affected by body weight	[60, 61]

MTX, the oldest systemic therapy for PSO, still remains one of the most successful treatments for PSO and PSA. MTX is a folate antagonist that competitively bind to dihydrofolatereductase hampering cell growth and arresting cell cycle in G1/S phases and has been used in the clinics since the fifteens for the treatment of different solid tumours (e.g. osteosarcoma, lung and breast cancer) [67] and in the therapy of autoimmune and inflammatory diseases as rheumatoid arthritis (RA) and PSO [12, 13]. It acts by suppressing the immune system and thereby stopping the inflammatory response that can direct to PSO and psoriatic flares [77–79]. MTX is one of the most effective therapeutic agents with a triple mode of action: it is anti-inflammatory, reduces cell proliferation and it is immunosuppressant. It is accessible to treat a variety of malignancies, such as osteosarcoma, non-Hodgkin's lymphoma, lymphocytic leukemia, choriocarcinoma, and head, neck, and breast cancers. MTX is also used against non-neoplastic conditions such as severe PSO and autoimmune diseases such RA [13, 79, 80]. It has some short-term side effects including bone marrow toxicity, nausea, aphthous stomatitis, and development of megaloblastic anaemia. Liver toxicity is the main limiting factor of MTX treatment in PSO. The incidence

of liver toxicity including liver fibrosis varies considerably depending on underlying risk factors [77, 80].

2.2.3 Biologic therapy in systemic therapy

A major expansion of the therapeutic efficiency against PSO has arrive with the approval of a number of "biologics" which have a good benefit-risk profile overall and are also successful in patients who cannot be treated satisfactorily with the systemic therapies available till now [73]. As of 2010, seven biologic drugs have obtained a food and drug administration (FDA) approval for the treatment of PSO and/or PSA [66]. **Biologics** are, by definition, genetically or biotechnologically generated products of living cells. They can be cytokines, fusion proteins composed of surface molecules, T cells or monoclonal antibodies towards the CD11 a subunit of LFA-1 (eg. efalizumab), or the p40 subunit of IL-12 /IL-23 (eg. ustekinumab) or to TNF-α (eg. adalimamub, infliximab and etanercept). Monoclonal antibodies therapy will compensate the disequilibrium of the inadequately regulated immune system, leading to improvement of the clinical manifestations and block specific molecular steps in the inflammatory cascade, thereby reducing activation and proliferation of KC [36, 81–83].

TNF-α inhibitors differ in mechanism of action and structure [40,81–84]. **Adalimumab** is a human monoclonal antibody to TNF-α and functions in the same way as infliximab. **Infliximab** is a chimeric mouse-human monoclonal antibody to TNF-α that can bind both soluble and membrane-bound TNF-α and successfully neutralize its activity [81, 82, 84]. **Etanercept** is a neutralizing recombinant soluble TNF-α receptor (human p75 TNF-receptor Fc fusion protein) and binds free TNF-α and lymphotoxin [40, 81, 83, 84].

The effectiveness of etanercept in the treatment of PSO is comparable to that of the antibodies [40]. **Golimumab**, a new anti-(human TNF-α) antibody, has already been used with success in patients with PSO [40]. The most common side effects included upper respiratory infections, nasopharyngitis, and headache [83, 85]. **Certolizumab,** a humanized antibody, TNF-α blocker that is effective in other immune-mediated diseases, such RA [40, 83]. Due to the considerable cost and risks related with TNF- α inhibitor therapy, these agents can only be used in patients with general skin disease or in patients with inadequate skin disease unresponsive to topical and/or targeted phototherapy [40, 82]. Despite this, it is likely that the therapeutic profit of TNF-α inhibitors is due not only to the obstruction of the soluble cytokine, but also to the neutralization of membrane bound TNF-α [40]. Recently, there are antibodies (anti-TNF-α) that may also act on the central IL-23–Th17 axis [40].

Efalizumab, is an antibody against the cell-surface adhesion molecule LFA-1 present on the T-cell surface, and inhibits the migration of inflammatory cells into the skin. It is effective only against PSO vulgaris. Successful treatment is accomplished after six months in about 40% of patients, but some patients can also profit from long-term therapy [36, 40]. Despite this, in 2009 it has been obliterated from the market due to progressive multifocal leukoencephalopathy [86, 87].

Alefacept is a fully human LFA3–IgG1 fusion protein that targets CD2 and inhibits T-cell activation and proliferation. Alefacept also promotes apoptosis of memory T-cells [40, 83]. It was the first FDA sanctioned biologic agent for the treatment of PSO [83].

Ustekinumab, a IL-12/23 inhibitor, is a human monoclonal antibody towards the p40 subunit, which is shared by both IL-12 and IL-23 cytok¬ines [82]. Furthermore, treatment was effective for at least 1 year while ustekinumab was administered every 12 weeks [40].

Briakinumab (ABT-874), human monoclonal antibody against the p40 subunit of IL-12 , has not received FDA approval as of yet, but has been studied in one clinical trial [40], [83].

Biological agents are listed on Table 2.2 are costly and demonstrate immunosuppressant activity, and are presently indicated for patients powerless to benefit from first- and second-line modalities [82, 83].

2.2.4 Phototherapy

For moderate-severe PSO or no respond to topical treatment alone, the application of ultraviolet light (UV) is suitable for inducing a remission but not for maintenance therapy, because its extended use is related with an elevated risk of skin cancer [12, 85]. UV radiation is broadly classified into three major spectrum ranges: UVA (320-400 nm), UVB (280-320 nm), and UVC (280-100 nm) [77]. At present, the most commonly used type of phototherapy is with the narrow-spectrum UV-B therapy. The application of narrow band (NB)-UVB has been possible on a widespread basis [17, 36].

Table 2.3- Phototerapy used in systemic treatment (Adapted from [7], [54], [71], [85])

Photo-therapy	Advantages	Disadvantages	Refs
PUVA	• Thick psoriatic plaques and nail disease • Involvement of palms and soles since • Failure to responds to UVB phototherapy	• Skin cancer risk occurs after prolonged photo-therapy with PUVA • Patient inconvenience • Higher running costs • Personal or family histo-ry of melanoma is an absolute contraindica-tion	[12, 71, 85]
NB-UVB	• Less risk than PUVA • Rapid and easy clear-ance on exposure to sunlight • effective, safe • Young age • Contemplates/reports pregnancy or lacta-tion.	• Daily treatment is not better • Personal or family histo-ry of melanoma is a rel-ative contraindication to UVB	

The application of PUVA: UVA radiation after the administration of a photosensitizer (psoralen) by the oral route or as a cream is highly effective although is difficult to deliver [23]. The efficacy of PUVA therapy in PSO and some other diseases has evidently been recognized, both as a clearance and as a maintenance treatment and, it can be improved in

combination with other treatments such as CyA plus PUVA and retinoid plus PUVA [12, 85]. Also, a combination of PUVA and MTX can decrease the duration of treatment, yet maintains its efficacy [77].

The advantages and disadvantages of phototherapy are described in Table 2.3. The application of systemic treatment and phototherapy is limited to treating severe PSO due to the carcinogenicity and their toxicity [54, 85].

The mode of action of each treatment applicable in phototherapy are shown in Table 2.4. Taking into account some factors such as relative efficacy, costs, availability, and side effects, phototherapy in general, and the NB-UV therapy, seems to suggest the best therapeutic option for patients affected with moderate to severe PSO [77].

Table 2.4 - Current treatment options for psoriasis phototherapy.

Agent	Mode of action	Refs
Ultraviolet B (UV-B)	Interaction between UV-B and DNA, generating pyrimidine dimers result in the inhibition of DNA synthesis. Reduce proliferation of lymphocytes and KC.	[12,85]
UV-A plus psoralen (PUVA)	Upon UV-A activation psoralen combine with DNA leading to the inhibition of DNA synthesis. Prevents cell hyperproliferation.	[12, 71, 85]
Methoxsalen	UV radiation activates methoxsalen to bind DNA inhibiting the DNA synthesis.	[78]

2.3 Skin as barrier and administration route

2.3.1 Histology of skin

Skin plays a vital role in maintaining homeostasis, defending against the invasion of microorganisms and providing protection from environmental attacks such as heat, chemicals and toxins [79]. The skin is the largest and the most versatile organ of our body making up 16% of body weight, with a surface area of 1.8 m^2 and direct contact with external environment [80]. The skin consists of three different layers: **epidermis, dermis and hypodermis/subcutis** as represented on **figure 2.5** [89, 90]**.** Usually, epidermis and dermis are considered more important from a penetration perspective [88, 89].

The epidermis is the outer layer, nonvascular and made of stratified squamous keratinized epithelium which synthesis the protein keratin [81]. The separate layers of the epidermis are formed by the differing stages of keratin maturation. These layers are ordered in five different strata (*stratum basale or* germinative (in contact with dermis), *stratum spinosum* or princkle cell layer, *stratum granulosum* or granular cell layer, *stratum lucidum or* horny layer and *stratum corneum* in contact with the external environment) as represented on Figure 2.6. So, epidermis is histologically classified as a stratified epithelial layer [88, 90].

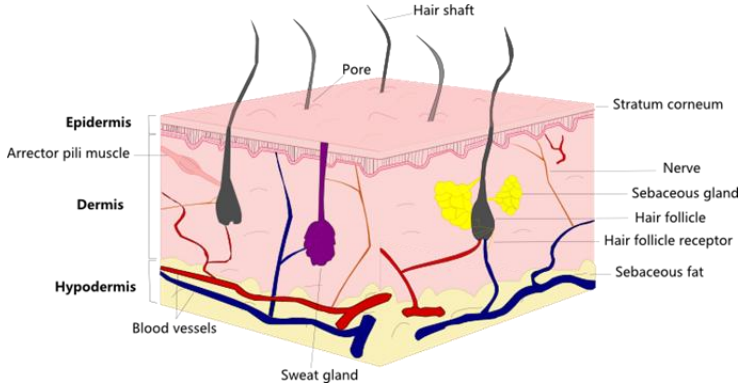

Figure 2.5 - Schematic representation of normal skin structure.

SC, the outermost portion of the epidermis is the main penetration barrier that protects the body from extreme water loss and damage due to toxic agents and microorganisms from the environment and which cells are embedded in highly ordered lipid layers [89–91]. *SC* is a lipophilic layer and contains ≈ 13% of water and it hydration is vital to keep away from mechanical collapse. Regulation is essential and guarantees preservation of *SC* enzyme activities [88,90, 92].

There are four categories of intercorneocyte lipids namely cholesterol and its derivatives, ceramides, free fatty acids and triglycerides [85]. Skin may also enclose aqueous pores that supply to the transdermal route of skin absorption [88, 89]. The barrier function provided of *SC* layer that is composed of corneocytes and intercellular lamellar lipid bilayers [86]. Under the epidermis is the vascular dermis, described by dense irregular connective tissue and responsible for the strength and flexibility of the skin. It contains nerves endings, sweat glands, hair follicles and blood vessels and its accountable to carry nutrients and oxygen to the epidermis, and as well clear the dermis from cell metabolic products and penetrated foreign agents [89, 90].

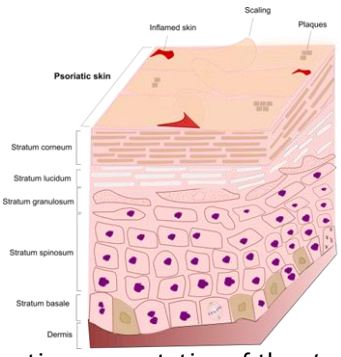

Figure 2.6 - Schematic representation of the *stratum corneum* structure.

Underneath the dermis is the **hypodermis or subcutis** (fat) layer of connective tissue composed of loose textured, white, fibrous connective tissue in which fat and elastic fibers are combined, that include two layers separated by a superficial fascia: the areolar layer, composed with large adipocytes arranged vertically and closest to the dermis and, the lamellar layer, a deeper layer, where the cells are smaller and arranged horizontally and the blood vessels are larger [87].

The histology of skin is analogous in dissimilar regions of the body, except in the thickness of the epidermis. Also present in the skin are sebaceous glands, sweat glands and hair follicles, closer to the connective tissue [88, 89]. It was not until 1960s–1970s that the scientists reached the accord that:

- *SC* is one of the most rate-limiting barrier against percutaneous drug penetration;
- Particular content, composition, and structure of the SC lipids hold selectively and efficiently the penetration of chemicals [86].

2.3.2 Skin for drug delivery

Drug delivery through skin can be separated into topical delivery, transdermal delivery and subcutaneous injection represented in Table 2.5 [79]. Skin is recognized as an attractive site for systemic drug delivery due to its large surface area, access convenience, and possibility of avoiding first pass metabolism in gastrointestinal tract and the liver [79]. The permeation barrier properties offered by human skin remains challenging as delivery routes for drugs and other compounds into the skin strata (topical delivery) and/or to the systemic exposure (transdermal delivery) [94, 96].

Topical delivery is mainly used for achieving local effect and several examples exist of its utility in the critically ill [79]. A drug can be directly applied to the skin for treatment of several dermatological diseases through several formulations such as gels, lotions, creams, foams, and ointments. Is can also be used for local anesthesia, local infection management and photodynamic therapy. These topically delivered drugs should reach the viable epidermis or dermis to take effect [79]. For optimum topical delivery of drugs into the skin, it is necessary that the carrier releases the encapsulated drug in the skin or mucous membrane, which can be additionally absorbed through the skin layers and through sub skin structures that are implicated in disease [87].

Transdermal drug delivery aims to deliver drugs through the skin to achieve systemic effect [89]. Offers an attractive non-invasive alternative and could be achieved through this route, possibly decreasing drug side effects and improving efficacy. Other advantages of this route drug delivery include ease of drug application and therapy cessation. Further, greater duration of action is seen for drugs with a short elimination half-life given transdermally [87, 97].

Subcutaneous drugs injected into the fatty subcutaneous tissue pass the epidermal and dermal layers of the skin and achieve the systemic circulation through capillaries or the lymphatic system depending on the drug molecular weight. Absorption of various drugs

through this way can be affected by formulation properties such injection volume, local degradation, viscosity and pH, formulation excipients and cellular uptake [79]. Theoretically, in this way a drug is applied in a moderately high dosage to the inside of a patch for an extensive period of time. Through a diffusion process, the drug go into the bloodstream directly through the skin [90].

Table 2.5 - Skin administration routes (topical, transdermal and subcutaneous) – formulation and applications (Adapted from [79])

	Topical	Transdermal	Subcutaneous
Skin layer	Epidermis or dermis	Viable epidermis or dermis	Subcutis (hypodermis)
Delivery mode	Local	Systemic	Systemic
Formulation	Gels, lotions, creams, foams, and ointments	Patches, gels, metered dose spray, and ointment	Solution
Medication	Treatment of skin disease Local anaesthesia Management of local infection Photodynamic therapy	Analgesia; smoking cessation; cardiovascular disease; Hormone replacement therapy	Growth hormones Insulin Epinephrine
Limitation	Local effects	Skin permeability	Limited injection volume

Compared to the other administration routes such as oral or intravenous, these delivery approaches, topical and transdermal, have the exceptional advantages namely [86]:

- for dermatological diseases, topical drug deliveries approaches directly deliver therapeutic agents into place of the diseased cells;
- lesser amounts of drugs are required to produce a therapeutic effect;
- plasma level peaking of drugs will be avoid;
- augment bioavailability since it avoids the hepatic first-pass metabolism;
- greatly improved patient compliance by eliminating recurrent dosing.

The micro and macromolecules can enter into the skin through three distinct pathways, as represented on Figure 2.7 :[94, 95]

- intercellular pathway, which is through the lipid matrix occupying the intercellular spaces of the KC;
- transcellular pathway, which is through the KC cells,
- transappendageal pathway, which is across hair follicles, sebaceous glands and sweat glands.

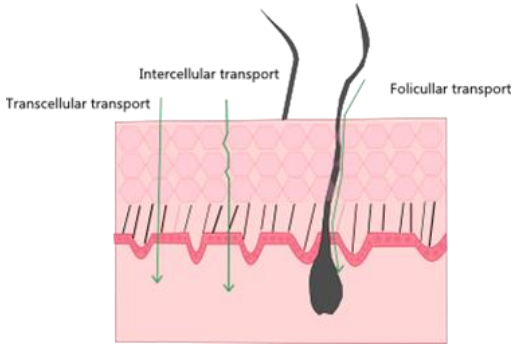

Figure 2.7 - Schematic representation of different entry pathways for molecules into the skin.

Thus, by limiting the analysis of potential penetration through the skin anatomical features, in healthy skin, only those agents lesser than 5–7 nm or 36 nm can respectively go through SC through intercellular route or aqueous pores, while larger ones (10,000–210,000 nm) could enter skin through the transfollicular route [80].

2.3.3 Novel therapeutic approaches

Presently, it has become clear that the development of new drug alone is not always sufficient to ensure progress and success in new therapies, since the major reasons for the failure of drugs stay behind poor drug solubility, insufficient drug concentration related to reduced absorption, rapid metabolism and removal, drug distribution and allocation to other tissues, high drug toxicity, and high fluctuation of plasma level due to unpredictable bioavailability [1, 97, 99, 100].

Treatment of PSO still remains a **challenging task** in spite of several therapeutic agents available due to absence of an ideal drug molecule. The main drawbacks are associated with side effects caused by an inappropriate drug location that could be overcome with an **efficient carrier for delivery of anti-psoriatic drugs**, and lack of a **suitable animal model** mimicking histological and immunophenotypic characteristics of PSO [93]. For these reasons, it has become necessary to find new solutions as novel drug carriers. Colloidal drug carriers can be generally classified on the basis of its components into **Lipid based colloidal carriers** and **Polymeric colloidal carriers** are represented on Figure 2.8.

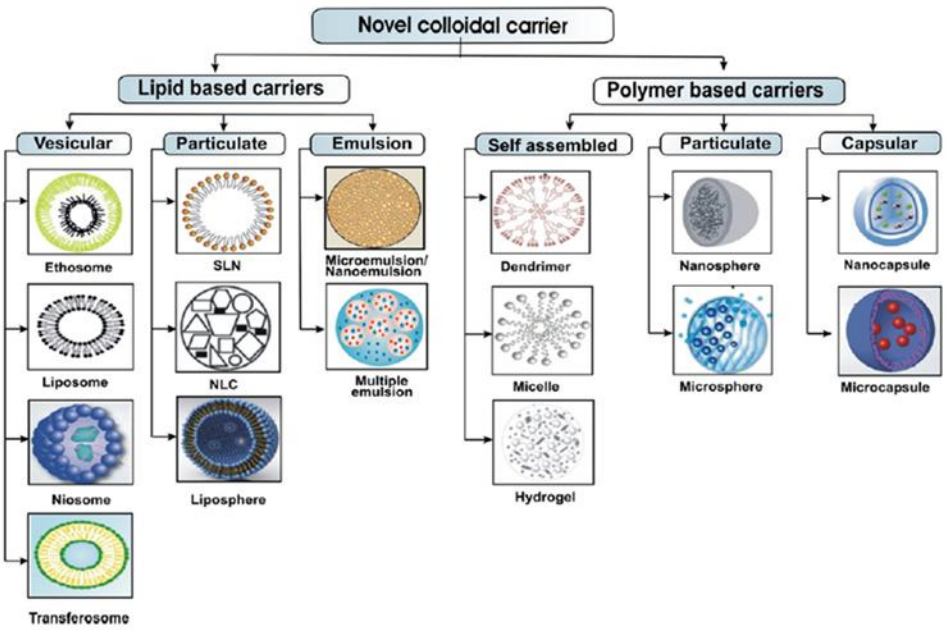

Figure 2. 8 - Classification of colloidal drug carriers. (Adapted from [94])

2.3.3.1 Drug carriers for topical delivery

In case of dermatological diseases such as PSO whose triggers are situated beneath the skin, it is preferable to manage drugs topically rather than systemically due to more efficient direct action with improvement of the local access for optimum amount of drug.

Topical administration also reduces the systemic burden and toxic effects of the drugs and it is considered the first-line of treatment currently used in moderate PSO as it is considered safe and well accepted by the patients with rates around (75-80%) [101, 103].

During the last decades, inorganic and colloidal particles such as nanocapsules, nanospheres, NLCs, among others, have been discovered for dermal/ transdermal drug delivery. The successful implementation of these systems for drug delivery entirely depends on their ability to go through numerous anatomical barriers, sustained release of their content and their stability in the nanometer size [1, 88]. Various particulate lipid based colloidal carriers have also found application in anti-psoriatic drug delivery, in particular SLN and NLC [93].

SLNs are the newest generation of lipid nanoparticles and are attracting attention as novel colloidal drug carriers for topical use. This kind of nanoparticles combine such advantages as sustained release of their content, insignificant skin irritation, organic solvent-free preparation process and protection of active compounds [104, 105]. **NLC**s are a second generation of SLNs, and have been used in topical drug formulations and cosmetic products. Their diminutive size ensures close contact to the SC and their composition provides selective drug delivery to skin layers [64]. They are formed by integrating solid lipids with spatially incompatible lipids leading to a lipid matrix with a particular structure with several imperfections, as represented on Figure 2.9. These imperfections are caused by a blend of a liquid and solid lipids, providing more space for drug accommodation [1, 106].

NLCs have the potential to adjust the drug release over an extended period with a reduced rate of systemic absorption. The lipid film formation above the skin and the succeeding occlusion effect was described for lipid nanoparticles with reduction of transepidermal water loss caused by this effect, leads to an augment in skin hydration after dermal application of SLNs or NLCs [74, 106, 107]. NLCs systems are a promising carrier for the topical delivery of antipsoriatic drugs as revealed by improved skin permeation and irritation, small and narrow size distribution, better bioavailability and the compatibility of the drugs [1, 106, 107].

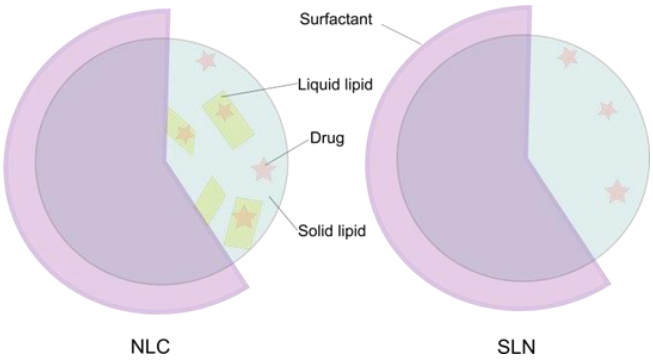

Figure 2.9 - Schematic representation of NLC and SLN structures.

2.3.3.2 Therapeutic agents review in the treatment of psoriasis

Lipid based carriers have attracted increasing scientific during the last few years as an alternative to polymeric nanoparticles and to overcome drawbacks associated with controlled release, stability, biodegradability and economical costs. Table 2.6 describes some applications of vesicular lipid based carriers in treatment of PSO.

Table 2.6 - List of lipid-based vesicular carriers for psoriasis topical therapy

Carrier	Drug	Composition	Size (nm)	Skin penetration tests	Refs
Liposomes	tacrolimus	DPPC:DLPC	77-88	*In vitro* porcine skin	[100]
	MTX	Hydrogenated soya PC/ egg PC/ cholesterol/ menthol		*In vitro* rat skin; *in vivo* animal studies	
	MTX	PC2:CHOL1; PC9:CHOL1: PC2.5:OA1	80-140	*In vitro* newborn pig skin	[101]
	tacrolimus	2% Lipoid S 100	146	*In vitro* SD rats skin	[102]
	psoralen	5% Lipoid S 100/ 1.5% cholesterol	198	*In vitro* rat skin	[103]
	Cy A	NAT 8539 /ethanol (10/10)	57 - 101	*In vitro* human skin	[104]
Ethosomes	tacrolimus	2% Lipoid S 100/ 30% ethanol	85	*In vitro* SD rats skin	[102]
	psoralen	5% Lipoid S 100/ 40% ethanol	120	*In vitro* rat skin	[103]
	psoralen	different ratios Lipoid S 100/ ethanol	56-159	*In vitro* rat skin; in vivo rat microdialysis assay	[105]
Transfersomes	hydrocortisone or dexamethasone	SPC: oxyethylene: polysorbate	100-200	*In vitro* porcine skin; *in vivo* mice	[106]

Lipid particulate carriers have application in anti-psoriatic drug delivery due to drug pay load and increased stability. Table 2.7 presents some applications in treatment of PSO using lipid particulate carriers.

Table 2.7 - List of lipid-based particulate carriers for psoriasis topical therapy

Carrier	Drug	Composition	Size (nm)	Skin penetration tests	Refs
SLN	psoralen	12% Precirol: 0.2% myverol or SPC: 2.4% PF68 or Tween 80	297	*In vitro* mice skin	[96]
	dithranol	Tricaprin/ soybean lecithin/ TDC	230-264	-	[107]
	tretinoin	Myristyl myristate/ PF68/ chitosan	163-285	-	[108]
	dithranol	Compritol 888 ATO/ Span60/ poloxamer 407	219	-	[109]
	tretinoin	Phosphatidylcholine /Tween 80/ BHT/ Compritol	82	*In vitro* mice skin; *in vivo* mouse tail model	[110]
	capsaicin	Compritol 888 ATO/ PC: PF68	182	*In vitro* rat skin; skin-irritation test	[111]
	mometasone furoate	GMS/ Tefose-63/ Tween 80	141-177	*In vitro* mice skin	[112]
	fluocinolone acetonide	Compritol1 888 ATO/ poloxamer 188/ soya lecithin	107	*In vitro* goat skin	[58]
NLC	psoralen	12% Precirol and/or squalene: 0.2% myverol or SPC: 2.4% PF68 or Tween 80	173-210	*In vitro* mice skin	[96]
	tretinoin	Phosphatidylcholine /Tween 80/ BHT/ IPM/ Compritol	79	*In vitro* mice skin; *in vivo* mouse tail model	[110]
	capsaicin	Compritol 888 ATO/ Oleic acid/ PC: PF68	145	*In vitro* rat skin; skin-irritation test	[111]
	MTX	Precirol ATO 5/ squalene/ Myverol/ PF68	270 -320	*In vitro* mice skin	[113]
	MTX	Witepsol1 S51/ oleic acid/ Tween 60 or Tween 80	274-298	-	[114]
	acitretin	Precirol ATO 5/ oleic acid/Tween 80	223	*in vitro* Human cadaver skin; Human clinical studies	[64]

Emulsion based carriers involve the dispersion of two or more immiscible liquids stabilized by a surfactant or emulsifier Table 2.8 presents the main application of this carrier in treatment of PSO.

Table 2.8 - List of lipid-based emulsion carriers for psoriasis topical therapy

Carrier	Drug	Composition	Size (nm)	Skin penetration tests	Refs
Microemulsion	8-methoxsalen	IPM and Tween 80: Span 80: 1,2-Octanediol	190-1240	*In vitro* newborn pig-skin	[78]
	CyA	Aerosol-OT/ Tween85/ IPM	-	*In vitro* rat skin; *in vivo* animals tests	[123, 124]
	ceramides	Lecithin or TCPL4	203-1279	*In vitro* human skin	[117]
	curcumin	Eucalyptol/ polysorbate 80/ ethanol	2-5	*In vitro* porcine skin	[118]
	betamethasone dipropionate	oleic acid:sefsol/ Teween 20/ isopropyl alcohol	60-190	*In vitro* rat skin; in vivo animals tests	[52]
Nanoemulsion	rice bran oil	sorbitan oleate/PEG-30 castor oil	45-303	*In vivo* clinical studies	[119]
	paclitaxel	Labrasol+vitamin E-TPGS/ Labrafil M1944CS	22	*In vitro* rat skin	[120]

Polymeric based carriers contain natural or synthetic polymer where polymer encapsulates drug. Self-assembled carriers include dendrimers, micelles, hydrogel and the main applications are shown in Table 2.9.

Table 2.9 - List of polymer-based self-assembled carriers for psoriasis topical therapy.

Carrier	Drug	Composition	Size (nm)	Skin penetration tests	Refs
dendrimers	8-methoxypsoralen	PAMAM G3 and G4	190-1240	*In vivo* rat skin tests	[121]
	dithranol	polypropylene imine (5.0 G)	6-8	I*n vitro* rat skin; *in vivo* animals tests	[122]
micelles	tacrolimus	MPEG-dihexPLA	10-50	*In vitro* human and porcine skin	[123]
	CyA	MPEG-dihexPLA	25-52	*In vitro* human and porcine skin	[124]
hydrogel	CyA	carboxyvinyl polymer/ propylene glycol/ diisopropanolamine/ polyoxyethylene glyceryl monostearate	-	*In vitro* rat skin	[125]
	MTX	acrylamide: acrylic acid monomers / terpenes/ ethanol	-	*In vitro* mice skin	[126]
	MTX	Propyl/ methylparaben/ carbomer/ triethanolamine	-	*In vitro* mice skin	[127]
	tretinoin	Carbopol® Ultrez 10 NF/ Imidazolidinyl urea	-	*In vitro* human skin	[128]
	linseed Oil	ethyl celulose/ sodium alginate/ carbopol 934/ carbopol 971/ HPMC	-	*In vitro* rat skin	[54]
	betamethasone dipropionate	carbopol 934/ salicylic acid	-	*In vivo* animal tests	[52]

Particulate polymer carriers (nano e micro spheres) and capsular polymeric based carriers are described in Table 2.10.

Table 2.10 - List of polymer-based particulate carriers for psoriasis topical therapy

Carrier	Drug	Composition	Size (nm)	Skin penetration tests	Refs
nanospheres microspheres	Trimethylpsoralen	PLGA/ Tween 80	243	*In vitro* human skin	[37]
	Psoralen	PLGA/ PVA	150–2900	*In vitro* rat skin	[38]
	Clobetasol propionate	PLGA/ PVA	8000-15000	-	[39]
	Naringenin and sericin		3875		[40]
nanocapsules	Dithranol	PCL/ Span® 60/ Tween® 80/ CCM	230–250	-	[41]

Chapter 3 - Methods

3.1 Materials

Chemical reagents were adquired from Sigma-Aldrich (St Louis, MO, USA) unless stated otherwise. All chemicals and solvents were of analytical grade and therefore used without further purification. Aqueous solutions were prepared with double-deionized water (Arium Pro, Sartorius AG, Göttingen, Germany), which possesses conductivity values lower than 0.1 μS cm^{-1}. Fetal bovine serum (FBS), penicillin-streptomycin antibiotics mixture and Dulbecco's Modified Eagle's Medium (DMEM) were purchased from Gibco® (Invitrogen Corporation, UK). L929 mouse fibroblast cell line was obtained from ATCC-LGC Standards (Barcelona, Spain) and HaCaT KC cell line was obtained from CLS (Eppelheim, Germany).

A. Solid lipids

Witepsol® E85

WITEPSOL E grades are hard fats with a melting range above body temperature, approximately 42–44°C [129]. They can be used to raise the melting point when associated with active ingredients that decrease the melting point. Also can be used as analgesics, anesthetics, antihypertonics and steroidal antirheumatics (corticosteroids). This lipid was kindly provided by Gattefossé (France)

Cetyl palmitate

Cetyl palmitate (*cetylis palmitas*) is a wax produced by catalytic esterification of fatty alcohol (cetylic alcohol) and fatty acid (palmitic acid). Besides palmitic acid, cetyl palmitate may contain myristin acid and stearic acid. Cetyl alcohol may be partly replaced by myristyl alcohol or stearyl alcohol. Cetyl palmitate is a white, with waxy plates which is supplied as pellets or flakes. Pure cetyl palmitate crystallizes in two modifications melting at 45-52ºC. According to the composition of the ester mixture the melting point is increased or decreased. Cetyl palmitate is practically insoluble in water, soluble in boiling ethanol and in methylene chloride, slightly soluble in light petroleum, practically insoluble in ethanol was kindly provided by Gattefossé (France) [130].

B. Liquid lipid

Miglyol® 812

Liquid lipids are fatty acid esters or alcohols (2-octyldodecanol). They are neutral carriers for various pharmaceutical applications. Because of their high polarity, they have superior solvent characteristics for active drugs [131]. Medium chain triglyceride (Triglycerida saturate media) is a synonym for Miglyol® 812. Consists of a mixture of triglycerides, mainly caprylic acid and capric acid and is an at room temperature liquid lipid (oil) of low viscosity. Miglyol® 812 is a colorless till light yellowish oily liquid which is insoluble in water but miscible with dichloromethane, ethanol, petroleum ether and fatty oils purchased by Acofarma (Spain) [131].

C. Surfactants

PVA

PVA is produced commercially from polyvinyl acetate, usually by a continuous process. It is an odorless and tasteless, translucent, white or cream colored granular powder. It is used as a moisture barrier film for food supplement tablets, food with inclusions that need to be protected from moisture uptake [132]. PVA is not known to occur as a natural product. Typically a 5% solution of polyvinyl alcohol exhibits a pH in the range of 5.0 to 6.5. Polyvinyl alcohol has a melting point of 180 to 190°C [132].

Tween 80

Tween 80 or polysorbate 80 (polyoxyethylene sorbitan fatty acid ester). Like any polysorbate, are stable to electrolytes and weak acids and bases. Also, in common with other polyoxyethylene surfactants, prolonged storage can lead to the formation of peroxides. Very soluble in water; soluble in alcohol, cottonseed oil, corn oil, ethyl acetate, methanol,toluene; insoluble in mineral oil [133]. It was used for the microemulsion which was applied on human skin, where polysorbate does not provoke irritations [133].

E. Psoriatic drugs

Methotrexate

MTX is a folate antagonist that competitively bind to dihydrofolatereductase (DFHR) enzyme hampering cell growth and arresting cell cycle in G1/S phases [134]. MTX, the oldest systemic therapy for PSO, still remains one of the most successful treatments for PSO and PSA that acts by suppressing the immune system and thereby stopping the inflammatory response that can direct to PSO and psoriatic flares [77, 78]. MTX is one of the most effective therapeutic agents with a triple mode of action: it is anti-inflammatory, reduces cell proliferation and it is immunosuppressant. It is accessible to treat a variety of malignancies, such as osteosarcoma, non-Hodgkin's lymphoma, lymphocytic leukemia, choriocarcinoma, and head, neck, and breast cancers, against non-neoplastic conditions such as severe PSO and autoimmune diseases (e.g. RA) [13, 79, 80]. However, it causes numerous adverse effects (e.g. hepatotoxicity, ulcerative colitis, nephrotoxicity) that hampers its therapeutic application [13, 77]. MTX was kindly provided by Excella (Feucht, Germany) as a gift.

Etanercept

Enbrel (etanercept) is a biologic medication that blocks TNF-α and other cells to cause inflammation. Enbrel helps lower the amount of TNF-α, which interrupts the inflammatory

cycle of PSO and PSA [135]. Approved in April 2004 by the U.S. Food and Drug Administration (FDA) for the treatment of moderate to severe plaque PSO. In January 2002, it was approved for PSA. It is also approved for treating RA [135].

3.2 Preliminary assessment of the production parameters influence on lipid nanoparticles

MTX solubilisation was studied in the presence of seven lipids (Cetyl Palmitate, Imwitor 308, Lipocire™ CM, Witepsol® E76, Witepsol® E85, Witepsol® H32, Witepsol® S51). MTX solubilized in Cetyl Palmitate, Imwitor 308, Lipocire™ CM and Witepsol® E85 and no drug crystals were observed (Table 3.1). So, the solid lipids Witepsol® E85, Lipocire™ CM and Cetyl Palmitate with a melting range above body temperature were selected to proceed with lipid nanoparticles production.

Table 3.1 - Solubility of MTX in solid lipids.

Solid lipid	Dissolved MTX?
Witepsol E76	-
Witepsol E85	+
Witepsol S51	-
Witepsol H32	-
Cetyl palmitate	+
Imwitor 308	+
LCM	+

NLCs were prepared using two different methods (1) **ultrasonication** (Figure 3.1) and (2) **emulsification-solvent evaporation** technique using as liquid lipid (Miglyol® 812) and the surfactants: PVA, polysorbate 60 (P60) and polysorbate 80 (P80). After defining the production method (Figure 3.1) and the solid lipid, the optimization was based in varying the amount of drug, surfactant and sonication conditions, following a sequential procedure represented in Figure 3.2. The goal was to obtained a formulation with size bellow 200 nm, as homogeneous as possible and with high drug entrapment efficiency (EE).

For the preparation of NLCs loaded with MTX two methods were considered as follow:

(1) **ultrasonication method**: the aqueous phase containing the surfactant and the lipid phase with the drug were prepared separately by heating at 60ºC in a water bath, then the lipid phase was added to the aqueous phase. The mixture was then homogenized using a probe-sonicator and left to cool down at room temperature.

(2) **emulsification-solvent evaporation technique**: the formulation was prepared from an emulsion using as aqueous phase the surfactant in water and as oil phase the solid lipid, liquid lipid and the drug in the organic solvents dichloromethane (DCM) or *dimethyl sulfoxide (DMSO)*. Then the emulsion was

subjected to ultraturrax (5 minutes) and probe-sonicator (10 minutes) producing a nanoemulsion.

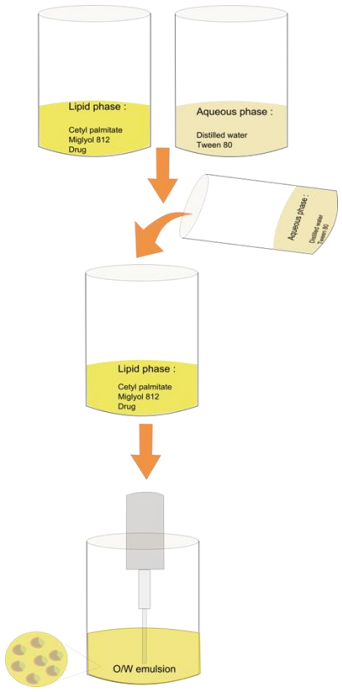

Figure 3.1 - Hot ultrasonication method for the production of NLCs.

Second step involved the choice of surfactant: P60, P80 or PVA while in the **third stage** consisted in the selection of solid lipid between Witepsol® E85, Lipocire™ CM and Cetyl Palmitate. The **fourth and fifth steps** were based on the evaluation of the influence of the amount of PVA surfactant (80, 100 and 120 mg) and (4, 20 and 40 mg) drug loading.

The **sixth and seventh steps** were related with sonication parameters such as time (10, 20 e 30 min) and amplitude (70 and 80%). At last, the **ninth stage**, evaluated the lipid ratio (solid/liquid: 70/30, 75/25 and 80/20).

Given the intended objectives, the final optimized MTX-loaded NLCs were prepared by hot ultrasonification with Witepsol® E85 (300 mg) and Miglyol® 812 (100 mg) in the lipid core, stabilized by the surfactant PVA (120 mg) and MTX at 10% (w/w) of total lipid mass.

The preparation required 10 minutes at 70% of amplitude as sonication parameters.

From this preliminary assessment it is clear the importance of several production parameters to produce the MTX-loaded NLCs. Based on this fact, a formulation design strategy was implemented to optimize the production of the formulation.

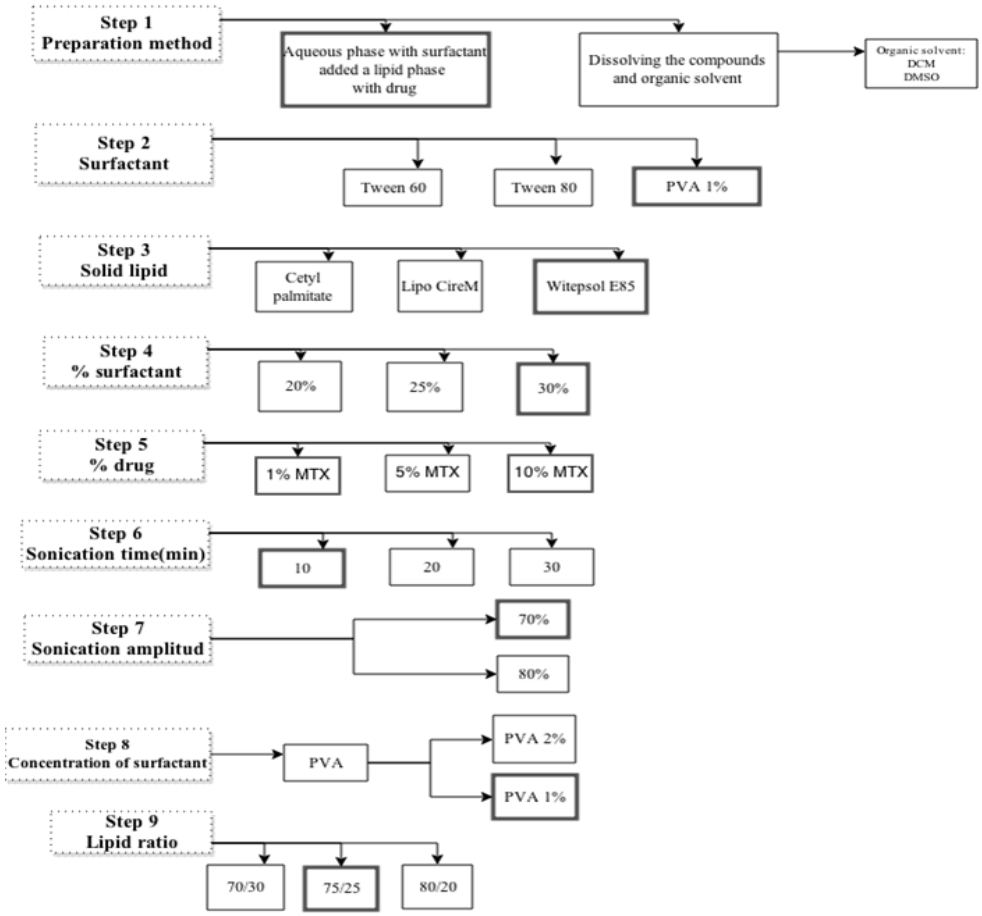

Figure 3.2 - Representation of the optimization process. Highlighted are the conditions with the more adequate performance.

3.3 Experimental design

In order to obtain an optimized formulation is useful to evaluate the influence of several parameters susceptible to affect the entire production process. A statistical experimental design was implemented to assess the influence of the amount of liquid lipid, surfactant and MTX in the NLCs's size, polydispersity and drug EE.

A full factorial design contains all possible combinations of a set of factors. In this design we performed total of 27 formulations with each coded level. Based on the results obtained a Box-Behnken experimental design was applied using 15 formulations at least three coded levels for each studied factor (Table 3.2) [146]. For each studied factor, the lower (-1), medium (0) and higher values (+1) were chosen on the basis of tested lower and upper values for each variable, according to pre-formulation studies and literature research. As we can see in the Table 3.2 coded levels are representative of the quantities of independent variables, X_1, X_2 and X_3, amount of liquid lipid, surfactant and drug, respectively. The data were analyzed using ANOVA by STATISTICA 10 (Statsoft®, Inc) software.

Table 3.2 - Variables with respective coded levels of the Box-Behnken design.

Factors	**Coded Levels**		
	Low Level	Medium Level	High Level
Independent variables	(-1)	(0)	(+1)
X_1 = Liquid lipid (mg)	40	50	60
X_2 = Surfactant (mg)	40	50	60
X_3 = Drug (mg)	2	10	20
Dependent variables		**Constrains**	
Y_1 = particle size		Optimum (250nm)	
Y_2 = Polydispersity index		Minimum	
Y_3 = Entrapment efficiency		Maximum	

The polynomial equation generated from the experimental design is given below:

$$Y = b_0 + b_1X_1 + b_2X_2 + b_3X_3 + b_{12}X_1X_2 + b_{13}X_1X_3 + b_{23}X_2X_3 + b_{11}X_1^2 + b_{22}X_2^2 + b_{33}X_3^2 , \quad (3.1)$$

where Y is the dependent variable, b_0 is the intercept, X_1, X_2, X_3 are the coded levels of independent variables, and b_1 to b_{33} are the regression coefficients computed throughout observed experimental values of Y; the terms X_1X_2 and X_i^2 (i = 1, 2 or 3) represent the interaction and quadratic terms, respectively. The polynomial equation was statistically validated using ANOVA, by statistical significance of coefficients and r^2 values. Statistical analysis were considered significant when the p values were ≤ 0.05.

3.4 Optimization and validation

The graphical and numerical analyses were done in order to obtain optimum values of the studied variables. The optimum variables were used to prepare a checkpoint NLC formulation and were compared with the predicted values to calculate the predicted error, in order to validate the chosen experimental domain and polynomial equation. Validation of this method was based on the formulation obtained throughout medium coded levels that correspond at sample #14 that is the formulation at central point, for estimating the experimental error. Optimized formulation was prepared in triplicate according to the obtained results after conclusion of this experimental design respecting the established criteria.

3.5. Determination of particle size, size distribution and surface charge

Theoretical principles

Particle size analysis can be achieved by dynamic light scattering (DLS) also called Quasi-Elastic Light Scattering (QELS) or Photon Correlation Spectroscopy (PCS) because when photons are scattered by mobile particles, the process is quasi-elastic [136]. This method was performed using a Brookhaven ZetaPALS DLS equipment, suitable to determine size and size distribution (polydispersity index, PDI) of particles with great accuracy, in a reduced time and as a non-invasive technique [106, 107, 145].

DLS technique measures the translational diffusion coefficient through interactions between a dispersion and a laser beam. Therefore disperse particles in a diluted suspension without interactions between particles moving to thermal Brownian movement or motion (random movement of the particles owing to bombardment by the solvent molecules that surround them) and so the size of the particles should be calculate using Stokes-Einstein equation [145, 146].

$$\boldsymbol{D_t = \frac{K_b\, T}{3\pi\eta D_h}} \;<=>\; \boldsymbol{D_h = \frac{K_b\, T}{3\pi\eta D_t}} \quad , \tag{3.2}$$

where D_h is hydrodynamic diameter value allows to calculate size particle, D_t is translational diffusion coefficient (we know this through DLS) , K_b is Boltzman´s constant (we know this), T is thermodynamic temperature (we control this) and η is dynamic viscosity (we know this)

This coefficient will depend not only on the size of particle but also concentration and type of ions in the medium [139].

Particle size distribution can be determined by analyzing the intensity of the scattered light as a function of angle between the incident and scattered beams using a suitable light scattering theory [140].

The size distribution is very important to determinate the physical stability of nanosuspensions. This parameter represents the quality of dispersion assessing the homogeneity of the size distribution of particles in solution [148, 149]. PDI is used to describe the width of the size distribution and the accurate value of this parameter for a homogeneous nanoparticles population is below 0.3 [150, 151].

Particle surface charge, also known as zeta potential (ζ-potential) and represented on Figure 33 , is the electrical potential that reflects the surface charge of nanoparticles in an aqueous medium. It is defined such as the distance away from the particle surface below the ions keep tightly attached to the particle when it moves through an electrical field [144].

Due to gravity or an electric field, the particles and ions move in the solution. The hydrodynamic shear is the region, or the slipping plane, the ions do not move with the parti-

cles. The electric potential at the slipping plane is called zeta potential, ζ-potential [145]. Generally, the ζ-potential values of -30 or +30 mV are considered to be sufficient and adequate for stabilization of NLCs [146].

For the ζ-potential measurement a laser Doppler electrophoresis is used to calculate the net velocity through an electric field applied to the nanoparticles [145, 155]. This procedure involves the Henry approximation:

$$\boldsymbol{\mu = \frac{2\zeta\varepsilon}{3\eta_0} f(kr)} \ , \tag{3.3}$$

where:

ζ - zeta-potential (main goal)
μ - electrophoretic mobility,
ε - dialectric constant,
η - viscosity of the water (in this case)
f (kr) - Henry function.

This function generally has value of 3/2 or 1 depending the Smoluchowski or Huckel approximation, respectively. To measure ζ-potential in this case, this term assumes the value 3/2 because is used an aqueous solution [145, 155].

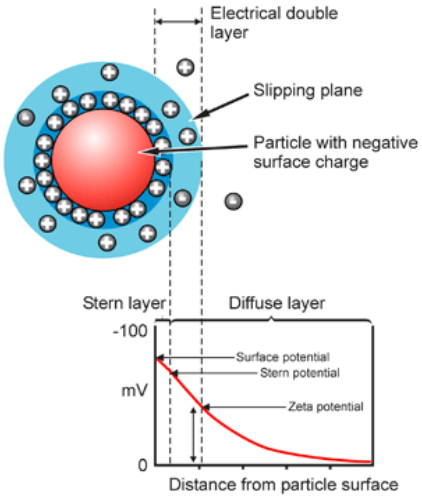

Figure 3.3 - Representation of the surface potential measurement. (Adapted from [148])

Experimental details

For each formulation a dilution of 1:400 was made using double deionized water followed by determination of particle size, PDI and ζ-potential at 25ºC using ZetaPALS (Brookhaven 153 Instruments Corporation, Holtsville, NY, USA). Photon correlations of spectroscopic measurements were carried out at a scattering angle of 90° with 10 cycles and 6 runs for each measure.

3.6 Entrapment efficiency

Theoretical principle

EE is defined as the ratio of entraped drug within the nanoparticles to total amount of drug used to formulate the NLCs[105, 157]. In this study, the drug EE was determined indirectly using the following equation [105, 157, 158].

$$\mathbf{EE}\ (\%) = \left(\frac{\mathbf{Initial\ drug - non - incorporated\ drug}}{\mathbf{initial\ drug}}\right) \times \mathbf{100}\,, \tag{3.4}$$

Absorption spectroscopy was used in order to determine the concentration of non-incorporated MTX [151].

This process, commonly referred to as spectrophotometry is one of the most flexible analytical method that allows measuring the non-incorporated drug through the amount of the light absorbed by a sample at a defined wavelength [152]. Transmittance (T) is defined as the ratio between incident radiation transmitted by the analyte and reference solutions (**Figure 3.4**) [152].

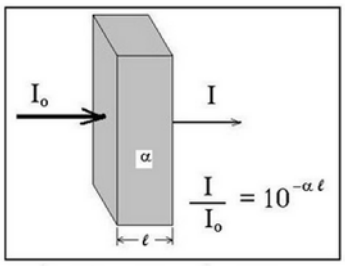

Figure 3.4 - Representation of the Beer Lambert law. (Adapted from [152].)

Experimental details

The MTX-loaded NLCs containing the entraped drug was retained in Amicon filter (Merck millipore, Germany) while the non-incorporated MTX remained in the supernatant.

The supernatant samples were analyzed using UV-vis spectrophotometer at λ_{max} 303 nm, which is the maximum absorption of MTX in aqueous solution [113]. A standard curve of MTX in water was used to determine the amount of the non-incorporated MTX and the EE.

3.7 Transmission electron microscopy

Theoretical principles

When electrons increase speed up to elevated energy levels and focused on a material, they can disperse or backscatter elastically or inelastically, or produce numerous

interactions, source of different signals such as X-rays, Auger electrons or light. Transmission electron microscopy (TEM) is a fundamental characterization tool for directly imaging nanomaterials to achieve quantitative measures of particle and/or grain size, size distribution, and morphology (Figure 3.5).. Successful imaging of nanoparticles by TEM depends on the contrast of the sample comparative to the background [161, 162].

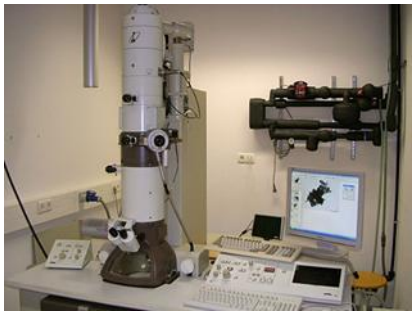

Figure 3.5 - TEM Jeol JEM 1400 microscope.

Experimental details

The shape and size of all of lipid nanoparticles was observed by TEM using a Jeol JEM 1400 microscope. Prior to analysis, samples were diluted with double deionized water, loaded on nickel grids with 300 mesh, dried at room temperature and stained with uranyl acetate for 30 seconds for contrast and then placed at the accelerating voltage of 60 kV.

3.8 Cryo-scanning electron microscopy

Theoretical principle

Cryo-SEM is an effective technique of imaging of samples containing moisture without causing drying artifacts. It is a quick and reliable way to overcome SEM preparation problems. There is a cryo chamber that embody a resistance heating vacuum evaporator to coat samples with gold. There are heaters that sublime the ice molded in samples. Then, liquid nitrogen needs to be quickly added to the samples to frozen them and finally loaded into the Cryo-SEM[155].

Experimental details

The morphology of nanoparticles was evaluated by cryogenic-scanning electron microscopy (cryo-SEM) using the experimental facilities at the Materials Centre of the University of Porto, Portugal (CEMUP). All lipid nanoparticles were filtered through a 0.80 μm filter to remove impurities of the water. A volume of these dispersions was dropped on an adequate support and rapidly cooled by plunging into sub-cooled nitrogen (slush nitrogen) and transferred under vacuum to the cold stage of the preparation chamber. Cryofactures were then performed using an ALTO 2500 (Gatan Alto 2500 (Pleasanton, CA, USA)), with subsequent sublimation for 180 seconds at -90ºC and coating with Au/Pd by sputtering for

35 seconds. Then, the samples were transferred to the Cryo-SEM chamber and observed at a temperature of -150ºC using a JSM 6301F microscope (JEOL, Tokyo, Japan).

3.9 Fourier transform infrared (FT-IR) spectroscopy

Theoretical principle

FT-IR measures the intensity of the infrared absorption radiation by a sample at a specific wavelength [156]. Some of the infrared radiation is absorbed by the sample and some is transmitted resulting in a spectrum that characterizes the molecular absorption and transmission; thus creating a molecular 'fingerprint' of the sample [157].

This technique can identify unknown materials, demonstrate if an compound is present in a solution and determine the amount of components in a mixture [157]. Furthermore, this method provides a fast and precise measurement [164, 165].

Experimental details

Prior FT-IR analysis the samples were lyophilized (LyoQuest-85 plus v.407, Telstar).

The freeze-dried optimized formulations of SLNs/NLCs with and without MTX, pure MTX, as well the used combinations as physical mixtures, were evaluated using an FT-IR Spectrophotometer (FrontierTM, PerkinElmer; Santa Clara, CA, USA) equipped with a horizontal attenuated total reflectance (ATR) sampling accessory with a diamond crystal. All samples were run in triplicate. At the first, we performed a background run (to remove the background noise of the instrument) and use a run with pure MTX as positive control.

The data was obtained for the mid-infrared absorbance region, between 4000 and 600 cm^{-1}, and the spectra were measured at a spectral resolution of 4 cm^{-1} with 200 scans co-added, to minimize differences between spectra due to baseline shifts. In order to perform the spectra comparison, spectra were truncated at 2000 and 750 cm^{-1}, based on the typical absorption bands for the analyzed compounds.

3.10 Storage stability

Stability of nanoparticles during storage was assessed by the appearance, size, PDI and drug content in comparison to the day of production. NLCs dispersions were stored after production in closed glass vials at room temperature and examined on the day of production and after 4 or 6 weeks of storage.

3.11 Targeted lipid nanoparticles for psoriasis

Theoretical principle

Functionalization is the procedure applied in surface engineering field to introduce a chemical functional group on the surface of the nanoparticles [158]. This targeting approach can improve nanoparticles efficacy and minimize the side effects of drugs because it results in an active targeting towards the target cell/ tissue [166–168]. Active targeting can be performed by an antibody, a peptide and can revolutionize the therapeutic potential offered by local topical therapy, particularly, in PSO [160].

In this work, the lipid nanoparticles were functionalized with a model globular protein (bovine serum albumin, BSA) and a monoclonal antibody (etanercept) (Figure 3.6). BSA is used in numerous biochemical applications due to its stability and lack of interference within biological reactions The monoclonal antibody, etanercept, is a fully human tumour necrosis factor (TNF) soluble receptor fusion protein that antagonizes the effects of endogenous TNF and it is approved to treat moderate-to-severe PSO cases where current systemic therapies have failed [161]. This two molecules were coupled throughout carbodiimide reaction using as a crosslinker, the water-soluble 1-etliyl-3-(3 dimethylaminopropyl) carbodiimide (EDC) and DSPE-PEG-NH_2 that was previsouly incorporated in the nanoparticles [162].

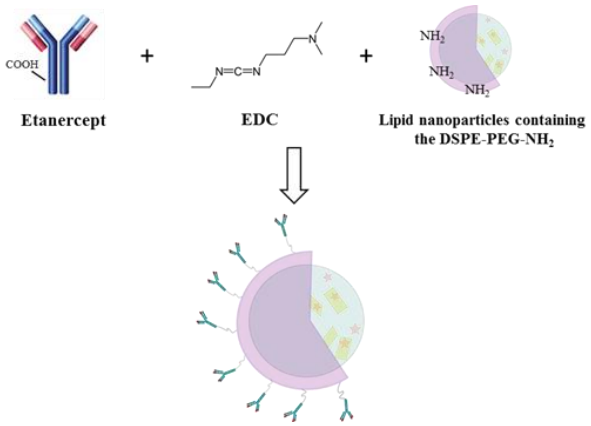

Figure 3.6 - Functionalization process of the lipid nanoparticles.

This procedure was performed according to carbodiimide method [163]. The coupling of the molecule of interest was carried out in PBS buffer in a three-step procedure. The first step consists in the activation of the carboxyl-groups. EDC is a powerful cross linker for peptides and proteins for use in numerous protein and cell biology detection and analysis methods that and reacts with various forms of amides and hydroxyl functional groups that's why with carboxylic groups to form an active O-acylisourea intermediate [171, 172].

The second step was the reaction of the amine function with the activated carboxylic functions [164]. The last step consists of binary covalent binding of an antibody with the lipid nanoparticles.

Experimental details

For targeting purposes, lipid nanoparticles were also performed by the ultrasonication method. Briefly, the lipid phase was prepared by melting 150 mg of Cetyl Palmitate, 45 mg of Miglyol®812 and 18 mg of MTX with an aqueous phase composed by 47 mg of polissorbate 80 in 7 mL of double-deionized water. For the functionalization, 5 mg of DSPE-PEG-NH_2 were added to the lipid phase. Both phases were heated to 60ºC in a water bath, separately. The aqueous phase was poured into the lipid phase and homogenized using a probe-sonicator (VCX130, Sonics & Materials, 115 Newtown, CT, USA) with amplitude frequency of 70% during 10 minutes, in order to obtain a nanoemulsion. Empty lipid nanoparticles were prepared in a similar way, without the drug. Similarly, SLN were prepared without the addition of the liquid lipid, Miglyol®812. Then, formulations were left to cool down at room temperature. Then, in another tube 100 μg of EDC were added in 200 mL of PBS mixed with the DSPE-PEG-NH_2 containing lipid nanoparticle, by vortex, and placed for 30 minutes at 4ºC. Then, 10 μL of Etanercept or BSA (corresponding to 500 μg) were added to 3.5 mL of nanoformulations/EDC solution. Fuctionalized nanoformulations were placed at 4ºC until further use.

3.12 Coupling efficiency of the functionalization

Theoretical principle

To determine the quantity of antibody or protein conjugated at surface of nanoparticles was used a commercial kit the BioRad™ DC Protein Assay Synergy™ HT Multi-mode microplate reader (BioTek Instruments Inc., Winooski, VT, USA). This is a colorimetric assay based on Biuret reaction for the determination of protein concentration [165]. Peptide bonds of proteins react with copper under alkaline conditions to produce Cu^+, which reacts with the Folin reagent through the Folin Ciocalteau reaction. The reactions result in a strong blue color, with maximum absorbance at 750 nm and minimum absorbance at 405 nm, which depends partly on the tyrosine and tryptophan content. The method is sensitive down to about 0.01 mg of protein.mL^{-1}, and is best used on solutions with concentrations in the range 0.01–1.0 mg.mL^{-1} of protein [173, 174].

Experimental details

In this work we used a Etanercept such a protein of interess due to its use in biological treatment of psoriasis and BSA for costs reasons and also be a protein it will have a similar behavior [167].

The procedure was based on the kit instructions. Briefly, standard solutions of BSA were prepared between 1.5 – 0.09 mg.mL^{-1}. To a 96-well plate 5 μL of each standard and samples were transferred in five replicates. After adding the reagents A and B the optical density was read in a Biotek (Sinergy HT) microplate reader. To determine the protein concentration, the absorbance at 750 nm was measured and compared with a blank containing the same amount of dye [168].

3.*13 In vitro* drug release

Theoretical principle

Dialysis is a powerful technique to separate biomolecules according to their molecular weight and can also be used to evaluate the compound release from the nanoparticles and in binding studies [169]. This method, separate biomolecules across a 'semi-permeable' membrane constituted by pores that retain the biggest molecules and is permeable at small molecules [170].

The dynamic release has been used to measure the drug release kinetics from the lipid nanoparticles. In this process, the drug release is achieved by diffusion across the dialysis membrane while nanoparticle-bound drug is prevented to pass through the membrane [179, 180].

Experimental details

The optimized formulation was subjected to *in vitro* release studies using 80 mL of phosphate buffer at pH 7.4 or acetate buffer at pH 5 as dissolution medium (maintained at 37 ± 0.5°C and 32 ± 0.5°C), which is equivalent to the pH of the skin and inflamed skin respectively. *In vitro* release studies were performed using the dialysis bag method, modified to maintain a sink condition and achieve satisfactory reproducibility, as illustrated in Figure 3.7. 1.5 mL of MTX-loaded NLC dispersion containing 250 μg of MTX was first poured into the dialysis bag (molecular weight cut off 6,000–8,000 Daltons, CelluSep1 T2; Membrane Filtration Products Inc., Frilabo, Portugal) with the two ends fixed by thread and placed into the preheated dissolution media. The suspension was stirred at defined temperatures, using a heating and magnetic stirring plate (IKAMAG1, Staufen, Germany) at 350 rpm. One mL of the sample was withdrawn at fixed time intervals and the same volume of fresh medium was added accordingly. The drug content determined spectrophotometrically (Jasco V-660 spectrophotometer, USA), using a standard curve of MTX in phosphate buffered saline (PBS) pH 7.4 and acetate buffer pH 5. The mathematical models for evaluation of drug release kinetics: zero order, first order, Higuchi, Peppas-Korsmeyer and Hixon-Crowell were fitted to the experimental data [173]. Regression coefficient (r^2) was calculated to determine the best-fit model.

Figure 3.7 - Image representing the setup of an *in vitro* drug release assay.

3.14 Cell culture and viability assessment

Theoretical principle

Cell viability and cytotoxicity assays are used for drug screening and toxic assessment of a certain chemicals or formulation. They are based on various cell functions such as enzyme activity, cell membrane permeability, cell adherence and nucleotide uptake activity [174].

In this work we used an enzyme-based viability methods, the MTT assay, to evaluate cell viability. It is based in the reduction of the mitochondrial dehydrogenases activity (Figure 3.8) [174]. MTT is reduced to purple crystals of formazan [174].

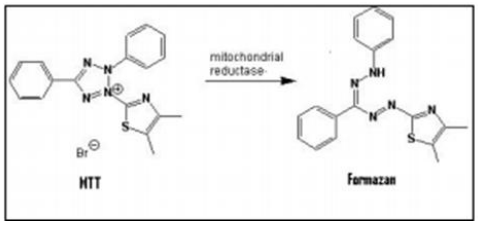

Figure 3.8 - Principle of the MTT assay.

Experimental details

Murine fibroblasts L929 from the American Type Culture Collection (Rockville, MD, USA) and HaCaT (human KC) were cultured in DMEM supplemented with 10% (v/v) FBS and 1% (v/v) penicillin-streptomycin. The cells were maintained in a humidified chamber at 37°C and 5% CO_2, and the cells were detached using a scraper when reaching 80% confluence. For assessment of the formulations effect on the cell viability a MTT assay was performed. Cells were cultured in 96-well plates at $5x10^4$ cells.mL^{-1} density and after 24-hours incubated with the all the lipid nanoparticles at different concentrations (ranging from 0.1-100 µg.mL^{-1} in MTX). Empty lipid nanoparticles were added at equivalent lipid concentration to the MTX-loaded lipid nanoparticles (15-250 µg mL^{-1}). Upon 24 or 48 hours of incubation, the culture medium was removed and replaced by 100 µL of MTT at 0.5 mg mL^{-1} in fresh culture medium. The plate was incubated for 3 hours at 37°C and formazan crystals were solubilized using 100 µL of DMSO. The absorbance (590 nm, 630 nm) was read using a Synergy™ HT Multi-mode microplate reader (BioTek Instruments Inc., Winooski, VT, USA).

3.15 Skin permeation studies

Theoretical principle

The assessment of molecules penetration through the skin is a crucial point in the evaluation and selection of drugs/ formulations for dermal or transdermal application [183, 184]. Several *ex vivo* and *in vitro* skin models with similarities with human skin, are frequently used to assess drug skin permeation profiles and kinetic parameters [175]. Also,

a wide range of animal models have been suggested as a suitable replacement for human skin such as primates, porcine, mouse, rat, guinea pig and snake models [175].

Anatomically and physiologically, pig skin is analogous to human skin. Indeed, pig *SC* is comparable to human *SC* in terms of lipid composition and the human viable epidermis is around 70 μm and the pig's from 66-72 μm [183, 185, 186].

Experimental details

To assess MTX permeation through the skin, samples of pig ear skin were mounted on standard Franz diffusion cells (Figure 3.9). The skin permeation of MTX, MTX-loaded NLCs/SLNs, void NLCs and functionalized-MTX loaded NLCs/SLNs were evaluated using a Franz cell assembly (9 mm unjacketed Franz Diffusion Cell with 5 mL receptor volume, o-ring joint, clear 216 glass, clamp and stir-bar; PermeGear, Inc., USA) [179]. The donor medium consisted of vehicle containing either free MTX or loaded on lipid nanoparticles systems, with an equivalent amount of 250 μg of MTX. In the receptor medium (4.7 mL) phosphate buffer, pH 7.4 containing 10% DMSO, added to maintain sink conditions. The available diffusion area between cells was 0.64 cm^2. The stirring rate and temperature of receptor were respectively kept at 600 rpm and 32±0.5ºC. At appropriate intervals, 500 μL aliquots of the receptor medium were withdrawn and immediately replaced with equal volumes of fresh buffer. The cumulative amounts of MTX permeated through the skin was determined by HPLC.

The quantification of MTX was conducted by HPLC rather than UV–vis spectrophotometer to overcome interferences from skin components released during the experiment. The HPLC system included MD-2015 multi-wavelength detector (Jasco, Easton, MD, USA) programmed for peak detection at 303 nm, a high-pressure pump (PU-2089), an autosampler (AS- 235 2057) and a controller (LC-Net II/ADC) mastered by ChromNAV software. A Chromolith 4.6-mm reversed-phase monolithic column (Merck, Darmstadt, Germany) connected to a guard column of the same material was used as a stationary phase. The MTX quantification was performed according to method previously described [180]. In particular, standard MTX solutions were prepared at 0.75, 1.5, 3, 6, 12.5, 25, 50 and 100 $\mu g.mL^{-1}$ in mobile phase and in permeation buffer enriched upon pig skin contact for defined times (1.5; 3; 4.5; 6 and 8 h).

Percentage of permeation of MTX through the skin was calculated by the next equation [181].

$$\text{Permeation } (\%) = \frac{\text{Drug amount in the receptor compartment}}{\text{Drug amount in the donor compartment}} \times 100 \quad , \tag{3.5}$$

Flux of MTX through the skin was obtained by applying the finite flux equation:

$$J = \frac{Q}{A \times t} \, , \tag{3.6}$$

where Q corresponds to the quantity of MTX traversing the skin in time t, with A being the area of exposed skin in cm^2 (in our study 0.64 cm^2, as previously stated).

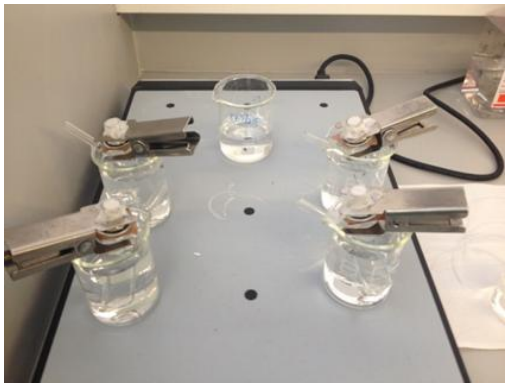

Figure 3.9 - Image of our skin permeation studies.

3.16 Hydrogel enriched with lipid nanoparticles

Theoretical principle

Currently, hydrogel enriched with nanoparticles have gained substantial attention as one of the most promising nanoparticulate drug delivery systems since it combines the characteristics of a hydrogel such their hydrophilicity, flexibility, versatility, high water content with the small size of nanoparticle [182].

Hydrogels are by definition polymeric networks with three-dimensional configuration, cross-linked with amounts of water or biological fluids. Their affinity to absorb water is attributed to the presence of hydrophilic groups in polymers forming hydrogel structures which allow chemical and biochemical modification resulting in many kinds of biopolymer-based materials. Due to their properties such good compatibility with tissues, ease of application and preparation, low cost, softness and excellent biocompatibility, hydrogels have been widely used in pharmaceutical and cosmetic applications. Their major disadvantage is their low mechanical strength [182]. Therefore, hydrogel was chosen in this work as a topical dosage form to add value for the topical therapy of PSO.

Carbomer is one of the polymers generally used in preparation of hydrogels with pharmaceutical applications. Carbopol® (made of carbomers) polymers are anionic polymers of acrylic acid, cross-linked. They are used as thickening, dispersing, suspending and emulsifying agents in pharmaceuticals and cosmetics [182], [183]. Their neutralized aqueous dispersions demonstrate high viscosity that decrease the turbidity of the dispersion and considerably increases its consistency. This occurs because the polymer chains elongates under the influence of electrostatic repulsion forces [182]. Specifically, Carbopol® 934, 940 and Ultrez 10 were reported by many to be of great applications pharmaceutically and cosmetically [184].

Experimental details

Hidrogels were produced using Carbopol® 934: a certain amount of polymer was hydrated in 25 mL of double-distilled water using a stirrer at a speed of 150 rpm overnight (Figure 3.10A).

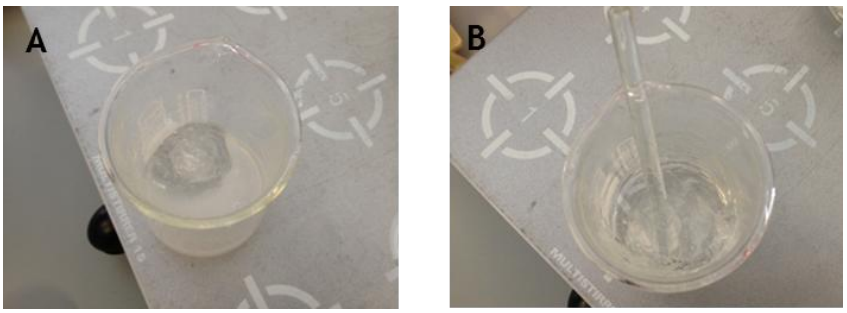

Figure 3.10 - Preparation of hydrogel. A) Carpobol hidratation B) NaOH neutralization.

NaOH solution (10%) was added dropwise to neutralize the solution until a transparent gel appeared and to confer a pH value within the range to 5.5-7.4, similar to the dermal conditions (Figure 3.10B). The pH was confirmed with universal pH strips. Because lipid nanoparticles suspension is liquid, different amounts of carbopol (Table 3.3) were tested in the hydrogels preparation. The gel with the concentration of carbopol that had the best consistency considering its spreadability and rheological behaviour was chosen, to incorporate the drug-loaded and void lipid nanoparticles functionalized and without functionalization.

Table 3.3 - Different concentration of carbopol® tested to prepare 25 g of hydrogel

	Gel 1	Gel 2	Gel 3	Gel 4
Carbopol® 934 (w/w%)	0.5	1	1.5	2
Double distilled water	25 mL			
NaOH solution (10%)	q.b to neutralize different concentrations of carbopol			

3.17 Hydrogel characterization

Theoretical principle

According to the definition, "Rheology is the science of the flow and deformation of matter under the effect of an applied force" that describe flow behavior through the viscosity, elasticity, and plasticity of liquid, solid and semisolid materials under physical deformations. [137, 138]. Rheological measurements provide useful information about interactions between nanostructures, vehicles and/or active compounds [138]. Viscosity is a measure of the internal resistance against flow [138,193]. The relation between viscosity and shear rate reveals the nature of the system which can be Newtonian or non-Newtonian (Figure 3.11)

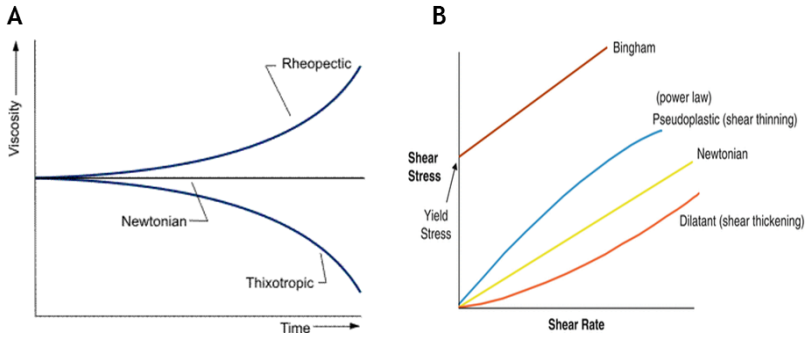

Figure 3.11- Non-Newtonian and Newtonian fluids. a) Non newtonian-time dependent b) Non newtonian-time independent behaviour. Adapted from [186].

A system is said to have Newtonian flow behavior when its viscosity is independent of shear rate, while in a non-Newtonian flow system the viscosity changes according to the rate of shear [139, 195]. Furthermore, Non-Newtonian systems can be viscoelastic, time-dependent (thixotropic or rheopectic) or time independent (plastic, pseudoplastic or dilatant) [140].

The time-dependent change in viscosity is the most wanted property in the pharmaceutical formulations due to their requirement of the flexibility in drug delivery and particularly thixotropy (rheological manifestation of viscosity exhibited by the pseudoplastic systems) is one of the most important property for topical applications of drugs. It represents phenomenon of the fluid which shows a reversible structural transition [188].

In viscosity measurements, Yield stress (τ_0) of a material can be defined as the minimum stress above which flow can be observed. Therefore, hydrogels or creams can be added to the liquid solid lipid dispersions and it gives rise at convenient dosage to obtain a topical application form [189].

Incompatibilities with ingredients from the hydrogel may occur due to interactions between the gel forming polymer, emulsifying agents, lipid and drug [198, 199] . Thus, its rheological studies are crucial in the development of a potential new drug delivery system for topical use because them can affect the semisolid consistency of the topical formulation [191]. Furthermore, the viscous and elastic properties of the dispersions are important for their application to skin [192].

Experimental details

Rheological measurements of the developed hydrogels were performed on a viscosimeter (Therme Haake VT550) equipped with a cone and plate test geometry (plate diameter 20 mm, cone angle 4°). All measurements were carried out at a temperature of 20 ± 0.1°C. The rheological properties were studied by continuous shear investigations, which were performed in order to evaluate the shear stress [Pa] as a function of shear rate [1/s]. The determination mode was set to flow-step measurement with shear rates from 0 to 500 1/s and back again to 0 1/s. The resulting shear stress and viscosity were measured.

3.18 Statistical analysis

Data is expressed as the mean ± standard deviation, for a minimum of three independent experiments. Statistical comparisons of the means were performed using one-way analysis of variance or Student's *t*-test with Welch's correction, Mean ± SD (n=3); * $p<0.05$, **$p<0.01$ obtained with one-way ANOVA analysis with GraphPad Prism 6 software (La Jolla, California, USA). The differences were considered to be significant when the *P*-value was < 0.05.

Chapter 4 - Results and discussion

4.1 Optimization of nanostructured lipid carriers loaded with methotrexate

Initial steps for formulation of MTX-loaded NLCs assessed the drug solubility in the solid lipids. Six lipids with different physicochemical properties were studied and MTX solubilized in Cetyl Palmitate, Imwitor 308, Lipocire™ CM and Witepsol® E85 with no drug crystals observed. So, the solid lipid Witepsol® E85 with a melting range above body temperature and exhibiting the higher solubility was selected to proceed with the optimization procedure.

Preliminary batches of NLCs were prepared to identify possible factors influencing the incorporation of MTX on NLCs, their size and polydispersity. The parameters studied were speed and time of sonication, type and amount of surfactant and optimum lipid loading in 10 mL of dispersion. Based on the preliminary formulation studies, three major variables affecting the particle size and drug EE of NLCs were identified: amount of liquid lipid, amount of surfactant and amount of drug.

4.1.1 Experimental design

Twenty seven experimental runs were conducted using full factorial analysis with a triplicate of the central point for estimation of the experimental error. The results could be shown in Table 4.1.

Table 4.1 - Formulation composition and the effect on different formulation variables on particle size (Y_1), polydispersity index (Y_2) and entrapment efficiency (Y_3) according full factorial design.

Sample	Factors			Responses		
	X_1 (mg)	X_2 (mg)	X_3 (mg)	Y_1 (nm)	Y_2	Y_3 (%)
1	40	40	2	257.9	0.066	67
2	40	40	10	275.9	0.079	92
3	40	40	20	258.6	0.067	95
4	40	50	2	261.2	0.073	65
5	40	50	10	275.4	0.072	91
6	40	50	20	263.4	0.089	95
7	40	60	2	261.8	0.078	68
8	40	60	10	273.9	0.055	89
9	40	60	2	258.4	0.052	95
10	50	40	2	257.2	0.09	65
11	50	40	10	282.9	0.033	89
12	50	40	20	266.6	0.062	95
13	50	50	2	286.1	0.051	66
14	50	50	10	265.5	0.088	89
15	50	50	20	285.4	0.039	95
16	50	60	2	242.3	0.062	61
17	50	60	10	239.8	0.091	89
18	50	60	20	255.5	0.085	90
19	60	40	2	290.3	0.042	54
20	60	40	10	291.7	0.058	90
21	60	40	20	284.2	0.041	94
22	60	50	2	243.7	0.108	60
23	60	50	10	262.2	0.067	89
24	60	50	20	256.5	0.092	94
25	60	60	2	260.8	0.056	52
26	60	60	10	257.4	0.084	58
27	60	60	20	275.2	0.069	88

Fifteen experimental runs were conducted using Box-Behnken design with a triplicate of the central point for estimation of the experimental error (Table 4.2)..

Table 4.2 - Formulation composition and the effect on different formulation variables on particle size (Y_1), polydispersity index (Y_2) and entrapment efficiency (Y_3) according Box-Behnken design

Sample	Factors			Responses		
	X_1 (mg)	X_2 (mg)	X_3 (mg)	Y_1 (nm)	Y_2	Y_3 (%)
1	40	40	10	275.9	0.079	92
2	60	40	10	291.7	0.058	90
3	40	60	10	273.9	0.055	89
4	60	60	10	257.4	0.084	58
5	40	50	2	261.2	0.073	65
6	60	50	2	243.7	0.108	60
7	40	50	20	263.4	0.089	95
8	60	50	20	256.5	0.092	94
9	50	40	2	257.2	0.090	65
10	50	60	2	242.3	0.062	61
11	50	40	20	266.6	0.062	95
12	50	60	20	255.5	0.085	90
13	50	50	10	265.5	0.088	89
14	50	50	10	250.0	0.069	88
15	50	50	10	269.9	0.087	88

Statistical analysis and calculated *p*-values were determined together with the fitting mathematical model involving the individual main effects and interaction factors are shown in Table 4.3. The positive sign before a factor revels that this response increases whereas the negative sign indicates that the response decreases with the factor. Interaction terms or quadratic relationships are represented by more than one factor or higher-order terms in regressions equations, respectively. It is also suggested non-linearity between factors and responses. A factor can produce a different degree of response when a factor is varied at different levels or more than one factor is varied simultaneously. The intercept correspond to the mean of the responses. Analysis of variance for the relevance of the model are shown in Table 4.4, where the model is statistically significant when F is higher that F_{critic} for all responses.

Effect on Particle Size

The particle size ranged from 242.3 nm (sample 10) to 291.7 nm (sample 2), with the selected levels of variables, while the mean was found to be 262.3 nm, which is the intercept of the model (Table 4.3). The most significant factors affecting particle size are the amount of surfactant (X_2) and amount of drug (X_3^2) (p<0.05). The amount of surfactant had a negative effect on particle size i.e, higher quantaties of surfactant gave rise a smaller size of particles. Higher amounts of surfactant may promote formation and stabilization of smaller particles due to the decrease in interfacial tension between the lipid and the external phase [193]. On the other hand, drug concentration has a positive effect, as expected, due to the rise molecular density in the inner phase. Interaction terms have non-statistically significant effects on Y_1.

Despite the significant effect of variables on particle size, and a correlation coefficient not as high as expected (r^2 0.863), the relatively small ranges of the responses support that the hot ultrasonication method is relatively robust to factor changes.

Table 4.3 - Summary of results of regression analysis for responses Y_1, Y_2 and Y_3

Parameter	Size (Y_1)		PDI (Y_2)		EE (Y_3)	
	Coefficient	*p*-value	Coefficient	*p*-value	Coefficient	*p*-value
Intercept	262.282	**0.000**	0.078	**0.000**	80.069	**0.000**
X_1	-3.009	0.334	0.005	0.150	-4.799	0.072
X_1^2	-3.431	0.157	-0.001	0.726	1.333	0.427
X_2	**-7.727**	**0.040**	0.000	0.922	**-5.494**	**0.048**
X_2^2	-3.031	0.202	**0.007**	**0.028**	1.708	0.319
X_3	4.700	0.155	-0.001	0.850	**15.375**	**0.001**
X_3^2	**6.492**	**0.026**	-0.004	0.164	**4.438**	**0.035**
X_1X_2	-8.075	0.097	**0.013**	**0.037**	-7.250	0.058
X_1X_3	2.307	0.585	-0.008	0.148	1.367	0.664
X_2X_3	1.086	0.795	**0.013**	**0.036**	0.110	0.972
R^2	**0.863**		**0.876**		**0.940**	

Effect on Polydispersity index

The PDI ranged from 0.055 (sample 3) to 0.108 (sample 6) (Tables 4.1 and 4.2), while the mean was 0.078 according to the model intercept (Table 4.3**)**. The only independent factor that seemed to influence on PDI is the amount of surfactant (X_2) since all the effects involving this variables were statistically significant (Table 4.3). The PDI value increases with the increase of surfactant concentration, probably in a non-linear relationship, as the *p*-value of the linear coefficient (X_2^2) was <0.05. In addition, the interaction terms involving the amount of surfactant (X_1X_2 and X_2X_3) are also significant (p<0.05). This phenomenon may be explained by the adsorption of PVA onto nanoparticle surface in a concentration dependent way, promoting aggregation due to its adhesive nature[193]. The same behavior may be achieved when two factor are changed simultaneously, i.e., increasing the amount of lipid (X_1) or the amount or drug (X_3).

Response surface analysis were plotted (Figure 4.1) based on the model polynomial function in a three-dimensional model depicting the effect of significant independent factors on the observed responses of particle size, PDI and EE.

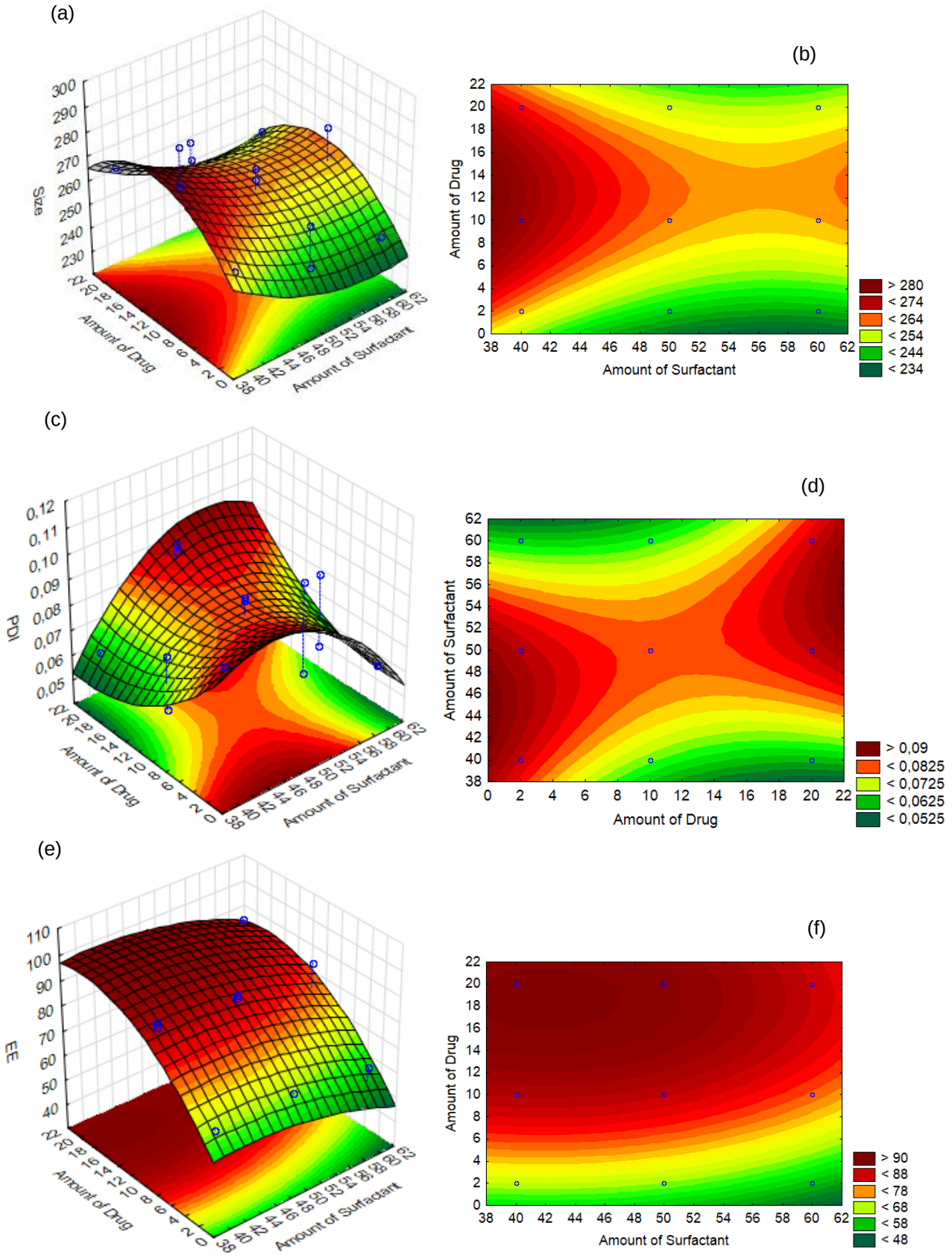

Figure 4.1 - Response surface and counter plots of Size (a,b) PDI (b,c) EE (d,e).

Table 4.4 - ANOVA results from particle size, polydispersity index and entrapment efficiency

Response	*Source*	*DF*	*Sum of squares*	*Mean of squares*	*F*	F_{critic}
Y_1	Model	9	19390.7000	1939.0700	30.8000	4.7700
	Error	5	3147.6980	62.9500		
	Cumulative total	14	22538.3980			
Y_2	Model	9	0.0027	0.0027	34.19	4.77
	Error	5	0.0004	0.0001		
	Cumulative total	14	0.0032			
Y_3	Model	9	2890.5920	2890.592	82.07	4.77
	Error	5	1761.0150	35220. 220		
	Cumulative total	14	2950.933			

Effect on entrapment efficiency

The EE varied from 58% (sample 4) to 95% (sample 7) for the level combinations (Tables 4.1 and 4.2, while the mean was 80.1%, according to the model intercept. The independent factors affecting EE were the amount of surfactant (X_2) and the amount of drug (X_3^2) (p<0.05), as seen in Table 4.3. The value of the correlation coefficient (r^2 0.940), indicating a good correlation between observed and predicted value.

The amount of surfactant has a negative impact on the EE, due the negative value of the regression coefficient, on the contrary of the amount of drug, which both coefficients (linear and quadratic) presented positive signs. This might indicate a non-linearity correlation between amount of drug and EE. The increase of EE in the presence of higher concentrations of drug was expected, as more drug is available to be entrapped. In the case of the surfactant level, the opposite was found, i.e., which could be explained by the partition phenomena, in which higher concentration of surfactant in the external phase might increase drug partition from internal to external phase, leading to drug solubilization. Interaction terms have non-significant effect on EE.

4.1.2 Optimization and validation

Desirability function of STATISTICA 10 was used to get the optimized formulation. Because the PDI was always below the desired value (<0.3), the formulation optimization were conducted regarding particle size (closer to 250 nm) and maximum EE [143]. Upon assessment of several responses and comprehensive search through desirability function, the composition of optimized formulation was 45 mg of liquid lipid, 47 mg of surfactant and 18 mg of drug, which fulfill the requirements of optimized formulations. Three repli-

cates of the checkpoint were analyzed. All the responses were considered to be in good agreement with the predicted values which confirmed on Figure 4.2. The optimized formulation has an average size of 252 ± 9 nm and an EE 87% ± 1%, which were in good agreement with the predicted values.

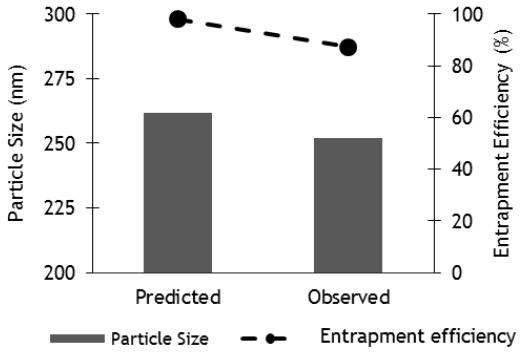

Figure 4.2 - Validation of the predicted optimal results with experimental values.

4.1.3. Physicochemical characterization of optimized NLC

Physicochemical characterization (size, polydispersity, surface potential, drug incorporation) was performed with optimized nanoparticles obtained throughout the experimental design. The results indicate that NLC size (246 ± 2 nm) increase with the incorporation of MTX to 252 ± 9 nm ($p<0.05$) and remaining homogenous, as suggested by the low values obtained for the PDI (<0.1). The optimized formulations exhibited a particle size below 300 nm, suitable for systemic and topical administrations [194]. It has been described that PDI values below 0.3 are indicative of homogeneity of the size distribution and with minimum tendency to aggregation [143]. These results are shown in Table 4.5.

Table 4.5 - Particle size, PDI, ζ-potential, drug entrapment efficiency of optimized NLCs

	Size (nm)	PDI	ζ-potential (mV)	EE (%)
NLC	246 ± 2	0.09 ± 0.02	-13 ± 2	
MTX loaded-NLC	252 ± 9*	0.06 ± 0.02	-14 ± 1	87 ± 1

Mean ± SD (n=3), *$p<0.05$

In order to confirm the incorporation of MTX in the NLCs infrared spectra of free MTX, NLC and MTX-loaded NLC were obtained, and are presented on Figure 4.3. MTX spectrum shows, at 1,638 cm^{-1}, a marked peak that indicates the presence of a C=C stretching vibration, which is characteristic of the drug molecule [195], [196]. This observation was present also in the MTX-loaded NLC, but not in the NLC, confirming the successful incorporation of MTX in the lipid nanoparticles. The characteristic peaks from NLC were not altered in the MTX-loaded NLC.

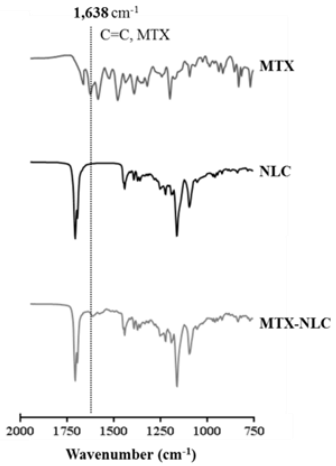

Figure 4.3 - FT-IR spectra of raw MTX powder and lyophilized nanoparticles NLCs and MTX-loaded NLCs.

4.1.4 Morphology of optimized NLCs

TEM studies revealed that MTX-loaded NLCs were spherical in shape with narrow size distribution (Figure 4.4). NLCs did not aggregated and no visible significant differences were observed between NLCs and MTX-loaded NLCs. The diameters of the particles observed by transmission microscopy (c.a. 250 nm) are in good agreement with the data obtained from dynamic light scattering (Table 4.5).

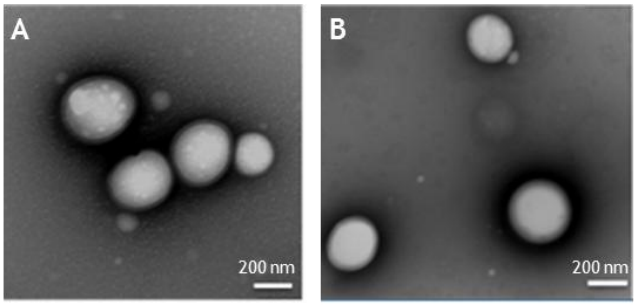

Figure 4.4 - Transmission electron microscopy images of NLCs (A) and MTX-loaded NLCs (B). Amplification of 80,000 x.

4.1.5 Storage stability assessment of optimized NLCs

Physical stability was assessed by analyzing changes in particle size, PDI and drug content of NLCs stored at room temperature. For all samples no particle aggregation was found through visual observations, up to 4 weeks. The stability studies of MTX-loaded NLCs suggested that these nanoparticles were quite stable for a month with no significant change in the mean particle size and drug content (Figure 4.5). As a broad conclusion, NLCs presented good stability after 4 weeks with average particle size between 211.5- 264.3 nm, PDI below 0.2 and EE remains higher than 85%.

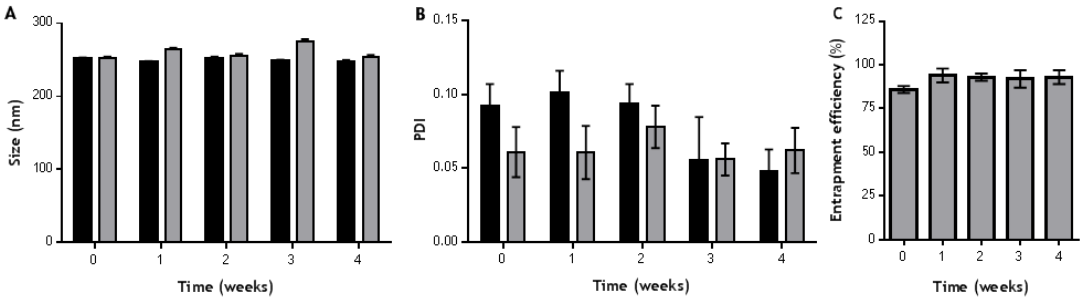

Figure 4.5 - Storage stability. Optimized MTX-loaded NLC were stored up to 4 weeks at room temperature and evaluated for (A) size, (B) polydispersity and (C) drug entrapment efficiency alterations. Unloaded (dark grey) and MTX-loaded (light grey). Data expressed as mean ± SD (n=3).

4.1.6 *In vitro* methotrexate release studies of optimized NLCs

The *in vitro* of MTX release profile from the NLCs was investigated using a dialysis membrane in three conditions defined to simulate physiological, inflammatory and topical environments in order to simulate a systemic therapy, inflammatory and skin environments they are closely related present in inflammatory diseases such or rheumatic arthritis and PSO, respectively. In Figure 4.6 shows the release profiles obtained that were further analyzed to determine the mechanism of release using the kinetic models first-order, Higuchi, Peppas-Korsmeyer and Hixson-Crowell.

Release simulation at physiological conditions

In vitro MTX release studies from the NLCs were performed at physiological conditions (37ºC, pH 7.4) to access the release profile upon systemic administration. The NLC formulations showed an initial fast release, the release reach 30% in 2 hours, followed by a sustained release up to 50% within 24 hours (Figure 4.6). The observed profile was analyzed by several drug release kinetic models Table 4.6, and fitted best to the Peppas-Korsemeyer model (r^2=0.9771), since the r^2 value is much higher than any other kinetic model. In this model, the value of *n* characterizes the release mechanism of drug. For the present case *n* was 0.55, indicative of non Fickian diffusion, as a combination of both diffusion and erosion controlled rate release [197].

Release simulation at inflammatory conditions

MTX is considered a reference drug for rheumatoid arthritis. We performed an *in vitro* release study simulating the inflammatory conditions (37°C, pH 5) in order to predict the MTX-loaded NLC *in vivo* kinetics [198]. The drug release from the formulation under this conditions exhibited a fast initial release (40% in 2 hours) followed by a sustained release up to 80% within 24 hours (Figure 4.6). Data fitted best to the Peppas-Korsemeyer model (r^2=0.9865) with an *n* value of 0.31, suggesting Fickian diffusion that occurs by the usual molecular diffusion of the drug.

Table 4.6 - Value of r^2 obtained from the release data for different models of mechanism of drug release

	Model	32°C	37°C	*n*
	First order		0.2860	
pH	Hixson-Crowell		0.2656	
7.4	Higuchi		0.5614	
	Korsmeyer-Peppas		**0.9771**	0.545
	First order	0.2380	0.4575	
pH	Hixson-Crowell	**0.9290**	0.7679	
5.5	Higuchi	0.7096	0.8901	
	Korsmeyer-Peppas	0.6389	**0.9865**	0.313

Release simulation at skin conditions

Topical administration of MTX could represent an interesting approach for skin inflammatory diseases, as PSO. Release conditions were set to simulate the drug administration through the skin (32ºC, pH 5). A slow release of the MTX from the NLC was observed reaching 30% after 24 hours (Figure 4.6). In this case, data fitted best to the Hixson-Crowell model (r^2=0.9290), that describes the drug releases by dissolution mechanism that occurs upon a change in surface area and diameter of particles [197]. A prolonged release is of interest for dermal formulations as it will contribute to a sustained effect.

Gathering the release studies data it is possible to consider the NLCs formulations suitable for systemic and topical administration of MTX under physiological and inflammatory conditions, conferring protection and allowing drug controlled release.

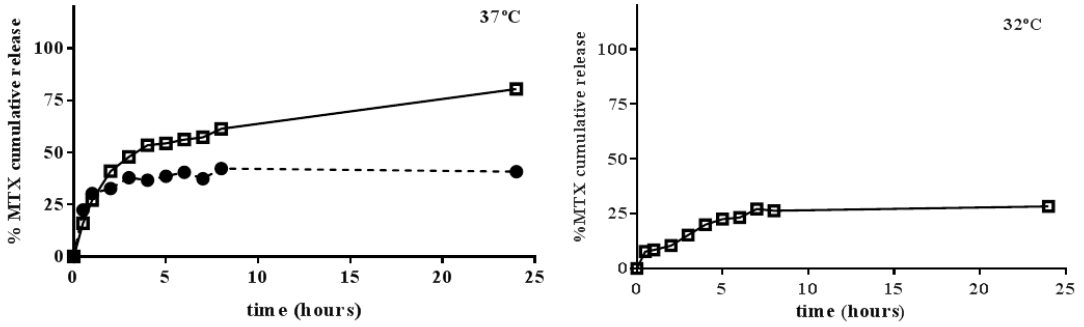

Figure 4.6 - MTX in vitro release from NLCs. On the left, drug cumulative release under physiologic (dark circles) and inflammatory environments (open squares). On the right, release simulation at skin environment. Data expressed as mean ± SD (n=2).

4.1.7 Cytotoxicity of the optimized formulation

To assess the effect of the formulations on cell viability, a MTT assay was performed on L929 fibroblasts. Cells were exposed to empty NLCs and MTX-loaded NLCs up to 250 $\mu g.mL^{-1}$ of MTX equivalent to 27 $mg.mL^{-1}$ in lipid for 24 and 48 hours. The fibroblasts tolerate well empty formulation as no toxicity was observed. While for MTX-loaded NLCs a slight effect on the viability of cells was observed in the presence of 250 $\mu g.mL^{-1}$ MTX-

loaded NLCs after 48 hours incubation. As for all studied conditions cell viability was above 80% it can be stated that the formulations are not toxic to the fibroblasts Figure 4.7. The NLC system represents a promising option for delivery of MTX, since it did not affect cell viability, confirming the safety profile of the optimized delivery system.

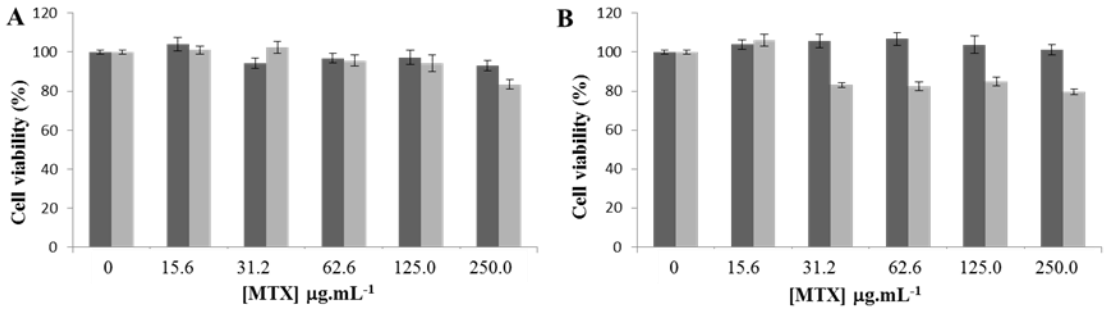

Figure 4.7 - Fibroblasts viability. Unloaded (dark grey) and MTX-loaded (light grey) NLCs incubated with fibroblasts for (A) 24 and (B) 48 hours. Data expressed as mean ± SD (n=3).

This lipid colloidal carrier show interesting properties for delivering MTX. Although further studies are required in order to evaluate the therapeutic potential of the optimized formulation in clinically relevant models, present result demonstrated that MTX loaded NLCs could be a promising modality for cancer and inflammatory diseases.

4.2 A targeted nanomedicine approach for psoriasis

To implement a targeted nanomedicine approach for topical therapy of psoriasis, lipid nanoparticles loaded with an anti-psoritic drug (MTX) where functionalized with an antibody targetting the inflammatory environment (Etanercept). It is expected to produce a dual drug delivery systmes, where MTX act as an anti-inflammatory drug and Etanercept suppress overactivity of the immune system. We used a carbodiimed reaction through the cross linker (EDC) and the lipid DSPE-PEG-NH_2. To improve its potential topical application a hydrogel will be prepared. Indeed, currently hydrogel enriched with nanoparticles have gained substantial attention as one of the most promising nanoparticulate drug delivery systems since it combines the characteristics of a hydrogel such their hydrophilicity, flexibility, versatility, high water content with the small size of nanoparticle [182].

4.2.1 Physicohemical characterization

Characterization was performed with empty lipid nanoparticles or loaded with MTX, before and after functionalization with eternecept.

The results indicate that all samples presented sizes closer to 400-nm with a slight increase after incorporation of MTX. There are significant differences ($p<0.05$) in particle

size when compared LNs to MTX-LNs and LNs-Etanercept to MTX loaded LNs-Etanercept maybe due to the decrease of inertial and hydrodynamic forces and the increase of aggregate strength with decreasing particle size [199]. With respect to PDI, all of the samples remaining homogenous also, as suggested by the low values obtained for the PDI (<0.3) [143]. Zeta potential was around -28 mV and the EE was more than 83%, suggesting the stability of this nanoformulations. These results are shown in Table 4.7.

Table 4.7 - Particle size, PDI, ζ-potential, drug entrapment efficiency of lipid nanoparticles

	Size (nm)	PDI	ζ-potential (mV)	EE (%)
NLC	421.6±2.2	0.278±0.005	-29.04±0.63	83.1 ±0.8
MTX loaded-NLC	458.3±5.0*	0.280±0.007	-23.53±0.60	
NLC-Etanercept	394.0±2.9	0.256±0.007	-24.85±0.76	
MTX loaded-NLC-Etanercept	443.0±4.6**	0.216±0.015*	-27.03±0.74	88.6±1.0*
SLN	396.5±4.2	0.270±0.009	-30.30±0.34	
MTX loaded-SLN	492.9±6.2*	0.268±0.001	-26.23±1.14	84.2±0.2
SLN-Etanercept	316.9±3.2	0.262±0.008	-30.55±0.82	
MTX loaded-SLN-Etanercept	356.4±2.0*	0.274 ± 0.007	-25.95 ± 1.13	88.1±0.7

Mean ± SD (n=3); * p<0.5, **p<0.01 obtained with one-way ANOVA analysis, Dunett test for comparison amoung LNs and F-LNs.

4.2.2 Morphology of targeted-lipid delivery systems

TEM and Cryo-SEM microscopies revealed that all of nanoformulations were spherical in shape with narrow size distribution and no visible differences between the LNs produced, as shown on Figures 4.8 and 4.9

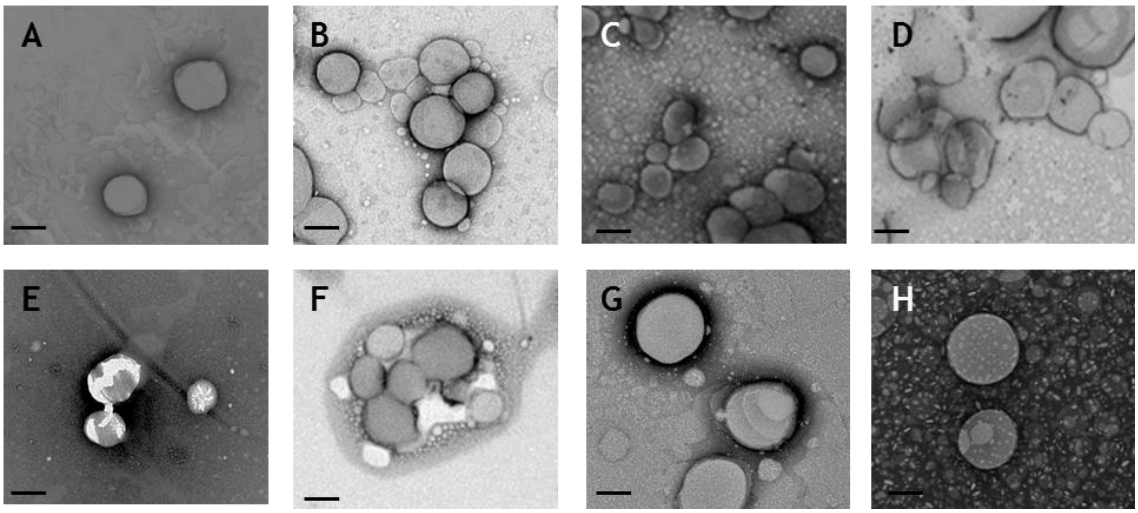

Figure 4.8 - Transmission electron microscopy of targeted SLNs and NLCs. On top panel empty SLNs (A), MTX-loaded SLNs (B), SLN-Etanercept (C) and MTX-loaded SLN-Etanercept (D); bottom panel: empty NLCs (E), MTX-loaded NLCs (F), NLCs-Etanercept (G) and MTX-loaded NLCs-Etanercept (H); the scale indicated pictures is of 100 nm. Amplification: 50,000x

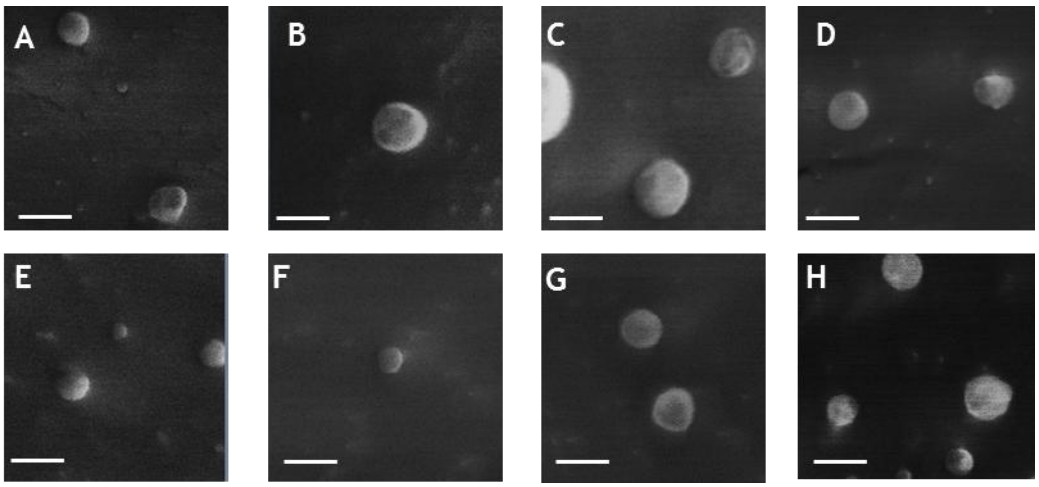

Figure 4.9 - Cryo-SEM microscopy of targeted SLNs and NLCs. On top panel empty SLNs (A), MTX-loaded SLNs (B), SLN-Etanercept (C) and MTX-loaded SLN-Etanercept (D); bottom panel: empty NLCs (E), MTX-loaded NLCs (F), NLCs-Etanercept (G) and MTX-loaded NLCs-Etanercept (H); the scale indicated pictures is of 300 nm. Amplification: 40,000x.

4.2.3 Protein coupling efficiency

The efficacy of Etanercept functionalization in the different prepared NLCs (empty and MTX loaded) and SLNs (empty and MTX loaded) was determined by Bradford method. The coupling efficiency indicates the amount of protein covalently bound to the lipid nanoparticle upon functionalization and is shown in Table 4.8. The results reveal that more than 78% of Etanercept initially added was bound to the LNs. Coupling efficiency with BSA revealed similar values with more than 82% of protein coupled to the LNs.

Table 4.8 - Protein coupling efficiency

Samples	Coupling efficiency (%)
NLC-Etanercept	94.3±0.1
SLN-Etanercept	78.4±0.2
MTX loaded-NLC-Etanercept	89.2±0.1
MTX loaded-SLN-Etanercept	90.6±0.2
NLC-BSA	95.6±0.4
SLN-BSA	90.1±0.6
MTX loaded-NLC-BSA	92.5±0.4
MTX loaded-SLN-BSA	82.4±0.2

4.2.4 Storage stability assessment

Physical stability was assessed by analyzing changes in particle size, PDI, zeta potential and drug content of lipid nanoparticles compared to freshly prepared nanoparticles, when stored at room temperature up to 6-weeks. For all samples no particle aggregation was found through visual observations. Data from size, PDI and surface potential analysis is represented on Figure 4.10 and shows no significant changes were observed upon storage.

Moreover, drug content remained similar to the observed upon preparation. With respect to size of nanoparticles and PDI parameters, all nanoformulations presented no statistical differences in first 4 weeks. However, for SLN at 6 weeks there are differences in size and PDI Figure 4.10 A and B. In zeta potential parameter after incorporation of MTX at week 0 for MTX-loaded NLC observe a decrease of this parameter. However this result may be associated with wrong measurment because previously conclude that durg incorporation no affect zeta-potential of nanoparticles. Relatively at drug content no significant diferrences were observed.

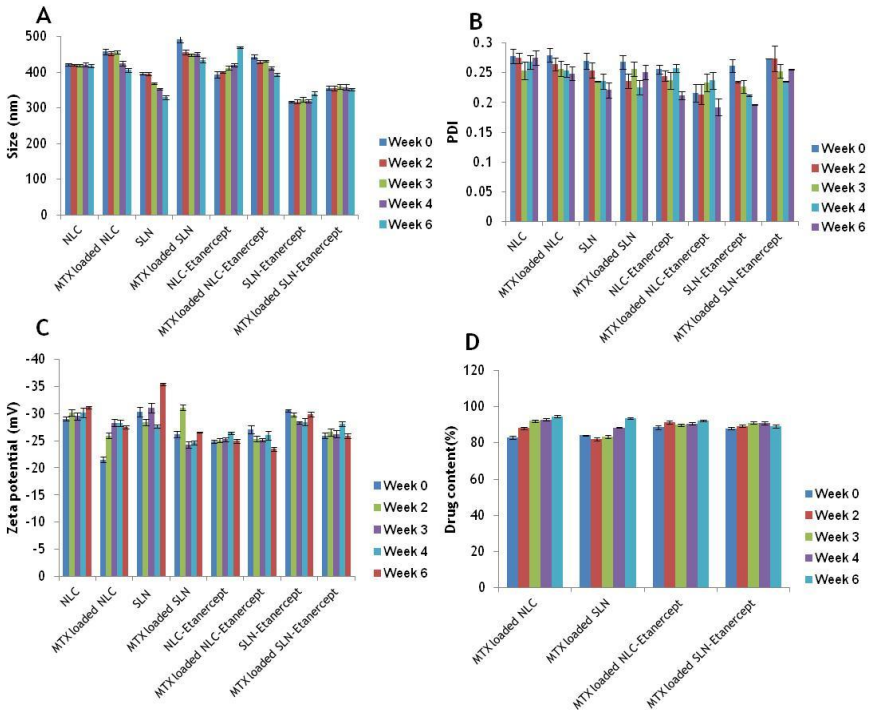

Figure 4.10 - Storage stability at room temperature for lipid nanoparticles. Empty and MTX-loaded SLNs and NLCs prior and after Etanercept-functionalization were stored at room temperature and assessed for stability parameters: size (A), PDI (B), zeta-potential (C) and drug content (D) for 6 weeks.

4.2.5 *In vitro* methotrexate release studies

Controlled drug release was observed for all studied nanoformulations. MTX gave a fastest drug release in the first 24 hours: 35-40% of its initial content was released in the first 2 hours and a sustained release around 49-60%, after 24 hours in physiologic environment; a 20-30% of its initial content was released within 2 hours while 50% was relased during 24 hours in inflamatory environment; and, in skin conditions a 20-30% was released in the first 2 hours and then a sustained release in 24 hours of 52-60% (Figure 4.11). A similar behavior was observed for all studied nanoparticles, displaying a biphasic profile that was described by an initial fast drug release followed by a sustained profile. The fast MTX release revealed in all nanoformulations can be explained by interactions stablished between drug-lipid in the LNs. The sustained release stage may be related with a diffusion-controlled mechanism provided by the lipid matrix: at first, MTX was effectively dissociated from the matrix and then diffuses to the external environment [200]. NLC and SLN formulations did not show significant differences between them as observed in Figure 4.11. Only MTX-loaded NLC-Etanercept nanoparticles, under skin stimulated conditions, released less drug when compared with non-functionalized NLCs (Figure 4.11F). This fact can be

explained due to structural integrity conferred by protein coupling (Etanercept) that might lead to a double barrier effect interfering negatively in drug diffusion [201].

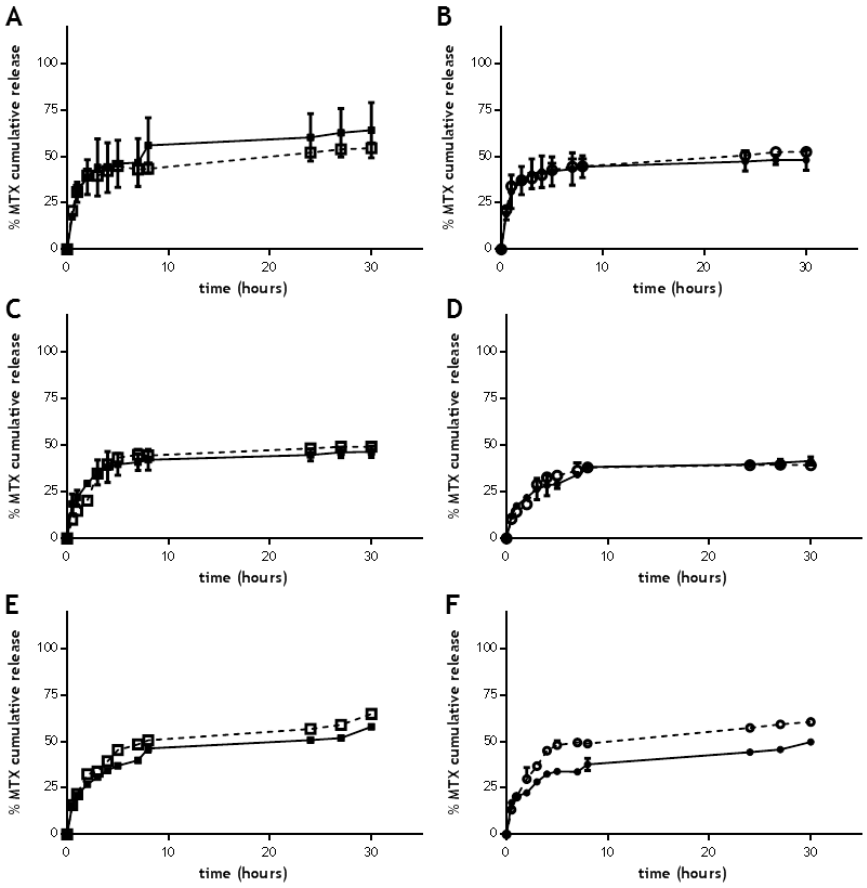

Figure 4.11 - MTX *in vitro* release from targeted lipid nanoparticles. The assays were conducted under simulated physiologic (37ºC, pH 7.4 – A and B), inflammatory (37ºC, pH 5 – C and D) and skin (32ºC, pH 5 – E and F) environments. Data expressed as mean ± SD (n=2) represents MTX-loaded SLN (open squares), MTX loaded SLN-Etanercept (closed squares) on graphs A, C and E; and MTX-loaded NLC (open circle), MTX-loaded NLC-Etanercept (closed circle) on graphs B,D and F .

The release profiles of the studied formulations were evaluated by fitting the experimental data to different kinetic equations (zero-order, first-order, korsemeyer-peppas, Hixson-Crowel and Higuchi equation) which are widely used in determining the release kinetics of lipid nanoparticles. The best kinetics of release profile of nanoparticles was found following korsemeyer-peppas model having the highest value of correlation coefficient r^2 (Table 4.9 and Table 4.10).

The parameter "*n*" in the Korsmeyer-Peppas equation is related to the mechanism of release of the drug, i.e. if the exponent n < 0.43, then the drug release mechanism is Fickian diffusion, if 0.43 < *n* < 0.85, then it is non-Fickian or anomalous diffusion and an exponent value is 0.85 or greater is indicative of Case-II Transport or typical zero-order release [209, 210].

In this case all formulations give a value of *n* below 0.45, so their release mechanism followed a Fickian diffusion.

This model, also known Power law has been used to describe the drug release from several different pharmaceutical modified release dosage forms [204].

Table 4.9 - Value of r^2 obtained from fit of different mathematical models of mechanism of drug release to the MTX release data from the SLNs nanoformulations

		Mathematical model	MTX-SLN	MTX-SLN-Etanercept
37ºC	**pH 7.4**	First order	0.4951	0.6233
		Hixson-Crowell	0.7104	0.7662
		Higuchi	0.5438	0.7059
		Korsmeyer-Peppas	**0.8275**	**0.8990**
		n	*0.21*	*0.31*
	pH 5.5	First order	0.8742	0.8645
		Hixson-Crowell	0.9373	0.9316
		Higuchi	0.9261	0.7854
		Korsmeyer-Peppas	**0.9502**	**0.9785**
		n	*0.45*	*0.29*
32ºC	**pH 5.5**	First order	0.8979	0.9246
		Hixson-Crowell	0.9564	0.9825
		Higuchi	0.9340	0.9246
		Korsmeyer-Peppas	**0.9857**	**0.9941**
		n	*0.39*	*0.37*

Table 4.10 - Value of r^2 obtained from fit of different mathematical models of mechanism of drug release to the MTX release data from the NLCs nanoformulations

		Mathematical model	MTX-NLC	MTX-NLC-Etanercept
37ºC	**pH 7.4**	First order	0.5615	0.5228
		Hixson-Crowell	0.7138	0.7415
		Higuchi	0.5766	0.5863
		Korsmeyer-Peppas	**0.9137**	**0.9275**
		n	*0.21*	*0.23*
	pH 5.5	First order	0.8989	0.8603
		Hixson-Crowell	0.9582	0.9546
		Higuchi	0.9182	0.8676
		Korsmeyer-Peppas	**0.9865**	**0.9857**
		n	*0.45*	*0.38*
32ºC	**pH 5.5**	First order	0.8989	0.8603
		Hixson-Crowell	0.9582	0.9546
		Higuchi	0.9182	0.8676
		Korsmeyer-Peppas	**0.9865**	**0.9857**
		n	*0.45*	*0.38*

4.2.6 Cytotoxicity of targeted nanoparticles

To evaluate the effect of the functionalization and the other nanoformulations on cell viability, a MTT assay was performed on L929 fibroblasts and HaCaT KC (Figure 4.12).

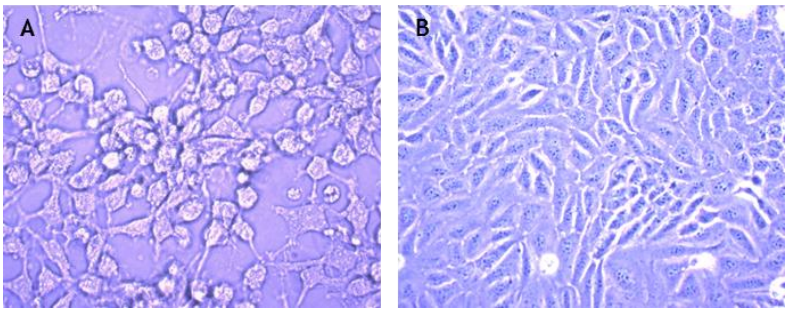

Figure 4.12 - L929 fibroblasts and HaCaT keratinocytes cells. Amplification of 40x.

Cells were exposed to empty LNs and MTX-loaded LNs with or without functionalization up to 250 $\mu g.mL^{-1}$ of MTX equivalent to 5 $mg.mL^{-1}$ in lipid for 24 hours. Free MTX was appied in HaCaT cell line and was observed a decrease on cells viability to 75% with 250 $\mu g.mL^{-1}$.

The fibroblasts and HaCaT tolerate well empty formulation as no toxicity was observed After incoporation of MTX in the presence of 250 $\mu g.mL^{-1}$ cell viability was reduced for 80% in both cell lines after 24h.

After Etanercept functionalization in nanoparticles loaded with MTX a slight effect on the viability of cells was observed and this parameter was reduced for 70%. As for all studied conditions cell viability was above 80% it can be stated that these nanoformulations and its functionalization is no toxic for both types of cells. So, these lipid system represents a promising option for delivery of MTX, since concentrations of MTX closer to 100 $\mu g.mL^{-1}$ no affect cell viability, confirming the safety profile of the delivery system.

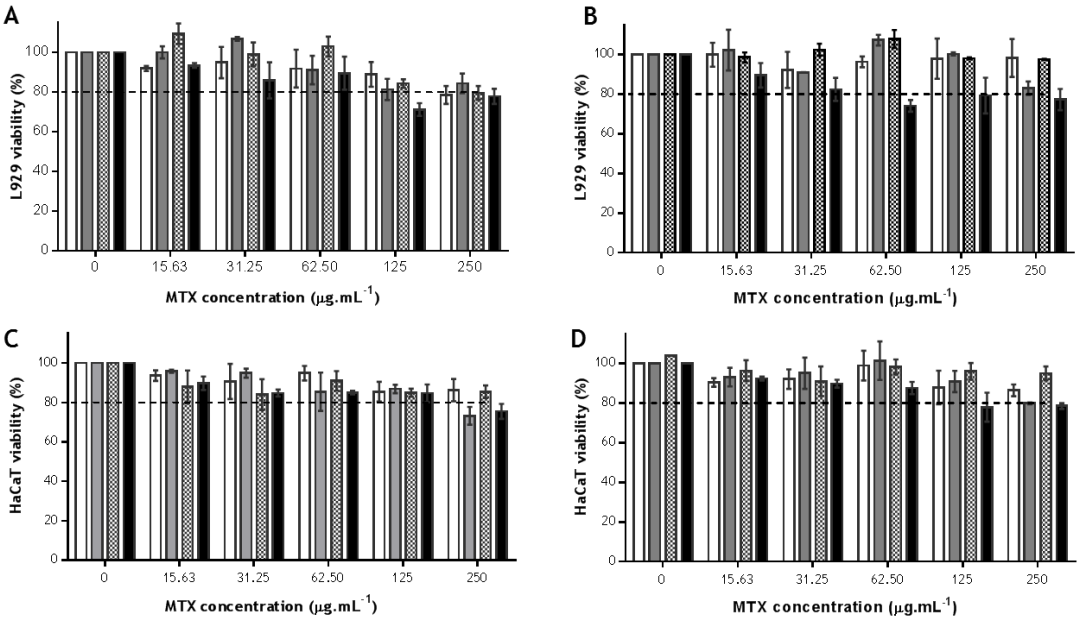

Figure 4.13 - L929 fibroblasts and HaCaT keratinocyte cell viability. Unloaded LNs (white bar), MTX-loaded LNs (light grey bar), Etanercept-functionalized LNs (squares bar), and MTX-loaded LNs-Etanercept (black bar) were incubated with fibroblasts (A, B) and keratinocytes (C, D) for 24 hours. The dotted line at 80% represents the viability limit defined. Data expressed as mean ± SD (n=3).

4.2.7 Rheological properties of hydrogel-enriched nanoparticles

In this work, we tested four different concentrations of Carpobol 934 (0.5; 1; 1.5 and 2% (w/w)) corresponding to 0.125, 0.250, 0.375 and 0.5 g of Carbopol 934® for 25 g of hydrogel. For all of these concentrations all hydrogels presented a clear, glossy and homogeneous aspect. However as LNs are liquid we had to exclude carbopol with lower concentrations, i.e., at 0.5 and 1% (w/w). In order to choose between Carbopol 1.5 and 2% we tested the addition of 10 mg of empty LNs. Upon the hydrogel enriched-nanoparticles preparation the rheological properties, namely shear stress and viscosity, were studied. The flow curves shown in Figure 4.14. A represent the two different concentrations of carbopol (1.5 and 2%). The different curves relate the measurement of shear stress (Pa) with increasing shear rate (1/s), and measurement of shear stress (Pa) with decreasing shear rate (1/s). It is possible to observe that ascending and descending curve of each hydrogel practically did not overlap, which indicates the existence of thixotropy (reflects a degradation behaviour of the semisolid structure after application of the shear stress and posterior returns to the initial apparent viscosity [205].

Furthermore, we can see in Figure 4.14 that two differente carbopol concentrations possess pseudoplastic characteristics, as the viscosity decreases with the increase of shear rate. Pseudoplastic properties are a desired of topical systems because at high shear stresses the material will flow rapidly [205]. For LNs incorporation we choose the Carbopol

1.5% due to its better spreadability properties as observed in the Figure 4.14 with a lower value of shear stress.

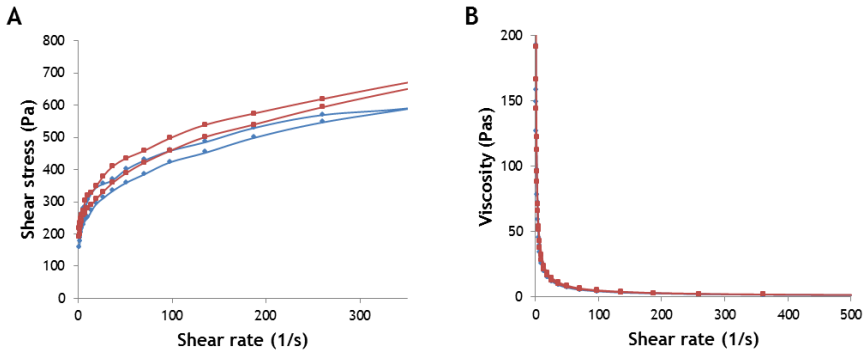

Figure 4.14 - The flow curves of carbopol gel placebo (A) Shear stress and (B) viscosity in blue Carbopol 1.5% and in red 2% of Carbopol.

Hydrogel 1.5% carbopol was enriched with 6 mg of free MTX and the rheological properties are shown in Figure 4.15. It is possible to observe that the hydrogel enriched with MTX did not retained thixotrophy. Flow curves are totally overlapped Figure 4.15A which indicates that MTX completely changes the hydrogel structure with respect to its thixotrophy. This results hampers the use of Carbopol 1.5% as carrier of free MTX in topical applications because it changes the thixotropic properties of the hydrogel base [188].

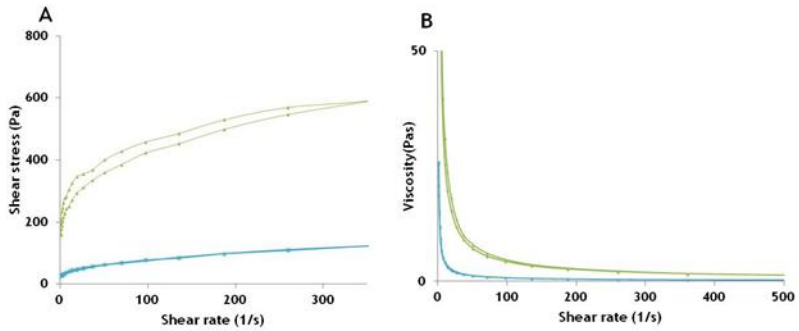

Figure 4.15 - The flow curves of carbopol gel enriched with MTX. (A) Shear stress and (B) viscosity in green Carbopol 1.5% and in blue Carpobol 1.5% - enriched MTX.

The rheological behavior of hydrogel carbopol 1.5%, enriched with empty and MTX-loaded SLN or NLC nanoparticles is presented in Figure 4.16. For all the hydrogels enriched with the LN produced it is possible to observe that curves did not overlap (Figure 4.16 A,B), which indicates the existence of thixotropy such as observed with carbopol placebo gel . The hysteresis loop reveals that the area of thixotropy is similar for all formulations.

However, empty and MTX-loaded NLCs seemed to present a greater area of thixotropy when compared with hydrogel enriched with SLNs, which means that NLCs containing hy-

drogels are easily spreadable in the skin. This result is also supported by the yield stress values (Table 4.11).

Table 4.11 - Yield stress values for all hydrogels

Hydrogel	Yield stress(τ_0-Pa)
Carbopol 1.5%	158.3
Carbopol 2%	191.0
SLN	198.4
NLC	176.2
MTX loaded SLN	248.2
MTX loaded NLC	185.8
SLN- BSA	240.5
NLC- BSA	198.4
MTX loaded SLN-BSA	207.2
MTX loaded NLC-BSA	169.6

The intersection on the stress axis is then taken as the yield stress, the assumption being that any stress below this is insufficient to cause the sample to flow. In general, lower values of the yield stress increase spreadability. Data of yield stress shows that hydrogel with Carbopol 1.5% have lower values of yield stress when compared with hydrogel carbopol 2%. Also, hydrogels enriched with NLC have lower yield stress values compared to SLN, so could represent the best choice for topical administration. For hydrogels containing MTX-loaded LNs, the yield stress value increases in comparison to the empty LNs, meaning that at is necessary more shear in the gel when drug is present, to cause the gel to flow. Furthermore, it was observed that all hydrogels mantained their pseudoplastic properties (Figure 4.16).

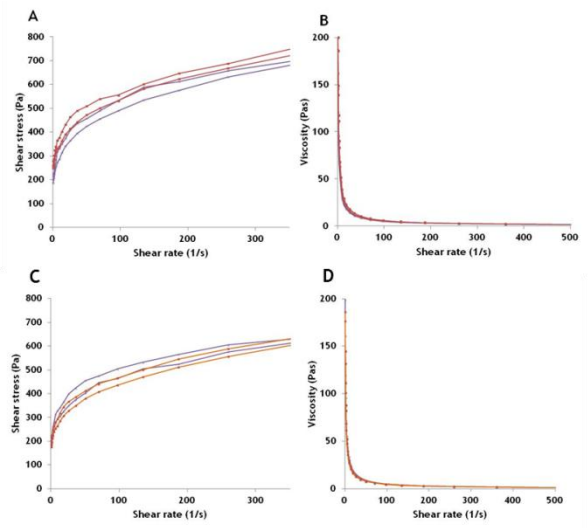

Figure 4.16 - Flow curves for hydrogel enriched LNs. (A) shear stress and (B) viscosity top images: in purple SLN and in red MTX loaded SLN; bottom images: purple NLC and orange MTX loaded NLC.

Figure 4.17 shows the pseudoplastic properties of hydrogels enriched with functionalized LNs. Results indicated that all of formulations maintaining thixotropy. Functionalized NLCs exhibit lower yield stress values compared to functionalized SLNs, as observed with the non-targeted LNs. Hydrogel enriched with functionalized NLCs represent a good choice for topical applications due to lower values of yield stress (Table 4.11), that is, higher spreadability. The hydrogels incorporating emtpy nanoparticles have higher spreadability than when MTX is present, as indicated by a higher area of thixitropy. The presence of drug, lowers these parameter translating a decreased ability of these two types of hydrogels to return of their initial properties, after application of shear stress. This could be explained because functionalization increase the viscosity of nanoparticles due to the aggregation of protein [213, 214].

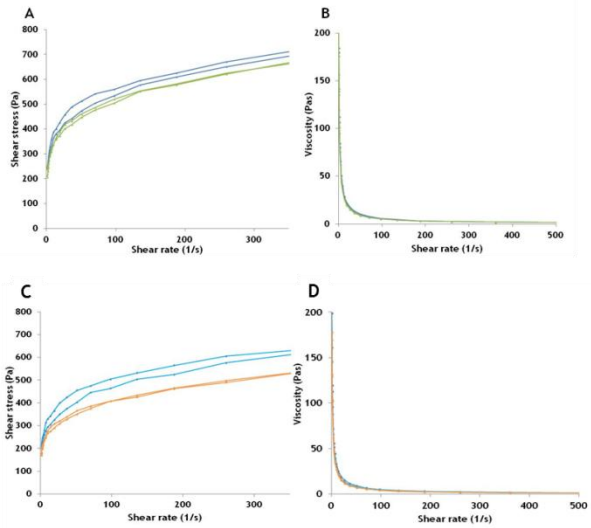

Figure 4.17 - Flow curves for LNs. (A) shear stress and (B) viscosity Top images: blue with SLN-BSA and green wit MTX loaded SLN-BSA and bottom images: ligth blue with NLC-BSA and orange with MTX loaded NLC-BSA.

4.2.7.1 Storage stablity of hydrogel enriched nanoparticles

Storage stability of hydrogel and -hydrogel enriched nanoparticles was assessed after 2 weeks of preparation. All of hydrogels appeared transparent, glossy and uniform within this period of time. Furthermore, their rheological parameters were measured in order to investigate any changes in the pseudoplastic properties and thixotropy. Figure 4.18 shows that no differences were observed in the hydrogel carbopol 1.5 and 2% between 0 an d 2 weeks storage at room temperature, as all curves are practically overlapped.

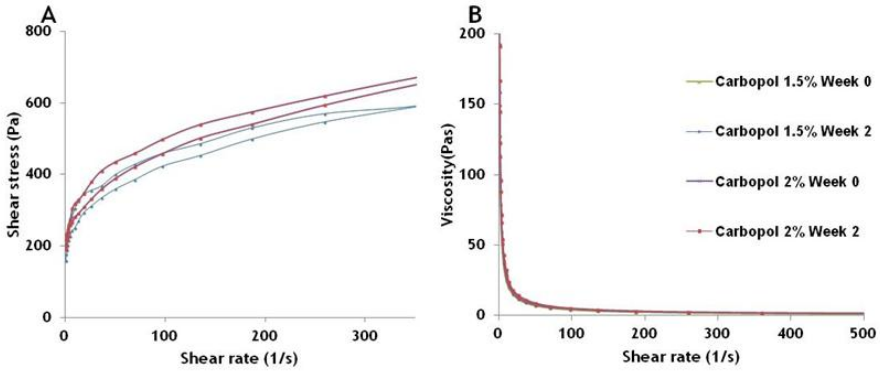

Figure 4.18 - The flow curves of carbopol gel placebo (A) Shear stress and (B) viscosity in blue Carbopol 1,5% and in red 2% of Carbopol at 0 and 2 weeks.

Rheological measurements after 2 weeks in hydrogels enriched LNs (with and without drug, functionalized or not) confirmed the reported values of low viscosity at week 0. Flow curves illustrated in Figure 4.19 and Figure 4.20 for LNs and functionalized LNs, respectively, revealed similar psedoplastic behaviour as showed in week 0 as all formulations presented thixotropy, reversible variation of viscosity. However, in shear stress along the time, we could see a small decrease of this value in two weeks that means that it is necessary small shear in gel to cause the gel to flow. This behaviour can be explained by the existence of certain internal structures that change with flowing; certain particles aggregates, formed by hydrogen bonds or van der Waals interactions, that could brake and promote a small decrease in its consistency [212, 215]. For these reasons it seems that altough the formulations presented a small decrease in shear stress they remained a good option for topical application, due to pseudoplastic and thixotropy properties.

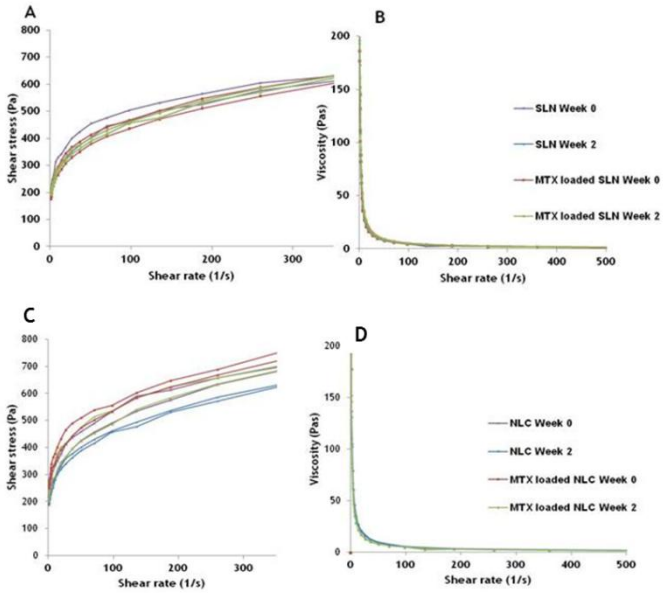

Figure 4.19 - Flow curves for hydrogels enriched LNs. (A) shear stress and (B) viscosity Top images: SLNs and bottom images with NLCs after 2 weeks of storage.

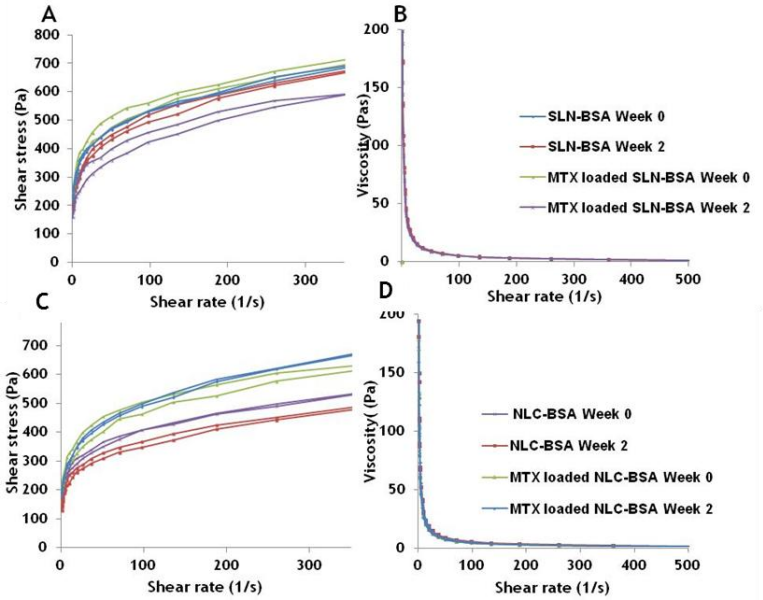

Figure 4.20 - Flow curves for hydrogels containing functionalized LNs. (A) shear stress and (B) viscosity Top images: SLNs-BSA as MTX loaded SLNs-BSA after 15days and bottom images with NLCs-BSA and MTX loaded NLCS-BSA.

4.2.8 Skin permeation studies

One of most important *in vitro* characterization study that a topical formulation can be subjected to is a permeation study (also referred to as penetration study) and in this case its crucial that this system mimics the psoriasis environment [209].

The aim of present section was to investigate topical deliver of both MTX and Etanercept drugs using lipid delivery systems. To assess *in vitro* MTX skin penetration, the Franz diffusion cells were used, as described on section 3.15. Diffusion rates of drug through the epidermis can also be influenced by membrane components, enzymes and transporters and also to be affected by surface charge, properties of the nanomaterial, drug-loading efficiency, mode of application and hydrogen bonding ability [95, 188, 217].

Figure 4.21 shows the MTX skin penetration as free drug and when incorporated in the lipid nanoparticles (functionalized or not). After 8 hours the amounts of MTX that permeated through pig skin were: 1.7 ± 0.1%, 4.8 ± 0.2%, 3.1 ± 0.01%, 2.97 ± 0.03% and 2.17 ± 0.01% for free MTX, MTX loaded -SLNs, - NLCs, -SLN-BSA and –NLC-BSA, respectively. The diferences between free drug and loaded nanoparticles can be explained because nanoparticles improve MTX penetration into the skin, as previously described [211]. From this, it can be concluded that both LNs play important role in controlling the MTX delivery and targeting through the skin. Functionalization with protein in both LNs acts as double barrier effect for drug diffusion through the structural integrity conferred by BSA coupling, therefore decreasing drug penetration profile [168].

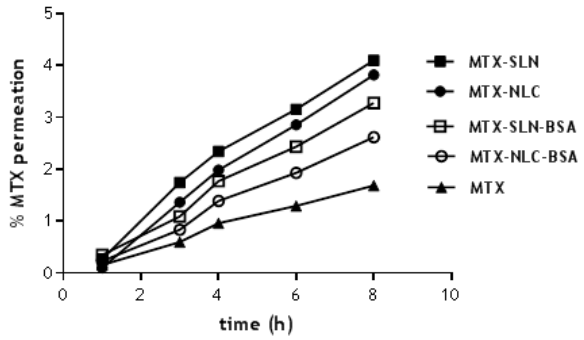

Figure 4.21 - MTX penetration through pig skin during 8 hours.

Furthermore we performed skin permeation studies with the hydrogel enriched with LNs. The drug flux rate through the skin during 8 hours was determined and listed on Table 4.12. In general, permeation profile is as follow: LNs> Hydrogel enriched with LNs.

In the case of hydrogel enriched with LNs the flux value decreased about 10 times for MTX loaded -SLNs, - NLCs, -SLN-BSA and –NLC-BSA, when compared to MTX loaded LNs and MTX loaded-BSA. LNs embedded hydrogel exhibited smaller amount of drug permeation. These results was also observed by other authors [198, 219, 220]. This fact could be explained due to the mucoadhesive properties of hydrogel that enhance the retention time of MTX [213].

However, when comparing free MTX permeation amounts with hydrogel loaded with equivalent amount of MTX, we observed that the latter could permeate a higher quantity of drug. This result can be explained through rheological properties described in section 4.2.7

Probably, free MTX changes the hydrogel structure with lost of consistency that could facilitate the drug penetration in skin.

Table 4.12 - MTX flux through pig ear skin upon 8 hours

Formulation code	Flux (μg/cm^2/h)
Free MTX	**0.71 ± 0.11**
H MTX	**1.23 ± 0.05**
MTX-SLN	**2.60 ± 0.10**
H MTX-SLN	**0.26 ± 0.01**
MTX-SLN-Etanercept	**1.76 ± 0.11**
H MTX-SLN-Etanercept	**0.13 ± 0.01**
MTX-NLC	**1.79 ± 0.09**
H MTX-NLC	**0.16 ± 0.01**
MTX-NLC-Etanercept	**1.04 ± 0.13**
H MTX-NLC-Etanercept	**0.14 ± 0.01**

It is described in the literature that when the skin barrier is compromised, nanoparticle penetration might be considerably enhanced. In psoriasis, with inflammation and KC hyperproliferation, there are some alterations of the SC that may favor the penetration of nanoparticles in psoriatic lesions [87].

Interestingly, NLC presents increased retention of MTX. So, there is no consensus on the use of NLC instead of SLN in order to increase skin penetration of certain drugs [214].

Functionalization with Etanercept allowed to obtain a targeted dual therapy and it was performed by a carbodiimide reaction. Both of proteins, BSA is a model protein usually used in replacement of more expensive proteins, as is the case of Etanercept [76, 83, 175].

In the skin permeation studies, we used BSA to functionalized the LNs instead of Etanercept since both are proteins with similar sizes (< 10 nm) [175, 222].

In order to evaluate if protein-bound to the nanoparticle is able to cross the skin barrier, we quantify the amount of BSA that permeate ear pig skin. Data indicated that 10-20% BSA could enter in the skin in the first 8 hours in contact with skin. So, we could infer that functionalized nanoparticles are suitable for topical application in treatment of psoriasis achiveing a dual therapeutic effect.

Chapter 5 - Conclusion

Psoriasis (PSO) is a commom chronic immune-mediated inflammatory disorder associated with abnormal differentiation and hyperproliferation of epidermal keratinocytes (KC) affecting 2–3% of the population. The *stratum corneum* (SC) is a physical barrier to most substances that come in contact with the skin. The success of dermatological products and, in this case, topical therapy of PSO, depends on the capability of the drug to overcome this barrier and to penetrate through skin in sufficient therapeutic amounts. Bearing that in mind, several systems have been developed to overcome this barrier. Among those nanocarriers, particulate lipid based nanocarriers such as SLN and NLC exhibit many features for dermal application of cosmetic and pharmaceutical products, such as, the controlled release and targeting of drugs, occlusion associated with penetration enhancement, increase of skin hydration and excellent tolerability. So, in this work SLN and NLC were chosen as systems to incorporate and deliver the MTX into the skin.

The first aim of this work consisted in the optimization of NLCs loaded with MTX for the treatment of psoriasis. In order to reduce the number of experiments and cost we performed a experimental design, full factorial and Box-Behnken design to improve the production of a particular system with certain properties. This study was able to evaluate the most important parameters in the production of NLC using Witepsol®E85, Miglyol®812 and PVA. With this conditions the amount of drug and surfactant have more impact in three responses (size, PDI and entrapment efficiency) assessed. NLC containing MTX were produced successfully by ultrasonication method with size closer to 200-300 nm, zeta potential values, in absolute values, were high enough to assure a good electrostatic stabilization, higher values of drug content, at least one month stable stored at room. Morphological investigations showed that all nanoparticles exhibit a spherical shape and a smooth surface independently of their composition. After analyzing the physical and chemical stability of loaded LNs, *in vitro* drug release and were performed and can be concluded that MTX release into NLCs revealed a fast initial drug release followed by a sustained drug release. As for all studied conditions cell viability was above 80% it can be stated that the formulations are not toxic to the fibroblasts and this NLC system represents a promising option for delivery of MTX, since it did not affect cell viability, confirming the safety profile of the optimized delivery system.

In short conclusion of the first approach of this work, the lipid colloidal carrier optimized shows interesting properties for delivering MTX. Although further studies are required in order

to evaluate the therapeutic potential of the optimized formulation in clinically relevant models, present result demonstrated that MTX loaded NLCs could be a promising platform for other inflammatory diseases and even cancer therapy.

The second aim of this work was to develop a targeted nanomedicine appoach for treatment of psoriasis. NLCs and SLNs were produced by ultrasonication method. Functionalization with Etanercept in order to obtain a dual target therapy. All nanoformulations present size closer to 400 nm, zeta potential values, in absolute values, were high enough to assure a good electrostatic stabilization and high values of drug content. Furthermore, morphological investigations by TEM and Cryo-SEM showed that all nanoparticles exhibit a spherical shape and a smooth surface independently of their composition. The physical and chemical stability of all formulation at 6 weeks was assessed. *In vitro* drug release and skin permeation studies were performed and can be concluded that MTX release from LNs reveal similar behaviour: fast initial drug release followed by a sustained drug release.This type of release is interest for drugs encapsulated in cosmetics that will thus have a more sustained and prolonged effect, as desired for anti-psoriasis therapy. Furthermore, we produced a hydrogel (Carbopol 934®) enriched with empty LNs MTX loaded LNs, F-LNs and MTX loaded F-LNs in order to assess its rheological properties, the ability to be applied in topical admnistration of MTX and their skin permeation behaviour. Rheological tests performed showed that all the designed formulations had a non-Newtonian, pseudoplastic, thixotropic behavior, suggesting that they are suitable for topical drug delivery with a small decrease of it consistency in 2 weeks. However this fact could be overcomed with a preservative. The rheological results showed that hydrogels enriched with LNs are good options to be applied in topical administration. Skin permeation assays demonstrated that, mimicking physiological values and temperature, LNs loaded with MTX have good levels of MTX and protein penetration through pig ear skin with small decrease of MTX permeation when LNs were embedded in the hydrogel.

Nevertheless, MTX incorporated in both LNs has already proved to gather several optimal characteristics that indicate that the proposed novel formulation can be an excellent administration MTX in a topical away for psoriasis therapy.

Future work, and before concluding about the real potentiality of these nanoformulations and the possibility of actually using these nanoparticles in a topical therapy for psoriasis, several experiments still need to be performed. DSC investigations should be performed to evaluate the possible polymorphic modifications that can occur in storage. To assess the behaviour of these systems in psoriatic environment we could performed permeation studies with psoriatic human skin and evaluate cell viability under inflammatory conditions. The hydrogels enriched LN should be characterized for their physicochemical properties such as color, odor and pH, mean size, zeta potential, loading efficiency, polymorphism and *in vitro* release. Furthermore hydrogel optimization (amount of carbopol, quantity of MTX and protein) should be conducted to improve the skin permeation results.

References

[1] A. Kuchekar, R. Pujari, S. Kuchekar, and S. Dhole, “Psoriasis : A comprehensive review,” *Int. J. Pharm. life Sci.*, vol. 2, no. 6, pp. 857–877, 2011.

[2] C. Griffi and J. Barker, “Pathogenesis and clinical features of psoriasis,” in *Psoriasis 1*, 2007.

[3] S. Dubois Declercq and R. Pouliot, “Promising new treatments for psoriasis.,” *ScientificWorldJournal.*, vol. 2013, p. 980419, Jan. 2013.

[4] P. Laws and H. Young, “Update of the management of chronic psoriasis : new approaches and emerging treatment options,” *Clin. Cosmet. Investig. Dermatol.*, vol. 3, pp. 25–37, 2010.

[5] I. Grozdev, N. Korman, and N. Tsankov, “Psoriasis as a systemic disease.,” *Clin. Dermatol.*, vol. 32, no. 3, pp. 343–50, 2014.

[6] U. Mrowietz, K. Kragballe, K. Reich, P. Spuls, C. E. M. Griffiths, a Nast, J. Franke, C. Antoniou, P. Arenberger, F. Balieva, M. Bylaite, O. Correia, E. Daudén, P. Gisondi, L. Iversen, L. Kemény, M. Lahfa, T. Nijsten, T. Rantanen, a Reich, T. Rosenbach, S. Segaert, C. Smith, T. Talme, B. Volc-Platzer, and N. Yawalkar, “Definition of treatment goals for moderate to severe psoriasis: a European consensus.,” *Arch. Dermatol. Res.*, vol. 303, no. 1, pp. 1–10, Jan. 2011.

[7] G. K. Perera, P. Di Meglio, and F. O. Nestle, “Psoriasis.,” *Annu. Rev. Pathol.*, vol. 7, pp. 385–422, Jan. 2012.

[8] G. S. Rasmussen, H. T. Maindal, and K. Lomborg, “Self-management in daily life with psoriasis: an integrative review of patient needs for structured education.,” *Nurs. Res. Pract.*, vol. 2012, p. 890860, Jan. 2012.

[9] C. Ryan, N. J. Korman, J. M. Gelfand, H. W. Lim, C. a Elmets, S. R. Feldman, A. B. Gottlieb, J. Y. M. Koo, M. Lebwohl, C. L. Leonardi, A. S. Van Voorhees, R. Bhushan, and A. Menter, “Research gaps in psoriasis: opportunities for future studies.,” *J. Am. Acad. Dermatol.*, vol. 70, no. 1, pp. 146–67, Jan. 2014.

[10] A. M. Bowcock and W. O. C. M. Cookson, “The genetics of psoriasis, psoriatic arthritis and atopic dermatitis.,” *Hum. Mol. Genet.*, vol. 13 Spec No, no. 1, pp. R43–55, Apr. 2004.

[11] R. G. B. Langley, G. G. Krueger, and C. E. M. Griffiths, “Psoriasis: epidemiology, clinical features, and quality of life.,” *Ann. Rheum. Dis.*, vol. 64 Suppl 2, pp. ii18–23; discussion ii24–5, Mar. 2005.

[12] R. Parisi, D. P. M. Symmons, C. E. M. Griffiths, and D. M. Ashcroft, “Global epidemiology of psoriasis: a systematic review of incidence and prevalence.,” *J. Invest. Dermatol.*, vol. 133, no. 2, pp. 377–85, Feb. 2013.

[13] A. K. M. A. S. M. Hani A. AlShobaili MD, Muhammad Shahzad MD, Abdullah Al-Marshood MBBS and I. B. MD, “Genetic Background of Psoriasis,” pp. 23–29, 2010.

[14] J. G. Krueger and a Bowcock, “Psoriasis pathophysiology: current concepts of pathogenesis.,” *Ann. Rheum. Dis.*, vol. 64 Suppl 2, pp. ii30–6, Mar. 2005.

[15] J. Shapiro, A. D. Cohen, M. David, E. Hodak, G. Chodik, A. Viner, E. Kremer, and A. Heymann, “The association between psoriasis, diabetes mellitus, and atherosclerosis in Israel: a case-control study.,” *J. Am. Acad. Dermatol.*, vol. 56, no. 4, pp. 629–34, Apr. 2007.

[16] P. Coto-Segura, N. Eiris-Salvado, L. González-Lara, R. Queiro-Silva, P. Martinez-Camblor, C. Maldonado-Seral, B. García-García, L. Palacios-García, S. Gomez-Bernal, J. Santos-Juanes, and E. Coto, “Psoriasis, psoriatic arthritis and type 2 diabetes mellitus: a systematic review and meta-analysis.,” *Br. J. Dermatol.*, vol. 169, no. 4, pp. 783–93, Oct. 2013.

[17] A. T. Ion and S. I. S. Found, “An overview of psoriasis and psoriatic arthritis,” *National psoriasis foundation*.

[18] M. a Lowes, M. Suárez-Fariñas, and J. G. Krueger, “Immunology of psoriasis.,” *Annu. Rev. Immunol.*, vol. 32, pp. 227–55, Jan. 2014.

[19] C. Tiemblo, “Información para pacientes de Psoriasis.” Available in http://microsite.20minutos.es/psorinfo/entrevista_cristina_tiemblo.html. Accessed in in 4 March of 2015 .

[20] Jamaludin, “Traditional Medicine for Skin Psoriasis,” *Multikhasiat., Jual Produk Herbal*, 2015. Available in https://obattradisionalpenyakitkulitpsoriasismultikhasiat.wordpress.com/2015/04/17/obat-tradisional-penyakit-kulit-psoriasis-multikhasiat/ Accessed in 4of March of 2015 .

[21] J. Berth-Jones, “Psoriasis,” *Medicine (Baltimore).*, vol. 41, no. 6, pp. 334–340, Jun. 2013.

[22] J. D. Bernhard, “Clinical Pearl : Auspitz sign in psoriasis scale,” p. 1990, 1991.

[23] U. Mrowietz and K. Reich, “Psoriasis--new insights into pathogenesis and treatment.,” *Dtsch. Arztebl. Int.*, vol. 106, no. 1–2, pp. 11–8, quiz 19, Jan. 2009.

[24] Y. Cai, C. Fleming, and J. Yan, “New insights of T cells in the pathogenesis of psoriasis.,” *Cell. Mol. Immunol.*, vol. 9, no. 4, pp. 302–9, Jul. 2012.

[25] M. a Lowes, W. Lew, and J. G. Krueger, “Current concepts in the immunopathogenesis of psoriasis.,” *Dermatol. Clin.*, vol. 22, no. 4, pp. 349–69, vii, Oct. 2004.

[26] K. Suresh, “Novel topical drug carriers as a tool for treatment of psoriasis: Progress and advances,” *African J. Pharm. Pharmacol.*, vol. 7, no. 5, pp. 138–147, Feb. 2013.

[27] J. A. O. Daly, “Psoriasis , a Systemic Disease Beyond the Skin , as Evidenced by Psoriatic Arthritis and Many Comorbities – Clinical Remission with a Leishmania Amastigotes Vaccine , a Serendipity Finding,” vol. 18, pp. 1–57, 2011.

[28] G. Monteleone, F. Pallone, T. T. MacDonald, S. Chimenti, and A. Costanzo, “Psoriasis: from pathogenesis to novel therapeutic approaches.,” *Clin. Sci. (Lond).*, vol. 120, no. 1, pp. 1–11, Jan. 2011.

[29] M. a Lowes, C. B. Russell, D. a Martin, J. E. Towne, and J. G. Krueger, “The IL-23/T17 pathogenic axis in psoriasis is amplified by keratinocyte responses.,” *Trends Immunol.*, vol. 34, no. 4, pp. 174–81, Apr. 2013.

[30] M. J. McGeachy, Y. Chen, C. M. Tato, A. Laurence, B. Joyce-Shaikh, W. M. Blumenschein, T. K. McClanahan, J. J. O’Shea, and D. J. Cua, “The interleukin 23 receptor is essential for the terminal differentiation of interleukin 17-producing effector T helper cells in vivo.,” *Nat. Immunol.*, vol. 10, no. 3, pp. 314–24, Mar. 2009.

[31] L. Flatz and C. Conrad, “Role of T-cell-mediated inflammation in psoriasis : pathogenesis and targeted therapy,” pp. 1–10, 2013.

[32] A. Balato, N. Balato, M. Megna, M. Schiattarella, S. Lembo, and F. Ayala, “Pathogenesis of Psoriasis : The Role of Pro-Inflammatory Cytokines Produced by Keratinocytes,” 2007.

[33] M. a Lowes, A. M. Bowcock, and J. G. Krueger, “Pathogenesis and therapy of psoriasis.,” *Nature*, vol. 445, no. 7130, pp. 866–73, Feb. 2007.

[34] S. K. Raychaudhuri, E. Maverakis, and S. P. Raychaudhuri, “Diagnosis and classification of psoriasis.,” *Autoimmun. Rev.*, vol. 13, no. 4–5, pp. 490–5, 2014.

[35] L. Naldi and D. Gambini, “The clinical spectrum of psoriasis.,” *Clin. Dermatol.*, vol. 25, no. 6, pp. 510–518, 2007.

[36] A. Menter, A. Gottlieb, S. R. Feldman, A. S. Van Voorhees, C. L. Leonardi, K. B. Gordon, M. Lebwohl, J. Y. M. Koo, C. a Elmets, N. J. Korman, K. R. Beutner, and R. Bhushan, “Guidelines of care for the management of psoriasis and psoriatic arthritis: Section 1. Overview of psoriasis and guidelines of care for the treatment of psoriasis with biologics.,” *J. Am. Acad. Dermatol.*, vol. 58, no. 5, pp. 826–50, May 2008.

[37] G. Wozel, “Psoriasis treatment in difficult locations: scalp, nails, and intertriginous areas.,” *Clin. Dermatol.*, vol. 26, no. 5, pp. 448–59, 2008.

[38] M. A. N. Johnson and A. W. Armstrong, “Clinical and histologic diagnostic guidelines for psoriasis: a critical review.,” *Clin. Rev. Allergy Immunol.*, vol. 44, no. 2, pp. 166–72, Apr. 2013.

[39] I. Zschocke, U. Mrowietz, E. Karakasili, and K. Reich, “Non-adherence and measures to improve adherence in the topical treatment of psoriasis.,” *J. Eur. Acad. Dermatol. Venereol.*, vol. 28 Suppl 2, pp. 4–9, May 2014.

[40] L. Uva, D. Miguel, C. Pinheiro, J. Antunes, D. Cruz, J. Ferreira, and P. Filipe, “Mechanisms of action of topical corticosteroids in psoriasis.,” *Int. J. Endocrinol.*, vol. 2012, no. iv, p. 561018, Jan. 2012.

[41] E. E. Bailey, E. H. Ference, A. Alikhan, M. T. Hession, and A. W. Armstrong, “Combination treatments for psoriasis: a systematic review and meta-analysis.,” *Arch. Dermatol.*, vol. 148, no. 4, pp. 511–22, Apr. 2012.

[42] P. Jensen, L. Skov, and C. Zachariae, “Systemic combination treatment for psoriasis: a review.,” *Acta Derm. Venereol.*, vol. 90, no. 4, pp. 341–9, Jul. 2010.

[43] E. Castela, E. Archier, S. Devaux, a Gallini, S. Aractingi, B. Cribier, D. Jullien, F. Aubin, H. Bachelez, P. Joly, M. Le Maître, L. Misery, M. Richard, C. Paul, and J. P. Ortonne, “Topical corticosteroids in plaque psoriasis: a systematic review of efficacy and treatment modalities.,” *J. Eur. Acad. Dermatol. Venereol.*, vol. 26 Suppl 3, pp. 36–46, May 2012.

[44] P. L. Scott, C. West, and S. R. Feldman, “Self-management in patients with psoriasis,” *Psoriasis targets Ther.*, pp. 19–26, 2014.

[45] G. De Gannes, C. Huang, Y. Zhou, and T. Afifi, “Topical therapies for psoriasis,” *Can. Fam. Phy*, vol. 51, pp. 519–525, 2005.

[46] V. N. Sehgal, P. Verma, and A. Khurana, “Pharmacology and therapeutics Anthralin / dithranol in dermatology,” *Int. J. Dermatol.*, pp. 449–460, 2014.

[47] E. Campione, E. J. Paternò, G. Costanza, L. Diluvio, I. Carboni, D. Marino, S. Chimenti, L. Bianchi, and A. Orlandi, “Tazarotene as alternative topical treatment for onychomycosis,” *Drug Des. Devel. Ther.*, vol. 9, pp. 879–886, 2015.

[48] a G. M. Hendriks, R. R. M. C. Keijsers, E. M. G. J. de Jong, M. M. B. Seyger, and P. C. M. van de Kerkhof, “Efficacy and safety of combinations of first-line topical

treatments in chronic plaque psoriasis: a systematic literature review.," *J. Eur. Acad. Dermatol. Venereol.*, vol. 27, no. 8, pp. 931–51, Aug. 2013.

[49] K. Tsuda, K. Yamanaka, H. Kitagawa, T. Akeda, M. Naka, K. Niwa, T. Nakanishi, M. Kakeda, E. C. Gabazza, and H. Mizutani, "Calcineurin inhibitors suppress cytokine production from memory T cells and differentiation of naïve T cells into cytokine-producing mature T cells," *PLoS One*, vol. 7, no. 2, 2012.

[50] G. Murphy and K. Reich, "In touch with psoriasis: topical treatments and current guidelines.," *J. Eur. Acad. Dermatol. Venereol.*, vol. 25 Suppl 4, no. Table 1, pp. 3–8, Jun. 2011.

[51] K. Reich and a Bewley, "What is new in topical therapy for psoriasis?," *J. Eur. Acad. Dermatol. Venereol.*, vol. 25 Suppl 4, pp. 15–20, Jun. 2011.

[52] S. Baboota, M. S. Alam, J. Ali, A. Kumar, and S. Sharma, "Nanocarrier-based hydrogel of betamethasone dipropionate and salicylic acid for treatment of psoriasis," *Int. J. Pharm. Investig.*, vol. 3, pp. 139–147, 2011.

[53] E. J. Samarasekera, L. Sawyer, D. Wonderling, R. Tucker, and C. H. Smith, "Topical therapies for the treatment of plaque psoriasis: systematic review and network meta-analyses.," *Br. J. Dermatol.*, vol. 168, no. 5, pp. 954–67, May 2013.

[54] S. Baboota, M. U. Rahman, A. Kumar, S. Sharma, J. Sahni, and J. Ali, "Submicron Size Formulation of Linseed Oil Containing Omega-3 Fatty Acid for Topical Delivery," *J. Dispers. Sci. Technol.*, vol. 33, no. 9, pp. 1259–1266, 2012.

[55] J. Ayer and H. S. Young, "Pimecrolimus for psoriasis.," *Expert Opin. Pharmacother.*, vol. 14, no. 6, pp. 767–74, 2013.

[56] W. Lapolla, B. a Yentzer, J. Bagel, C. R. Halvorson, and S. R. Feldman, "A review of phototherapy protocols for psoriasis treatment.," *J. Am. Acad. Dermatol.*, vol. 64, no. 5, pp. 936–49, May 2011.

[57] E. Sbidian, a Maza, H. Montaudié, a Gallini, S. Aractingi, F. Aubin, B. Cribier, P. Joly, D. Jullien, M. Le Maître, L. Misery, M. Richard, C. Paul, J.-P. Ortonne, and H. Bachelez, "Efficacy and safety of oral retinoids in different psoriasis subtypes: a systematic literature review.," *J. Eur. Acad. Dermatol. Venereol.*, vol. 25 Suppl 2, pp. 28–33, May 2011.

[58] M. Pradhan, D. Singh, and M. R. Singh, "Development characterization and skin permeating potential of lipid based novel delivery system for topical treatment of psoriasis.," *Chem. Phys. Lipids*, vol. 186, pp. 9–16, Nov. 2014.

[59] R. Sivaramakrishnan, C. Nakamura, W. Mehnert, H. C. Korting, K. D. Kramer, and M. Schäfer-Korting, "Glucocorticoid entrapment into lipid carriers--characterisation by parelectric spectroscopy and influence on dermal uptake.," *J. Control. Release*, vol. 97, no. 3, pp. 493–502, Jul. 2004.

[60] G. G. Krueger, M. a. O'Reilly, M. Weidner, S. H. Dromgoole, and F. P. Killey, "Comparative efficacy of once-daily flurandrenolide tape versus twice- daily diflorasone diacetate ointment in the treatment of psoriasis," *J. Am. Acad. Dermatol.*, vol. 38, no. 2 I, pp. 186–190, 1998.

[61] M. Lebwohl and S. Ali, "Treatment of psoriasis. Part 1. Topical therapy and phototherapy.," *J. Am. Acad. Dermatol.*, vol. 45, no. 4, pp. 487–98; quiz 499–502, Oct. 2001.

[62] B. Sebok, B. Bonnekoh, M. Kerenyi, and H. Gollnick, “Tazarotene induces epidermal cell differentiation in the mouse tail test used as an animal model for psoriasis,” vol. 13, no. 5, 2000.

[63] U. Mrowietz, “Advances in systemic therapy for psoriasis,” *Clin. Exp. Dermatol.*, vol. 26, no. 4, pp. 362–367, Jun. 2001.

[64] Y. Agrawal, K. C. Petkar, and K. K. Sawant, “Development, evaluation and clinical studies of Acitretin loaded nanostructured lipid carriers for topical treatment of psoriasis.,” *Int. J. Pharm.*, vol. 401, no. 1–2, pp. 93–102, Nov. 2010.

[65] a Maza, H. Montaudié, E. Sbidian, a Gallini, S. Aractingi, F. Aubin, H. Bachelez, B. Cribier, P. Joly, D. Jullien, M. Le Maître, L. Misery, M. Richard, J.-P. Ortonne, and C. Paul, “Oral cyclosporin in psoriasis: a systematic review on treatment modalities, risk of kidney toxicity and evidence for use in non-plaque psoriasis.,” *J. Eur. Acad. Dermatol. Venereol.*, vol. 25 Suppl 2, pp. 19–27, May 2011.

[66] M. P. Heffernan, “Combining traditional systemic and biologic therapies for psoriasis.,” *Semin. Cutan. Med. Surg.*, vol. 29, no. 1, pp. 67–9, Mar. 2010.

[67] S. S. Abolmaali, A. M. Tamaddon, and R. Dinarvand, “A review of therapeutic challenges and achievements of methotrexate delivery systems for treatment of cancer and rheumatoid arthritis,” *Cancer Chemother. Pharmacol.*, vol. 71, no. 5, pp. 1115–1130, 2013.

[68] C. G. Shinde, M. P. Venkatesh, T. M. P. Kumar, and H. G. Shivakumar, “Methotrexate: a gold standard for treatment of rheumatoid arthritis.,” *J. Pain Palliat. Care Pharmacother.*, vol. 28, no. 4, pp. 351–8, Dec. 2014.

[69] H. Montaudié, E. Sbidian, C. Paul, a Maza, a Gallini, S. Aractingi, F. Aubin, H. Bachelez, B. Cribier, P. Joly, D. Jullien, M. Le Maître, L. Misery, M. Richard, and J.-P. Ortonne, “Methotrexate in psoriasis: a systematic review of treatment modalities, incidence, risk factors and monitoring of liver toxicity.,” *J. Eur. Acad. Dermatol. Venereol.*, vol. 25 Suppl 2, no. January, pp. 12–8, May 2011.

[70] A. Ion and S. Found, “Systemic medication,” *Natl. psoriasis f.*

[71] C. Silva, V. Kossel, K. Leszczynski, T. Melnik, and R. Riera, “Methotrexate for psoriasis (Protocol),” in *John*, The Cochrane Library, 2013.

[72] J. Kay and R. Westhovens, “systemic medicaion,” *Ann Rheum Dis*, pp. 1081–1083, 2009.

[73] M. H. a Rustin, “Long-term safety of biologics in the treatment of moderate-to-severe plaque psoriasis: review of current data.,” *Br. J. Dermatol.*, vol. 167 Suppl , pp. 3–11, Nov. 2012.

[74] H. Coope, D. J. Mckenna, and A. B. Alexandroff, “Long-term safety of biologics in the treatment of psoriasis,” *Psoriasis: targets and thera*, pp. 1–9, 2013.

[75] R. K. Sivamani, H. Goodarzi, M. S. Garcia, S. P. Raychaudhuri, L. N. Wehrli, Y. Ono, and E. Maverakis, “Biologic therapies in the treatment of psoriasis: a comprehensive evidence-based basic science and clinical review and a practical guide to tuberculosis monitoring.,” *Clin. Rev. Allergy Immunol.*, vol. 44, no. 2, pp. 121–40, Apr. 2013.

[76] J. Yost and J. E. Gudjonsson, “The role of TNF inhibitors in psoriasis therapy: new implications for associated comorbidities.,” *F1000 Med. Rep.*, vol. 1, no. May, pp. 4–7, Jan. 2009.

[77] H. Matz, “Phototherapy for psoriasis: what to choose and how to use: facts and controversies.,” *Clin. Dermatol.*, vol. 28, no. 1, pp. 73–80, 2010.

[78] B. Baroli, M. A. Lopez-quintela, M. Begona, and A. M. Fadda, “Microemulsions for topical delivery of 8-methoxsalen,” vol. 69, pp. 209–218, 2000.

[79] X. Liu, P. Kruger, H. Maibach, P. B. Colditz, and M. Roberts, “Using skin for drug delivery and diagnosis in critically ill.,” *Adv. Drug Deliv. Rev.*, Oct. 2014.

[80] B. Baroli, “Penetration of Nanoparticles and Nanomaterials in the Skin : Fiction or Reality ?,” vol. 99, no. 1, pp. 21–50, 2010.

[81] “Chapter Skin structure and function,” in *Aromaderma*, pp. 1–11.

[82] P. M. Elias, “Structure and function of the stratum corneum extracellular matrix.,” *J. Invest. Dermatol.*, vol. 132, no. 9, pp. 2131–3, Sep. 2012.

[83] G. Imokawa, A. Akihito, K. Jin, Y. Higaki, M. Kawashima, and A. Hidano, “Decreased Level of Ceramides in Stratum Corneum of Atopic Dermatitis: An Etiologic Factor in Atopic Dry Skin?” 1991.

[84] J. M. Jungersted, H. Scheer, M. Mempel, H. Baurecht, L. Cifuentes, J. K. Høgh, L. I. Hellgren, G. B. E. Jemec, T. Agner, and S. Weidinger, “Stratum corneum lipids, skin barrier function and filaggrin mutations in patients with atopic eczema.,” *Allergy*, vol. 65, no. 7, pp. 911–8, Jul. 2010.

[85] M. Gomes, “Lipid nanoparticles for topical and transdermal application for alopecia treatment,” 2012.

[86] Z. Zhang, P.-C. Tsai, T. Ramezanli, and B. B. Michniak-Kohn, “Polymeric nanoparticles-based topical delivery systems for the treatment of dermatological diseases.,” *Wiley Interdiscip. Rev. Nanomed. Nanobiotechnol.*, vol. 5, no. 3, pp. 205–18, 2013.

[87] P. Desai, R. R. Patlolla, and M. Singh, “Interaction of nanoparticles and cell-penetrating peptides with skin for transdermal drug delivery.,” *Mol. Membr. Biol.*, vol. 27, no. 7, pp. 247–59, Oct. 2010.

[88] K. S. Paudel, M. Milewski, C. L. Swadley, N. K. Brogden, P. Ghosh, and A. L. Stinchcomb, “Challenges and opportunities in dermal/transdermal delivery,” *Ther. Deliv.*, vol. 1, no. 1, pp. 109–131, 2010.

[89] O. Uchechi, J. D. N. Ogbonna, and A. A. Attama, “Nanoparticles for Dermal and Transdermal Drug Delivery,” *Appl. Nanotechnol. drug Deliv.*, pp. 194–235, 2014.

[90] R. Paper, G. Manish, and S. Vimukta, “Targeted drug delivery system : A Review,” vol. 1, no. 2, 2011.

[91] V. J. Mohanraj and Y. Chen, “Nanoparticles – A Review,” vol. 5, no. June, pp. 561–573, 2006.

[92] N. S. Ranpise, S. S. Korabu, and V. N. Ghodake, “Second generation lipid nanoparticles (NLC) as an oral drug carrier for delivery of lercanidipine hydrochloride,” *Colloids Surfaces B Biointerfaces*, vol. 116, pp. 81–87, 2014.

[93] M. Pradhan, D. Singh, and M. R. Singh, “Novel colloidal carriers for psoriasis: current issues, mechanistic insight and novel delivery approaches.,” *J. Control. Release*, vol. 170, no. 3, pp. 380–95, Sep. 2013.

[94] Y. Rahimpour and H. Hamishehkar, “Niosomes as Carrier in Dermal Drug Delivery,” *Recent Adv. Nov. drug Carr. Syst.*, 2012.

[95] R. Sonawane, H. Harde, M. Katariya, S. Agrawal, and S. Jain, “Solid lipid nanoparticles-loaded topical gel containing combination drugs: an approach to offset psoriasis.,” *Expert Opin. Drug Deliv.*, vol. 11, no. 12, pp. 1833–47, Dec. 2014.

[96] J.-Y. Fang, C.-L. Fang, C.-H. Liu, and Y.-H. Su, “Lipid nanoparticles as vehicles for topical psoralen delivery: solid lipid nanoparticles (SLN) versus nanostructured lipid carriers (NLC).,” *Eur. J. Pharm. Biopharm.*, vol. 70, no. 2, pp. 633–40, Oct. 2008.

[97] P. Ekambaram, A. A. H. Sathali, and K. Priyanka, “Solid lipid nanoparticles: a review,” vol. 2, no. 1, pp. 80–102, 2012.

[98] F. Tamjidi, M. Shahedi, J. Varshosaz, and A. Nasirpour, *Nanostructured lipid carriers (NLC): A potential delivery system for bioactive food molecules*. Elsevier B.V., 2013.

[99] S. G. Lee, J. H. Jeong, K. M. Lee, and H. Yang, “Nanostructured lipid carrier-loaded hyaluronic acid microneedles for controlled dermal delivery of a lipophilic molecule,” pp. 289–299, 2014.

[100] P. Srisuk, P. Thongnopnua, U. Raktanonchai, and S. Kanokpanont, “Physico-chemical characteristics of methotrexate-entrapped oleic acid-containing deformable liposomes for in vitro transepidermal delivery targeting psoriasis treatment.,” *Int. J. Pharm.*, vol. 427, no. 2, pp. 426–34, May 2012.

[101] N. Ø. Knudsen, L. Jorgensen, J. Hansen, C. Vermehren, S. Frokjaer, and C. Foged, “Targeting of liposome-associated calcipotriol to the skin: effect of liposomal membrane fluidity and skin barrier integrity.,” *Int. J. Pharm.*, vol. 416, no. 2, pp. 478–85, Sep. 2011.

[102] G. Li, C. Fan, X. Li, Y. Fan, X. Wang, M. Li, and Y. Liu, “Preparation and in vitro evaluation of tacrolimus-loaded ethosomes.,” *ScientificWorldJournal.*, vol. 2012, p. 874053, Jan. 2012.

[103] Y.-T. Zhang, L.-N. Shen, Z.-H. Wu, J.-H. Zhao, and N.-P. Feng, “Evaluation of skin viability effect on ethosome and liposome-mediated psoralen delivery via cell uptake.,” *J. Pharm. Sci.*, vol. 103, no. 10, pp. 3120–6, Oct. 2014.

[104] D. D. Verma and a Fahr, “Synergistic penetration enhancement effect of ethanol and phospholipids on the topical delivery of cyclosporin A.,” *J. Control. Release*, vol. 97, no. 1, pp. 55–66, May 2004.

[105] Y. Zhang, L. Shen, J. Zhao, and N. Feng, “Evaluation of psoralen ethosomes for topical delivery in rats by using in vivo microdialysis,” *Int. J. n*, pp. 669–678, 2014.

[106] G. Cevc and G. Blume, “Hydrocortisone and dexamethasone in very deformable drug carriers have increased biological potency, prolonged effect, and reduced therapeutic dosage.,” *Biochim. Biophys. Acta*, vol. 1663, no. 1–2, pp. 61–73, May 2004.

[107] M. E. Carlotti, S. Sapino, E. Peira, M. Gallarate, and E. Ugazio, “On the Photodegradation of Dithranol in Different Topical Formulations: Use of SLN to Increase the Stability of the Drug,” *J. Dispers. Sci. Technol.*, vol. 30, no. 10, pp. 1517–1524, 2009.

[108] D. M. Ridolfi, P. D. Marcato, G. Z. Justo, L. Cordi, D. Machado, and N. Durán, “Chitosan-solid lipid nanoparticles as carriers for topical delivery of tretinoin.,” *Colloids Surf. B. Biointerfaces*, vol. 93, pp. 36–40, May 2012.

[109] M. S. Gambhire, M. R. Bhalekar, and B. Shrivastava, “Investigations in photostability of dithranol incorporated in solid lipid nanoparticles,” *Pharm. Chem. J.*, vol. 46, no. 4, pp. 256–261, Aug. 2012.

[110] K. Raza, B. Singh, S. Lohan, G. Sharma, P. Negi, Y. Yachha, and O. P. Katare, “Nano-lipoidal carriers of tretinoin with enhanced percutaneous absorption, photostability, biocompatibility and anti-psoriatic activity.,” *Int. J. Pharm.*, vol. 456, no. 1, pp. 65–72, Nov. 2013.

[111] U. Agrawal, M. Gupta, and S. P. Vyas, “Capsaicin delivery into the skin with lipidic nanoparticles for the treatment of psoriasis.,” *Artif. Cells. Nanomed. Biotechnol.*, no. August, pp. 1–7, Sep. 2013.

[112] J. R. Madan, P. a Khude, and K. Dua, “Development and evaluation of solid lipid nanoparticles of mometasone furoate for topical delivery.,” *Int. J. Pharm. Investig.*, vol. 4, no. 2, pp. 60–4, Apr. 2014.

[113] Y. Lin, Z. Huang, R. Zhuo, and J. Fang, “Combination of calcipotriol and methotrexate in nanostructured lipid carriers for topical delivery,” pp. 117–128, 2010.

[114] M. F. Pinto, C. C. Moura, C. Nunes, M. a. Segundo, S. a. Costa Lima, and S. Reis, “A new topical formulation for psoriasis: Development of methotrexate-loaded nanostructured lipid carriers,” *Int. J. Pharm.*, vol. 477, no. 1–2, pp. 519–526, 2014.

[115] H. Liu, Y. Wang, F. E. I. Han, H. Yao, and S. Li, “Gelatin-Stabilised Microemulsion-Based Organogels Facilitates Percutaneous Penetration of Cyclosporin A In Vitro and Dermal Pharmacokinetics In Vivo,” vol. 96, no. 11, pp. 3000–3009, 2007.

[116] H. Liu, Y. Wang, Y. Lang, H. Yao, Y. Dong, and S. Li, “Bicontinuous Cyclosporin A Loaded Water-AOT / Tween 85-Isopropylmyristate Microemulsion : Structural Characterization and Dermal Pharmacokinetics In Vivo,” vol. 98, no. 3, pp. 1167–1176, 2009.

[117] F. F. Sahle, J. Wohlrab, and R. H. H. Neubert, “Controlled penetration of ceramides into and across the stratum corneum using various types of microemulsions and formulation associated toxicity studies.,” *Eur. J. Pharm. Biopharm.*, vol. 86, no. 2, pp. 244–50, Feb. 2014.

[118] C. L. Iu and F. C. Hang, “Development and Characterization of Eucalyptol Microemulsions for Topic Delivery of Curcumin,” vol. 59, no. 2, pp. 172–178, 2011.

[119] D. S. Bernardi, T. a Pereira, N. R. Maciel, J. Bortoloto, G. S. Viera, G. C. Oliveira, and P. a Rocha-Filho, “Formation and stability of oil-in-water nanoemulsions containing rice bran oil: in vitro and in vivo assessments.,” *J. Nanobiotechnology*, vol. 9, no. 1, p. 44, Jan. 2011.

[120] S. Khandavilli and R. Panchagnula, “Nanoemulsions as versatile formulations for paclitaxel delivery: peroral and dermal delivery studies in rats.,” *J. Invest. Dermatol.*, vol. 127, no. 1, pp. 154–62, Jan. 2007.

[121] K. Borowska, S. Wołowiec, A. Rubaj, K. Głowniak, E. Sieniawska, and S. Radej, “Effect of polyamidoamine dendrimer G3 and G4 on skin permeation of 8-methoxypsoralene--in vivo study.,” *Int. J. Pharm.*, vol. 426, no. 1–2, pp. 280–3, Apr. 2012.

[122] U. Agrawal, N. K. Mehra, U. Gupta, and N. K. Jain, “Hyperbranched dendritic nano-carriers for topical delivery of dithranol.,” *J. Drug Target.*, vol. 21, no. 5, pp. 497–506, May 2013.

[123] M. Lapteva, K. Mondon, M. Mo, R. Gurny, and Y. N. Kalia, “Polymeric Micelle Nanocarriers for the Cutaneous Delivery of Tacrolimus: A Targeted Approach for the Treatment of Psoriasis,” 2014.

[124] M. Lapteva, V. Santer, K. Mondon, I. Patmanidis, G. Chiriano, L. Scapozza, R. Gurny, M. Möller, and Y. N. Kalia, “Targeted cutaneous delivery of ciclosporin A using micellar nanocarriers and the possible role of inter-cluster regions as molecular transport pathways.,” *J. Control. Release*, vol. 196, pp. 9–18, Dec. 2014.

[125] T. Tamura, T (Tamura, K. Takayama, K (Takayama, H. Satoh, H (Satoh, K. Tanno, K (Tanno, and T. Nagai, T (Nagai, “Evaluation of oil/water-type cyclosporine gel ointment with commercially available oral solution,” 1997.

[126] R. Prasad, V. Koul, S. Anand, and R. Khar, “Effect of DC/mDC iontophoresis and terpenes on transdermal permeation of methotrexate: In vitro study,” vol. 33, 2007.

[127] H. P. Singh, P. Utreja, A. K. Tiwary, and S. Jain, “Elastic liposomal formulation for sustained delivery of colchicine: in vitro characterization and in vivo evaluation of anti-gout activity.,” *AAPS J.*, vol. 11, no. 1, pp. 54–64, Mar. 2009.

[128] A. F. Ourique, A. Melero, C. de Bona da Silva, U. F. Schaefer, A. R. Pohlmann, S. S. Guterres, C.-M. Lehr, K.-H. Kostka, and R. C. R. Beck, “Improved photostability and reduced skin permeation of tretinoin: development of a semisolid nanomedicine.,” *Eur. J. Pharm. Biopharm.*, vol. 79, no. 1, pp. 95–101, Sep. 2011.

[129] C. Health, “Witepsol- Fatty bases for suppositories,” *Cremer- Oleo Div.*

[130] “Cetylis palmitas,” *Eur. pharmacopoeia*, p. 95, 2005.

[131] S. S. Glycolate, B. Paraben, M. Paraben, E. Cellulose, Z. Citrate, M. Citrate, D. H. Citrate, and P. Citrate, “Excipients for pharmaceuticals,” pp. 1–3.

[132] S. Saxena, “Polyvinyl Alcohol (Pva),” *Int. J. Toxicol.*, vol. 1, no. 3, pp. 3–5, 2004.

[133] “2 2.1 Materials-,” *Lipid and Waxes*, vol. 812, pp. 169–171.

[134] S. Padmanabhan, D. N. Tripathi, a. Vikram, P. Ramarao, and G. B. Jena, “Methotrexate-induced cytotoxicity and genotoxicity in germ cells of mice: Intervention of folic and folinic acid,” *Mutat. Res. - Genet. Toxicol. Environ. Mutagen.*, vol. 673, no. 1, pp. 43–52, 2009.

[135] W. I. It, H. Does, I. Work, W. Can, T. It, W. Should, and N. Take, “Remicade (infliximab) How Does It Work ? Who Should Not Take It ? How Is It Used ? Can It Be Used With Other Treatments ?,” no. April 2004, 2006.

[136] U. Haustein and M. Rytter, “Methotrexate in psoriasis : 26 years ’ experience with low-dose long-term treatment,” pp. 382–388, 2000.

[137] S. Li, D. A. Xing, and J. Li, “Dynamic Light Scattering Application to Study Protein Interactions in Electrolyte Solutions,” pp. 313–324, 2004.

[138] M. Zimbone, L. Calcagno, G. Messina, P. Baeri, and G. Compagnini, “Dynamic light scattering and UV–vis spectroscopy of gold nanoparticles solution,” *Mater. Lett.*, vol. 65, no. 19–20, pp. 2906–2909, Oct. 2011.

[139] M. Instruments, “Dynamic Light Scattering : An Introduction in 30 Minutes,” *techical note*, pp. 1–8.

[140] A. Achouri, Y. Zamani, and J. I. Boye, “Stability and Physical Properties of Emulsions Prepared with and without Soy Proteins,” *J. Food Res.*, vol. 1, no. 1, pp. 254–267, Jan. 2012.

[141] L. Wu, J. Zhang, and W. Watanabe, “Physical and chemical stability of drug nanoparticles.,” *Adv. Drug Deliv. Rev.*, vol. 63, no. 6, pp. 456–69, May 2011.

[142] S. Kashanian, A. H. Azandaryani, and K. Derakhshandeh, “New surface-modified solid lipid nanoparticles using N-glutaryl phosphatidylethanolamine as the outer shell.,” *Int. J. Nanomedicine*, vol. 6, pp. 2393–2401, 2011.

[143] P. Pathak and M. Nagarsenker, “Formulation and evaluation of lidocaine lipid nanosystems for dermal delivery.,” *AAPS PharmSciTech*, vol. 10, no. 3, pp. 985–992, 2009.

[144] E. Lasoń, E. Sikora, and J. Ogonowski, “Influence of process parameters on properties of Nanostructured Lipid Carriers (NLC) formulation *,” vol. 60, no. 4, pp. 773–777, 2013.

[145] D. J. Shaw, D. H. Everett, I. D. Ross, S. and Morrison, and J. Lyklema, “Zeta Potential An Introduction in 30 Minutes,” 2000.

[146] B. Mukherjee, “Preparation , characterization and in-vitro evaluation of sustained release protein-loaded nanoparticles based on biodegradable polymers,” vol. 3, no. 4, pp. 487–496, 2008.

[147] R. Tantra, P. Schulze, and P. Quincey, “Effect of nanoparticle concentration on zeta-potential measurement results and reproducibility,” *Particuology*, vol. 8, no. 3, pp. 279–285, Jun. 2010.

[148] MinaTec, “Characterization Techniques,” *Micro and nanotechnologies*, 2009. .

[149] H. Yuan, L.-L. Wang, Y.-Z. Du, J. You, F.-Q. Hu, and S. Zeng, “Preparation and characteristics of nanostructured lipid carriers for control-releasing progesterone by melt-emulsification.,” *Colloids Surf. B. Biointerfaces*, vol. 60, no. 2, pp. 174–9, Nov. 2007.

[150] Z. Zhang and S.-S. Feng, “The drug encapsulation efficiency, in vitro drug release, cellular uptake and cytotoxicity of paclitaxel-loaded poly(lactide)-tocopheryl polyethylene glycol succinate nanoparticles.,” *Biomaterials*, vol. 27, no. 21, pp. 4025–33, Jul. 2006.

[151] S. Das, W. K. Ng, and R. B. H. Tan, “Are nanostructured lipid carriers (NLCs) better than solid lipid nanoparticles (SLNs): development, characterizations and comparative evaluations of clotrimazole-loaded SLNs and NLCs?,” *Eur. J. Pharm. Sci.*, vol. 47, no. 1, pp. 139–51, Aug. 2012.

[152] C. A. Praveen, “Absorption / Transmission / Reflection Spectroscopy,” *Oxford Instruments company*, 1999. .

[153] “Chapter 3,” *Transm. electron Microsc.*, pp. 21–42.

[154] S. A. N. D. Iego, “Transmission electron microscopy analysis of nanoparticles,” *nanoComposix*, vol. 1.1, pp. 1–7, 2012.

[155] B. Cryo, “Introducing Cryo Scanning Electron Microscopy 1.,” no. C, pp. 3–5, 2011.

[156] B. Stuart, “Infrared Spectroscopy: Fundamentals and Applications,” in *John Wiley*, 2004, pp. 5–79.

[157] T. Nicolet and C. All, “Introduction to Fourier Transform Infrared Spectrometry,” *A Thermo Electron Bussines*, pp. 1–8, 2001.

[158] R. Subbiah, M. Veerapandian, and K. S. Yun, “Nanoparticles: functionalization and multifunctional applications in biomedical sciences.,” *Curr. Med. Chem.*, vol. 17, no. 36, pp. 4559–4577, 2010.

[159] E. a. Bender, M. F. Cavalcante, M. D. Adorne, L. M. Colomé, S. S. Guterres, D. S. P. Abdalla, and A. R. Pohlmann, “New strategy to surface functionalization of polymeric nanoparticles: one-pot synthesis of scFv anti-LDL(−)-functionalized nanocapsules,” *Pharm. Res.*, vol. 31, no. 11, pp. 2975–2987, 2014.

[160] D. Papakostas, F. Rancan, W. Sterry, U. Blume-Peytavi, and A. Vogt, “Nanoparticles in dermatology,” *Arch. Dermatol. Res.*, vol. 303, no. 8, pp. 533–550, 2011.

[161] C. E. M. Griffiths, T. a. Luger, Y. Brault, J. M. Germain, and L. Mallbris, “Retreatment in patients with psoriasis achieving response with etanercept after relapse due to

treatment interruption: results from the CRYSTEL study," *J. Eur. Acad. Dermatology Venereol.*, vol. 29, no. 3, pp. 468–473, 2015.

[162] B. P. Albumin, "Albumin from bovine serum," *SigmaAldrich*, vol. 815, no. 1, pp. 2–5, 1990.

[163] C. C. Procedure and C. Method, "chemicell Covalent Coupling Procedure on SiMAG-Amine by Carbodiimide Method Introduction : Equipment and reagents :," pp. 2–4.

[164] C. R. Cammarata, M. E. Hughes, and C. M. Ofner, "Carbodiimide Induced Cross-Linking, Ligand Addition, and Degradation in Gelatin," *Mol. Pharm.*, p. 150206143522009, 2015.

[165] R. Wood, "DC Protein Assay Instruction Manual."

[166] J. H. Waterborg and H. R. Matthews, "The lowry method for protein quantitation.," *Methods Mol. Biol.*, vol. 1, pp. 1–3, 1984.

[167] A. Hawe, W. L. Hulse, W. Jiskoot, and R. T. Forbes, "Taylor dispersion analysis compared to dynamic light scattering for the size analysis of therapeutic peptides and proteins and their aggregates," *Pharm. Res.*, vol. 28, no. 9, pp. 2302–2310, 2011.

[168] S. Shilpi, V. D. Vimal, and V. Soni, "Assessment of lactoferrin-conjugated solid lipid nanoparticles for efficient targeting to the lung," *Prog. Biomater.*, vol. 4, no. 1, pp. 55–63, 2015.

[169] Interchim, "Separation techniques (Proteins) Desalting / Dialysis, Ultrafiltration," vol. 33, no. 0.

[170] "Fundamentals of Membrane Dialysis." [Online]. Available: http://www.spectrumlabs.com/dialysis/Fund.html.

[171] S. Modi and B. D. Anderson, "Determination of Drug Release Kinetics from Nanoparticles: Overcoming Pitfalls of the Dynamic Dialysis Method," 2013.

[172] S. J. Wallace, J. Li, R. L. Nation, and B. J. Boyd, "encapsulation and release methodology," vol. 2, no. 4, pp. 284–292, 2013.

[173] M. Barzegar-Jalali, K. Adibkia, H. Valizadeh, M. R. S. Shadbad, A. Nokhodchi, Y. Omidi, G. Mohammadi, S. H. Nezhadi, and M. Hasan, "Kinetic analysis of drug release from nanoparticles.," *J. Pharm. Pharm. Sci.*, vol. 11, no. 1, pp. 167–77, 2008.

[174] J. C. Stockert, A. Blázquez-Castro, M. Cañete, R. W. Horobin, and Á. Villanueva, "MTT assay for cell viability: Intracellular localization of the formazan product is in lipid droplets," *Acta Histochem.*, vol. 114, no. 8, pp. 785–796, 2012.

[175] B. Godin and E. Touitou, "Transdermal skin delivery: Predictions for humans from in vivo, ex vivo and animal models," *Adv. Drug Deliv. Rev.*, vol. 59, no. 11, pp. 1152–1161, 2007.

[176] F. P. Schmook, J. G. Meingassner, and A. Billich, "Comparison of human skin or epidermis models with human and animal skin in in-vitro percutaneous absorption," *Int. J. Pharm.*, vol. 215, no. 1–2, pp. 51–56, 2001.

[177] T. P. Sullivan, W. H. Eaglstein, S. C. Davis, and P. Mertz, "The pig as a model for human wound healing," *Wound Repair Regen.*, vol. 9, no. 2, pp. 66–76, 2001.

[178] F. Cilurzo, P. Minghetti, and C. Sinico, "Newborn pig skin as model membrane in in vitro drug permeation studies: a technical note.," *AAPS PharmSciTech*, vol. 8, no. 4, p. E94, 2007.

[179] K. Zhang, S. Lv, X. Li, Y. Feng, X. Li, L. Liu, S. Li, and Y. Li, "Preparation, characterization, and in vivo pharmacokinetics of nanostructured lipid carriers loaded with oleanolic acid and gentiopicrin," *Int. J. Nanomedicine*, vol. 8, pp. 3227–3239, 2013.

[180] M. F. Pinto, C. C. Moura, C. Nunes, M. a. Segundo, S. a. Costa Lima, and S. Reis, “A new topical formulation for psoriasis: Development of methotrexate-loaded nanostructured lipid carriers,” *Int. J. Pharm.*, vol. 477, no. 1–2, pp. 519–526, Dec. 2014.

[181] M. J. Gomes, S. Martins, D. Ferreira, M. a. Segundo, and S. Reis, “Lipid nanoparticles for topical and transdermal application for alopecia treatment: Development, physicochemical characterization, and in vitro release and penetration studies,” *Int. J. Nanomedicine*, vol. 9, no. 1, pp. 1231–1242, 2014.

[182] H. B. Patel, H. L. Patel, Z. H. Shah, and M. K. Modasiya, “Review on Hydrogel Nanoparticles in Drug Delivery,” vol. 1, no. 3, 2011.

[183] C. Gonçalves, P. Pereira, and M. Gama, “Self-assembled hydrogel nanoparticles for drug delivery applications,” *Materials (Basel).*, vol. 3, no. 2, pp. 1420–1460, 2010.

[184] G. Z. Abdullah, M. F. Abdulkarim, C. Mallikarjun, E. S. Mahd, M. Basri, M. A. Sattar, and and A. M. Noor, “Carbopol 934, 940 and Ultrez 10 as viscosity modifiers of palm olein esters based nano-scaled emulsion containing ibuprofen,” *Pak. J. Pharm. Sci*, pp. pp.75–83, 2013.

[185] “Rheology. Definition of viscosity. Non-newtonian behaviour.”

[186] S. M. Richardson, “Non-newtonian fluids,” 2000. .

[187] R. P. Chhabra, “Non-Newtonian fluids: An introduction,” *Rheol. Complex Fluids*, pp. 3–34, 2010.

[188] C. H. Lee, V. Moturi, and Y. Lee, “Thixotropic property in pharmaceutical formulations,” *J. Control. Release*, vol. 136, no. 2, pp. 88–98, 2009.

[189] a. Lippacher, R. H. Müller, and K. Mäder, “Preparation of semisolid drug carriers for topical application based on solid lipid nanoparticles,” *Int. J. Pharm.*, vol. 214, no. 1–2, pp. 9–12, 2001.

[190] K. Bhaskar, J. Anbu, V. Ravichandiran, V. Venkateswarlu, and Y. M. Rao, “Lipid nanoparticles for transdermal delivery of flurbiprofen: formulation, in vitro, ex vivo and in vivo studies.,” *Lipids Health Dis.*, vol. 8, p. 6, 2009.

[191] E. B. Souto, S. a. Wissing, C. M. Barbosa, and R. H. Müller, “Evaluation of the physical stability of SLN and NLC before and after incorporation into hydrogel formulations,” *Eur. J. Pharm. Biopharm.*, vol. 58, no. 1, pp. 83–90, 2004.

[192] R. H. Müller, M. Radtke, and S. a. Wissing, “Solid lipid nanoparticles (SLN) and nanostructured lipid carriers (NLC) in cosmetic and dermatological preparations,” *Adv. Drug Deliv. Rev.*, vol. 54, no. SUPPL., pp. 131–155, 2002.

[193] J. das Neves and B. Sarmento, “Precise engineering of dapivirine-loaded nanoparticles for the development of anti-HIV vaginal microbicides,” *Acta Biomater.*, no. February, 2015.

[194] a. K. Kohli and H. O. Alpar, “Potential use of nanoparticles for transcutaneous vaccine delivery: Effect of particle size and charge,” *Int. J. Pharm.*, vol. 275, no. 1–2, pp. 13–17, 2004.

[195] N. Kohler, C. Sun, J. Wang, and M. Zhang, “Methotrexate-modified superparamagnetic nanoparticles and their intracellular uptake into human cancer cells.,” *Langmuir*, vol. 21, no. 19, pp. 8858–8864, 2005.

[196] M. S. Khan, M. Priyadarshini, S. Sumbul, and B. Bano, “Methotrexate binding causes structural and functional changes in lung cystatin,” *Acta Biochim. Pol.*, vol. 57, no. 4, pp. 499–503, 2010.

[197] H. Sciences, S. Dash, P. N. Murthy, L. Nath, and P. Chowdhury, “Kinetic modeling on drug release from controlled drug delivery systems.,” *Acta Pol. Pharm.*, vol. 67, no. 3, pp. 217–23, 2010.

[198] R. H. Müller, K. Mäder, and S. Gohla, “Solid lipid nanoparticles (SLN) for controlled drug delivery - A review of the state of the art,” *Eur. J. Pharm. Biopharm.*, vol. 50, no. 1, pp. 161–177, 2000.

[199] B. Faure, G. Salazar-Alvarez, A. Ahniyaz, I. Villaluenga, G. Berriozabal, Y. R. De Miguel, and L. Bergström, “Dispersion and surface functionalization of oxide nanoparticles for transparent photocatalytic and UV-protecting coatings and sunscreens,” *Sci. Technol. Adv. Mater.*, vol. 14, no. 2, p. 023001, 2013.

[200] Y. Li, H. Wu, X. Yang, M. Jia, Y. Li, Y. Huang, J. Lin, S. Wu, and Z. Hou, “Mitomycin C-soybean phosphatidylcholine complex-loaded self-assembled PEG-Lipid-PLA hybrid nanoparticles for targeted drug delivery and dual-controlled drug release,” *Mol. Pharm.*, vol. 11, no. 8, pp. 2915–2927, 2014.

[201] A. Jain, G. Chasoo, S. K. Singh, A. K. Saxena, and S. K. Jain, “Transferrin-appended PEGylated nanoparticles for temozolomide delivery to brain: in vitro characterisation.,” *J. Microencapsul.*, vol. 28, no. 1, pp. 21–28, 2011.

[202] S. Jose, J. F. Fangueiro, J. Smitha, T. a. Cinu, a. J. Chacko, K. Premaletha, and E. B. Souto, “Predictive modeling of insulin release profile from cross-linked chitosan microspheres,” *Eur. J. Med. Chem.*, vol. 60, pp. 249–253, 2013.

[203] N. Peppas, “Commentary on an exponential model for the analysis of drug delivery: Original research article: a simple equation for description of solute release: I II. Fickian and non-Fickian release from non-swellable devices in the form of slabs, spheres, cylinders,” 1987.

[204] P. Costa and J. M. Sousa Lobo, “Modeling and comparison of dissolution profiles,” *Eur. J. Pharm. Sci.*, vol. 13, no. 2, pp. 123–133, 2001.

[205] A. Ortan, C. D. Parvu, M. V. Ghica, L. M. Popescu, and L. Ionita, “Rheological study of a liposomal hydrogel based on carbopol,” *Rom. Biotechnol. Lett.*, vol. 16, no. 1 SUPPL., pp. 47–54, 2011.

[206] A. Kandamchira, S. Selvam, N. Marimuthu, S. K. Janardhanan, and N. N. Fathima, “Influence of functionalized nanoparticles on conformational stability of type i collagen for possible biomedical applications,” *Mater. Sci. Eng. C*, vol. 33, no. 8, pp. 4985–4988, 2013.

[207] A. Petriccione, M. Zarrelli, V. Antonucci, and M. Giordano, “Aggregates of Chemically Functionalized Multiwalled Carbon Nanotubes as Viscosity Reducers,” pp. 3251–3261, 2014.

[208] M. E. Carlotti, V. Rossatto, M. Gallarate, M. Trotta, and F. Debernardi, “Vitamin A palmitate photostability and stability over time.,” *J. Cosmet. Sci.*, vol. 55, no. 3, pp. 233–252, 2004.

[209] K. Valdés, “Lipid nanoparticles for the topical delivery of retinoids and derivatives,” vol. 10, pp. 253–269, 2015.

[210] M. Gupta, U. Agrawal, and S. P. Vyas, “Nanocarrier-based topical drug delivery for the treatment of skin diseases,” *Expert Opin. Drug Deliv.*, vol. 9, no. 7, pp. 783–804, 2012.

[211] F. V. Tosta, L. M. Andrade, L. P. Mendes, J. L. V. Anjos, A. Alonso, R. N. Marreto, E. M. Lima, and S. F. Taveira, “Paclitaxel-loaded lipid nanoparticles for topical application:

the influence of oil content on lipid dynamic behavior, stability, and drug skin penetration," *J. Nanoparticle Res.*, vol. 16, no. 12, p. 2782, 2014.

[212] S. H. Song, K. M. Lee, J. B. Kang, S. G. Lee, M. J. Kang, and Y. W. Choi, "Improved Skin Delivery of Voriconazole with a Nanostructured Lipid Carrier-Based Hydrogel Formulation," *Chem. Pharm. Bull*, vol. 62, no. 8, pp. 793–798, 2014.

[213] S. N. ˇ C. ELISABET GONZALEZ-MIRA, A. C. CALPENA, M. A. EGEA, E. B. SOUTO, and M. L. GARCIA1, "Improved and Safe Transcorneal Delivery of Flurbiprofen by NLC and NLC-Based Hydrogels."

[214] A. K. Jain, A. Jain, N. K. Garg, A. Agarwal, A. Jain, S. A. Jain, R. K. Tyagi, R. K. Jain, H. Agrawal, and G. P. Agrawal, "Adapalene loaded solid lipid nanoparticles gel: an effective approach for acne treatment.," *Colloids Surf. B. Biointerfaces*, vol. 121, pp. 222–9, Sep. 2014.

[215] B. Jachimska, M. Wasilewska, and Z. Adamczyk, "Characterization of globular protein solutions by dynamic light scattering, electrophoretic mobility, and viscosity measurements.," *Langmuir*, vol. 24, no. 13, pp. 6866–6872, 2008.